Environmental Controls on δ^{11}B in Unconventional Biogenic Carbonate Archives

by

Yi-Wei Liu

**A dissertation submitted in partial fulfillment
of the requirements for the degree of
Doctor of Philosophy
(Geology)
in the University of Michigan
2015**

Doctoral Committee:

　　Assistant Professor Sarah M. Aciego, Chair
　　Professor Joel D. Blum
　　Associate Professor Terese M. Olson
　　Associate Professor Alan D. Wanamaker Jr., Iowa State University

Acknowledgements

First and foremost, I would like to thank Assistant Professor Sarah M. Aciego for her guidance and support throughout the past four years. I have learned a lot under her supervision in a wide variety of aspects from basic scientific writing and presentation, experimental design, trouble shooting, logical thinking, to scientific social networking. I also appreciate her moral support so that I can overcome the obstacles and frustrations in pursuing my Ph. D. degree.

I am also thankful to Associate Professor Alan D. Wanamaker Jr. for his technical, scientific and moral supports to my dissertation work. His constructive suggestions and encouragements help me a lot to keep being optimistic working on my dissertation. I would also thank to my other dissertation committee Professor Joel D. Blum and Associate Professor Terese M. Olson for their helpful comments and suggestions to my dissertation work.

Thanks to Assistant Professor Aradha Tripati, Dr. Robert Eagle, Dr. Michael Carroll for providing me opportunities to extend my dissertation work. I would also like to thank to Professor Larry Ruff, Associate Professors Nathan Sheldon, Ingrid Handy, and David Lund for their help and suggestions. Thanks the Department of Earth and Environmental Sciences, and Rackham Graduate School in the University of Michigan.

Many thanks to my colleagues, Bryan, Emily, Sarah, Carli, Mark, and Molly for their accompanies, suggestions and supports so that I can survive from the intense dissertation work. Living in a foreign country is hard; thanks to all my friends that have helped me to set up my life in Michigan, all the people that have helped me out with my fieldwork in Norway and all the friends I have in the past four years for their accompanies in my life. Because of them, I can find my balance between work and life and therefore be able to keep pursuing my degree.

In the end, I would like to thank to Dad, Mom, Xavier and all my family members. I would not be able to complete my degree aboard without all their supports. Thanks to auntie Jennifer for her warm e-mails in the past four years. Special thanks to auntie Lesley and uncle Albert for their help to go through my dissertation thesis and provide grateful comments to my writing and presentation. Thanks to Xavier for his moral and technical supports, helping me to cross those lows and downs and providing me mathematical and statistical supports in my study. Of course, I gratefully appreciate Dad and Mon being my strongest moral support all the time.

Table of Contents

Chapter III   Environmental Controls on the Boron and Strontium Isotopic Composition of Aragonite Shell Material of Cultured *Arctica islandica*…..

Chapter IV   Geochemical constraints on the vesicle pH of the coccolithophore *Pleurochrysis carterae* and its response to CO_2-induced ocean acidification

Chapter V   Summary and Outlook

Appendices

List of Tables

List of Figures

List of Appendices

Abstract

A method for high-throughput boron purification coupled with total evaporation thermal ionization mass spectrometry was developed to allow investigation of how the seawater pH varies spatially and temporally with respect to elevated atmospheric carbon dioxide level, and the impacts of ocean acidification on marine organisms. Using this method, we are able to measure boron isotopic composition in carbonate with less then 1 ng of boron in the sample and further reconstruct calcification pH for biogenic carbonate as a biogeochemical archive. In this dissertation, we applied this method to investigate how environmental factors influence the boron incorporation in two unconventional biogenic carbonate archives: aragonite bivalve shells and calcite coccolithophores. In the bivalve shell *Arctica islandica* study, we found that shells regulate their calcification pH, and that boron incorporation into the shell has a potential temperature dependence. Therefore, a culture experiment with fixed temperature and salinity, but variable pH is required to evaluate the species-specific relationship between boron and ambient seawater pH and the potential use of this proxy in this species. In the coccolithophorid species *Pleurochrysis carterae* study, we observed an ability for this organisms to adapt to ocean acidification. The boron isotopic composition in the coccoliths suggests it regulates vesicle pH to sustain calcification with decreasing environmental pH. With other geochemical constraints including the particulate inorganic carbon to particulate organic carbon ratio (PIC/POC) and stable isotopic compositions we found this coccolitophorid species is likely to change usage of inorganic carbon species from HCO_3^- to $CO_{2(aq)}$ as ambient medium pH decreases. This dissertation work provides insights on the diverse response of marine organisms to ocean acidification. Extending work on boron to pH calibration in unconventional species will help reconstruct seawater pH records over a wide geographic range through geologic time. Further applications in different marine calcifiers will help us better understand the mechanisms for diverse

biological responses to ocean acidification and to predict the potential capacity to sequestrate exceeded atmospheric CO_2 in the ocean.

Chapter I   Introduction

I.1   Motivation

I.1.1   Elevated atmospheric CO_2 and ocean acidification

The carbon cycle is one of the most important aspects of geologic study and climate change. Since the 20th century, an increasing level of anthropogenic activity has substantially raised the concentration of CO_2 in the atmosphere and is exacerbating the natural greenhouse effect leading to global climate change (IPCC, 2013). Atmospheric CO_2 dissolves into seawater and dissociates into bicarbonate and carbonate ions (Figure I.1). This process leads to the release of hydrogen ions and results in a decrease of ocean pH. The ocean is one of the largest carbon reservoirs on earth and it plays an important role in mediating or amplifying the effects of atmospheric CO_2 fluctuations. Approximately half of the anthropogenic CO_2 that is released into the atmosphere is sequestered by the oceans (Sabine *et al.*, 2004). Although seawater has a large buffering capacity, the dissolved CO_2 can still cause a marked decrease in the pH of well-buffered marine systems (Orr *et al.*, 2005). Recent observations suggest that ocean acidification has environmentally impacted diverse regions over the past one to two decades (Byrne *et al.*, 2010; Feely *et al.*, 2008; Findlay *et al.*, 2010; Hönisch *et al.*, 2012; Krief *et al.*, 2010; Vázquez-Rodrıguez *et al.*, 2012). Decreasing ocean pH associated with increasing atmospheric CO_2 may also likely impact marine organisms, particularly those which produce carbonate skeletons or shells. Therefore, it is essential to understand the relationship of increasing atmospheric CO_2 upon seawater carbon chemistry and its impact on different marine calcifiers as a means to understand climate change.

In addition to direct air-sea exchange of CO_2 into seawater, there are many other

environmental factors that could potentially influence seawater pH, especially in sensitive coastal areas. Alkalinity, the sum of weak base concentration in solution, is one of the factors that controls the aqueous carbonate system. The higher the alkalinity of a solution, the greater the buffering capacity. The alkalinity of the open ocean might not vary greatly due to level of organic formation and destruction and carbonate precipitation, except for the case with coccolithophorid blooms during seasonal warming; however, alkalinity varies spatially in coastal regions. River input is the major contributor for alkalinity in coastal seawater. River water may contain varied concentrations of particulate and dissolved organic and minerals depending on different geologic, ecologic, and climatic settings thus influencing local seawater chemistry. As increasing levels of anthropogenic CO_2 in the atmosphere are exacerbating the greenhouse effect, rising global temperature is not the only result. A change to the global climate system, including precipitation patterns may occur, which in turn may influence the chemical weathering processes. Therefore the source of alkalinity might not only differ from place to place, but also differ from time to time for the same location. Additionally, carbonate precipitation and dissolution will also change coastal seawater alkalinity and pH, which even complicates the regional seawater chemistry, as well as the overall carbon cycle (Figure I. 1). Causality for regional temporal seawater pH and how the seawater pH changes with respect to the increasing level of atmospheric CO_2 are not well known. To better understand how the CO_2 concentration in the air affects ocean pH, and further evaluate the potential storage capacity of the ocean for increasing anthropogenic carbon load, more direct and indirect seawater pH data is needed.
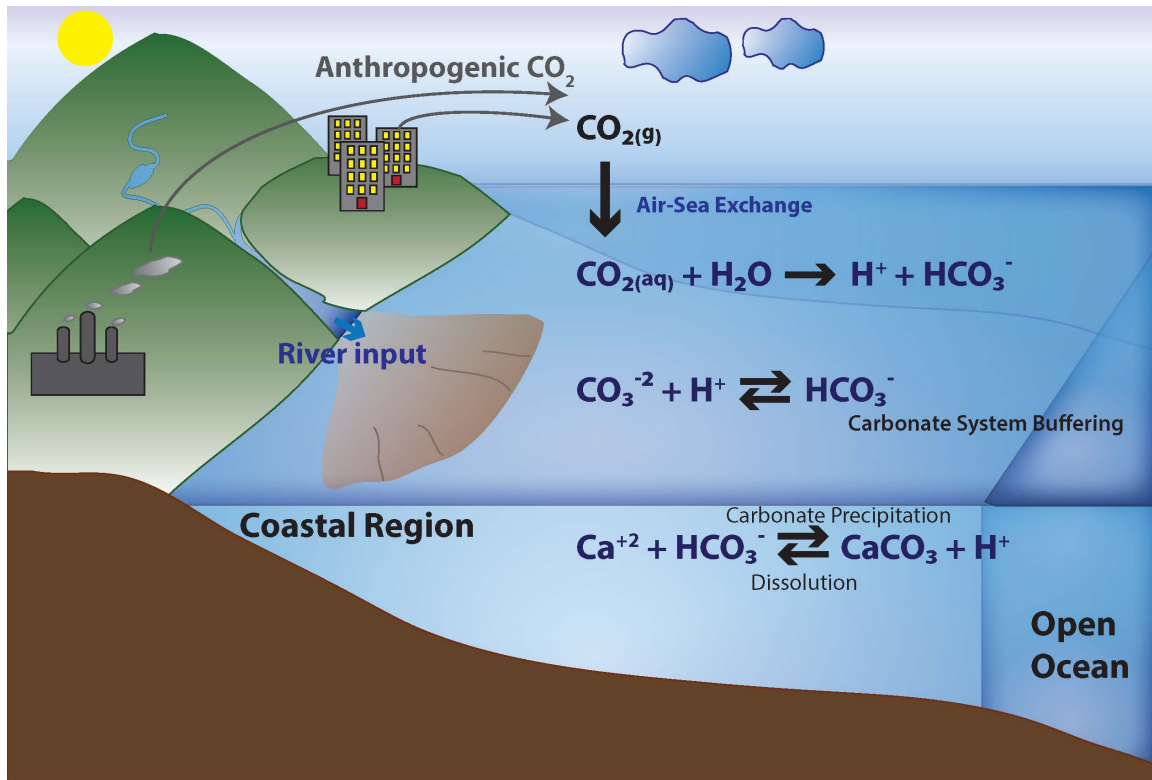
Figure I. 1   Illustration of increasing CO_2 in the atmosphere and seawater carbonate chemistry in coastal region.

Potential sources that would influence seawater pH in coastal region: (a) direct air-sea CO_2 exchange, (b) river input, and (c) carbonate precipitation.

I.1.2   The limited instrumental records

Research on the ocean carbon cycle is vitally important due to the projected impacts of atmospheric CO_2 on global temperatures, ocean chemistry and resulting climate change. Atmospheric CO_2 measured directly at the Mauna Loa station has increased from 315 ppm in 1958 to 400 ppm in May 2013, and records from ice cores indicate that the total CO_2 increase is on the order of 90 ppm since the beginning of the Industrial Revolution. However, complete data logs of direct seawater pH measurements are scarce and the behavior of ocean pH chemistry over different temporal and spatial scales is largely unknown. The earliest seawater pH measurement was made at the beginning of the 20th century by Sorensen and Palitzsch (1910). Since then many more seawater pH measurements have been reported, however, the data is only restricted to a small regime and measurements taken within a few days (Boyer *et al.*, 2013). Moreover, the pH measurements made before 1988 were

mostly conducted by the potentiometric method and have proven to be problematic (Dickson, 1993). Longer instrumental records started to be included into oceanographic studies later in the 21st century. However, compared to the other physicochemical seawater data logging (temperature, salinity or chemical composition data such as nutrients, stable oxygen or carbon records), seawater pH received less attention in oceanographic data collection. Such records are necessary in order to understand the trends and range of natural variability in ocean pH to predict the consequences of continued CO_2 increase on ocean chemistry.

One technique that has been widely used to reconstruct seawater pH is by measuring boron isotopic composition in biogenic archives such as temperate corals or foraminiferas. This work is largely based on the fact that the boron isotopic composition in seawater is a constant throughout the past 20 million years because of its long residence time in seawater, and the isotopic composition in the two dominant boron species, boric acid ($B(OH)_3$) and borate ion ($B(OH)_4^-$), are pH dependent. Based on the assumption that only borate ions will incorporate into biogenic carbonates, one can reconstruct the ambient seawater pH when the carbonate formed. However, foraminifera records are limited by time resolution and coral records are restricted by their habitat. New marine archives are still highly desired to resolve the seawater pH records in the geological past.

In addition to alkalinity, river inputs may also affect the temperature and salinity of coastal seawater thus influencing the boron partitioning into the carbonate and potentially changing the seawater isotopic composition thus complicating the interpretation of boron isotopic composition recorded in the biogenic carbonate. Furthermore, it has been observed that there might be a species-specific fractionation or systematically pH self-regulation in some marine calcifying organism. Hence, it is important to calibrate the boron to seawater pH dependency in different species when applying boron isotopic composition in a new biogenic carbonate species as an archive for pH in coastal areas.

I.1.3   The potential impacts on marine organisms

The potential application of using boron isotopic composition in biogenic carbonate to reconstruct historic seawater pH can be extended to investigate the impacts of ocean acidification on marine calcifying organisms. It is expected that the increasing CO_2-induced ocean acidification will threaten marine organisms because it could dramatically change the habitat. More specifically to calcifying organisms, decreasing seawater pH will reduce the carbonate saturation state ($\Omega = \frac{[Ca^{2+}][CO_3^{2-}]}{K_{sp}}$), which can cause shell or skeleton dissolution. In general, when $\Omega > 1$, calcium carbonate can precipitate from solution; when $\Omega < 1$, dissolution will occur. However, it has been suggested that for marine calcifiers, dissolution might happen even when $\Omega > 1$, if the saturation state is lower than a certain threshold (e.g., $\Omega < 5$ or 6) (Casareto *et al.*, 2009; Feely *et al.*, 2004; Kleypas *et al.*, 1999). Therefore, many arguments have focused on potential large-scale marine extinctions having been caused by ocean acidification (Abbasi and Abbasi, 2011; Bignami *et al.*, 2013; Doney *et al.*, 2009; Hofmann *et al.*, 2010).

Recent studies suggest that marine organisms might have different responses to the changing seawater acidity. Those species with a higher ability to pump protons from their calcification sites might have a better ability to raise their pH for calcification and may be less sensitive to ambient seawater pH. Some phytoplankton species, depending on the carbonate species used for photosynthesis and calcification, might even favor a lower pH environments because more dissolved inorganic carbon will be available. The complexity of biological responses and corresponding mechanisms have not been resolved yet and more studies are required to understand the impacts of ocean acidification on different species and changes to marine ecosystems in the projected high CO_2 partial pressure (pCO_2) future.

I.2   Boron isotopes as seawater pH proxy in biogenic carbonates

Boron has two natural stable isotopes, ^{10}B and ^{11}B, which comprise 19.9(7) % and 80.1(7) % of total boron, respectively (Berglund and Wieser, 2011). The dominant aqueous species of boron in seawater are boric acid ($B(OH)_3$) and borate ion ($B(OH)_4^-$).

The relative proportion of these two species is a function of pH with the following relationship:

$$B(OH)_3 + H_2O \rightleftharpoons B(OH)_4^- + H^+ \tag{Eq. I.1}$$

At low pH, boron exists as $B(OH)_3$ in solution, and conversely, at high pH, boron exists as $B(OH)_4^-$. The governing reaction for isotope exchange between these two species is:

$$^{10}B(OH)_3 + {}^{11}B(OH)_4^- \rightleftharpoons {}^{11}B(OH)_3 + {}^{10}B(OH)_4^- \tag{Eq. I.2}$$
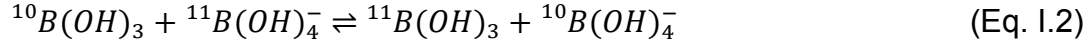
The stable isotope ^{11}B is enriched in $B(OH)_3$ compared to $B(OH)_4^-$, and the combination of Equations (I.1) and (I.2) can be used to determine the distribution of the two boron species and the isotopic composition of each for a given pH. The isotopic composition of boron is generally reported as:

$$\delta^{11}B = \left[\frac{(^{11}B/^{10}B)_{sample}}{(^{11}B/^{10}B)_{SRM\ 951a}} - 1 \right] \times 1000 \ (\permil) \tag{Eq. I.3}$$

where SRM 951 is the internationally recognized boron isotope standard. Because the residence time of seawater boron is approximately 14 million years (Lemarchand *et al.*, 2000), the boron isotopic composition in the ocean is constant over this time period, with an average seawater $\delta^{11}B$ value of 39.61 ‰ (Foster *et al.*, 2010). Therefore, $\delta^{11}B$ has the following relationship: at low pH, the isotopic composition of $B(OH)_3$ is equal to the isotopic composition of the total dissolved boron (39.61 ‰). In contrast, at high pH the isotopic composition of $B(OH)_4^-$ is equal to the isotopic composition of the total dissolved boron, therefore the $\delta^{11}B$ is enriched in $B(OH)_3$ by about 20 ‰ with respect to $B(OH)_4^-$ at any equilibrium pH based on a constant fractionation factor (Figure I. 1).
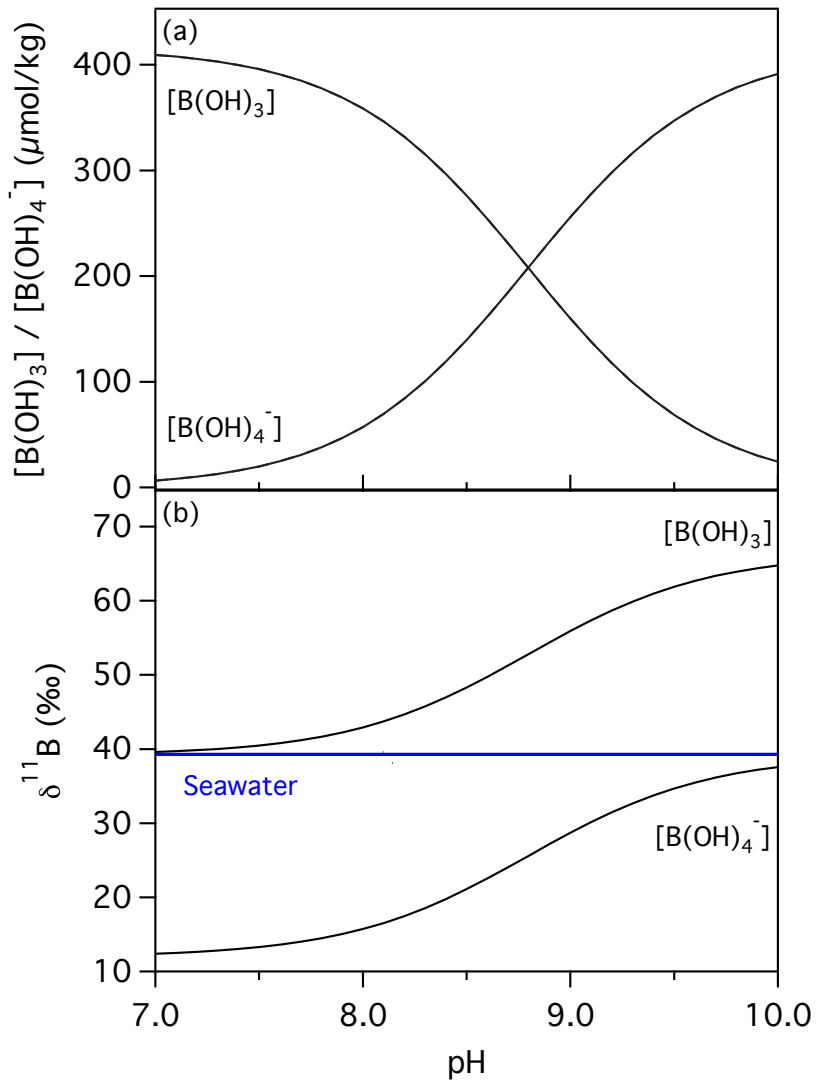
Figure I. 2 **Distribution of boric acid and borate concentrations and boron isotopic composition in seawater.**

During skeletal or shell growth, marine organisms primarily incorporate $B(OH)_4^-$ into the carbonate structure. Building on these relationships, Hemming and Hanson (1992) demonstrated that seawater pH dictates the amount of $B(OH)_4^-$ in seawater and thus the isotopic composition of boron in marine carbonates. Therefore, seawater pH can be reconstructed from $\delta^{11}B$ of carbonates from the following equation:

$$pH = pK_b - \log\left(\frac{\delta^{11}B_{sw} - \delta^{11}B_{carbonate}}{\alpha\delta^{11}B_{carbonate} - \delta^{11}B_{sw} + 1000(\alpha-1)}\right) \qquad \text{(Eq. I.4)}$$

where pK_b is the pK value for boric acid at a given temperature and salinity, and is 8.5975 at 25°C and 35 PSU salinity (DOE, 1994), $\delta^{11}B_{sw}$ is the isotopic composition of seawater, and α is the equilibrium isotopic fractionation factor between boric acid and borate ion $\left(\alpha \equiv \frac{\left(^{11}B / ^{10}B \right)_{Boric\,acid}}{\left(^{11}B / ^{10}B \right)_{Borate\,ion}} \right)$. Among these variables, only the seawater composition can be considered known and constant for all geographic locations and carbonate-precipitating species. Temperature, salinity, and the fractionation factor must be estimated. Two empirical and analytical values of α are suggested for seawater: (1) α = 1.0194, a theoretical result of Kakihana *et al.* (1977), which has been applied widely on paleo-reconstructions (Hönisch *et al.*, 2004; Kakihana *et al.*, 1977; Sanyal *et al.*, 1995); and (2) α = 1.0272, which was empirically obtained from Klochko *et al.* (2006) and is considered to better describe the distribution of the two boron species in nature today (Foster, 2008; Klochko *et al.*, 2006; Pagani *et al.*, 2005). However, due to the ability of calcifying organisms to buffer their own local environments, species specific fractionation factors and transfer functions are likely more appropriate than theoretical α values (Anagnostou *et al.*, 2012; Hönisch *et al.*, 2004; Krief *et al.*, 2010; Rae *et al.*, 2011; Reynaud *et al.*, 2004; Reynaud *et al.*, 2008; Trotter *et al.*, 2011).

I.3 Application of boron isotopic composition in biogenic carbonates

So far the $\delta^{11}B$-pH relationship (Eq. I.4) has been tested extensively on the biogenic marine carbonate foraminifera and coral with broad success. However, the applications of Boron isotopes in both types of carbonates have limitations.

Foraminifera have been analyzed extensively since the mid 1990s, with applications ranging across large timescales and water masses. Initial studies by Spivack et al. (1993) and Sanyal et al. (1995) reconstructed ocean pH using carbonate shells of foraminifera, which prompted the scientific community to focus on the foraminifera record of pH. The study from Hönisch and Hemming (2005) revealed that boron isotopic composition recorded in the foraminifera demonstrates the coupling of surface ocean chemistry and atmospheric pCO_2 over two full glacial cycles (0 – 140 and 300 – 420

kyr). Foster (2008) reconstructed a seawater pH record and investigated the carbon system in the Caribbean Sea over the last 130 ka. Palmer et al. (2010) showed that the northern Arabian Sea was a source of CO_2 to the atmosphere in the transition out of the Last Glacial Maximum. Recently, the utility of the $\delta^{11}B$-pH relationship was affirmed across a wide range of species of benthic foraminifera (Rae et al., 2011) and the $\delta^{11}B$-pH proxy was largely applied to reconstruct pCO_2 since the Pliocene (Foster and Sexton, 2014; Martinez-Boti *et al.*, 2015a; Martinez-Boti *et al.*, 2015b).

The wide range in habitat of planktonic and benthic foraminifera can provide average open ocean chemical records, but availabilities to achieve those records are limited by the location of drilled sediment cores and temporal resolution. Figure I. 3 shows the location of sediment cores from which foraminifera samples have been shown to preserve seawater boron ($\delta^{11}B$ or B/Ca) in the north Atlantic. Even Holocene sediment cores, which were dated with high-precision ^{14}C have age errors (e.g., 30 – 300 years, Schmidt *et al.* (2004)) that preclude continuous seasonal to decadal records of rapid ocean chemistry changes and regional climate controls.

Coral based studies have only recently been initiated for high-resolution pH studies. The positive relationship between $\delta^{11}B$ and pH was established using culture experiments (Hönisch *et al.*, 2004) and has been quickly utilized because the banded coral skeletons provide seasonal to yearly resolution records which are not available from foraminifera samples taken from most sediment cores. Pelejero *et al.* (2005) produced a coral *Porites* pH record with interdecadal variability indicating that changes in CO_2 concentrations due to seawater circulation caused abrupt shifts in pH in Pacific coral reefs. More recently, a series of papers have expanded the database of $\delta^{11}B$ in corals. Liu *et al.* (2009) found a 3 ‰ increase in the $\delta^{11}B$ of coral samples from the South China Sea (SCS) through the Holocene and then an abrupt decrease in the last 1 ka, which was attributed to a change in control on the seawater pH in the SCS from regional climate to global atmospheric CO_2. Wei *et al.* (2009) found a similar influence of regional climate on pH (and $\delta^{11}B$) of the seawater around the Great Barrier Reef, which is reflected in the *Porites* coral record. In order to probe the $\delta^{11}B$-pH relationship in corals further, Douville *et al.* (2010) applied the technique to an ancient *Porites* sample

of coral spanning the Younger Dryas (12.8 – 11.5 ka), a time period with a well-resolved change in atmospheric CO_2 concentration (40 ppm; Monnin et al., 2001). They observed an abrupt pH drop at the end of the Younger Dryas, providing further evidence of distinct changes in the properties of the water masses in the equatorial Pacific. In addition, a more recent study from D'Olivo *et al.* (2014) compared coral records from inner-shore and off-shore coastal Australia and showed that large river input may also change the water boron isotopic composition; consequently the $\delta^{11}B$ recorded in the inner-shore specimens can be used to trace the water quality. These recent works indicate that coral skeletons can record aspects of the chemical environment from the marine realm. However the applicability of the $\delta^{11}B$-pH relationship in surface corals is confined by their habitat: tropical to subtropical warm waters. Deep, cold-water corals have been found much farther north, but their usefulness as ocean chemistry and pH monitors still need to be studied (Farmer *et al.*, 2015) .

Brachiopods are used extensively for paleo-oceanic and paleo-climate work for deep time (> 180 Ma) because their chemical structure is stable. Understanding the $\delta^{11}B$-pH relationship for these carbonates, and the large observed $\delta^{11}B$ values (Hemming and Hanson, 1992), have been hampered by potential species-specific variability in their $\delta^{11}B$-pH transfer function (Penman *et al.*, 2012). Recent work from Penman *et al.* (2012) not only indicates that parts of the brachiopod shell structure do show a correlation with ambient pH, but also highlights the necessity of careful species-specific calibrations and sampling.

Taking advantage of boron isotopic composition recorded in biogenic carbonates, one can gain more knowledge about the paleo seawater pH or the corresponding pCO_2. Broadening the $\delta^{11}B$-pH technique to species produce high resolution records at mid-to-high latitudes (e.g., bivalve shell *A. islandica*) will complement the biogenic carbonate work that has been done previously.
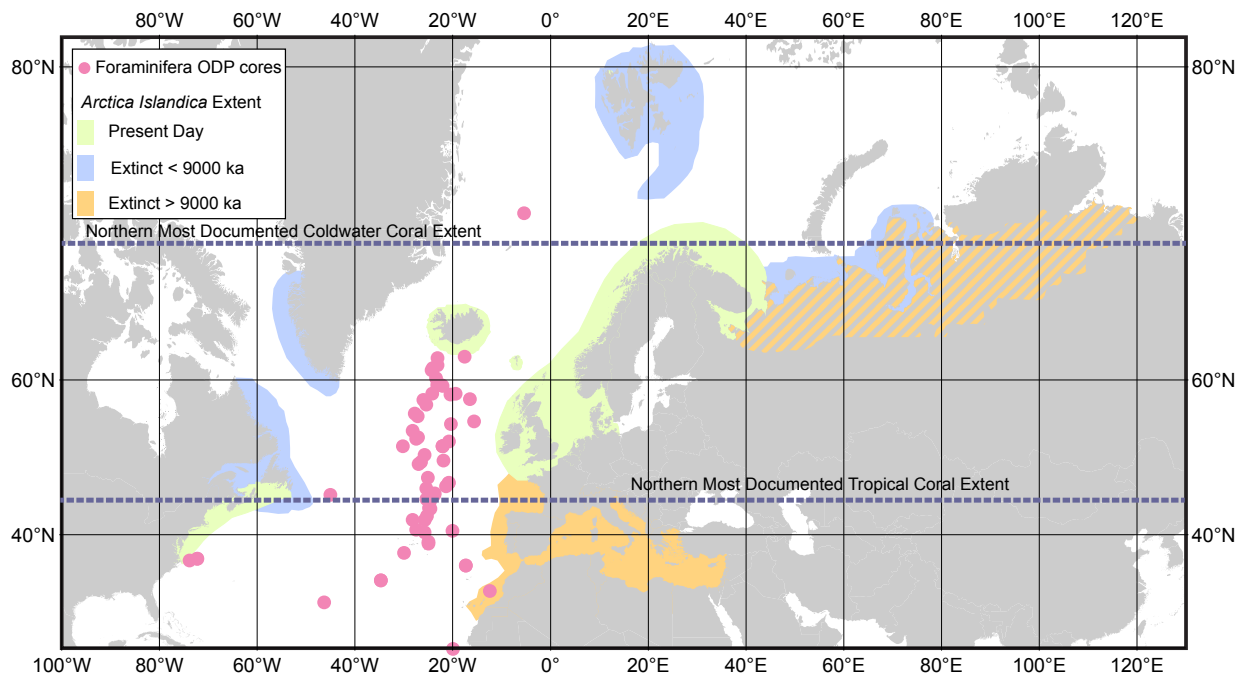
Figure I. 3   Biogenic carbonates of the north Atlantic.
Sediment core locations that show foraminifera accurately recording seawater boron composition (either δ^{11}B or B/Ca) from Brown *et al.* (2011); Foster *et al.* (2008); Rae *et al.* (2011); Sanyal *et al.* (1995); Yu and Elderfield (2007); Yu *et al.* (2007); Yu *et al.* (2008); Yu *et al.* (2013). Northern most extent of live coral in tropical and coldwater from Frank *et al.* (2011); Lindberg *et al.* (2007); Wells (1988). Present-day and historical extent of *A. islandica* modified from Dahlgren *et al.* (2000).

I.4   Species-specific responses to changing environments

According to previous boron isotope studies, for different foraminifera or coral species, species-specific calibration is required to apply the δ^{11}B-pH proxy (Henehan *et al.*, 2013; Hönisch *et al.*, 2004). Many boron studies further indicated self-regulation of the vesicle pH for corals. This suggests that different species might have different strategies for calcification in a range of seawater pH. Therefore, in addition to investigating the potential of extending δ^{11}B-pH proxy to a wider range of marine biogenic carbonates, it is also important to learn how those organisms respond to changing environments.

Ries *et al.* (2009) have reported net calcification rates in 18 species of marine organism in a pCO_2 controlled experiment and shown different patterns of the changing calcification rate to carbonate saturation state. A later study by Ries (2011) further summarizes marine biological response to six different patterns with respect to pCO_2 and proposed a proton-pumping model to explain the different trends. In addition to the

different abilities to regulate their internal pH, it has been also suggested that the marine organisms can change their photosynthesis and calcification strategies for survival (Delille *et al.*, 2005; Krief *et al.*, 2010). Although in an acidic environment the lower carbonate saturation state may cause partial dissolution of the carbonate shells, thicker external shells might also provide shields to protect the soft body. For photoautotrophic species, depending on the energy cost between two processes, different organisms change the photosynthesis to calcification ratio. This has been observed from different studies, which can be determined from the particulate inorganic carbon to particulate organic carbon ratios (PIC/POC) (Casareto *et al.*, 2009; Iglesias-Rodriguez *et al.*, 2008; Rickaby *et al.*, 2010; Riebesell *et al.*, 2000). Due to the complexity of the biological processes, the actual impacts of ocean acidification to marine ecosystems are not fully understood, and the mechanisms for the biological responses are still largely unknown.

I.5   Thesis outline

This work focuses on using boron isotopes in biogenic carbonates to investigate the impacts of ocean acidification. This study can provide a potential means to reconstruct paleo seawater pH records over a wider temporal and geographical range and provide insights on how different marine calcifiers will adapt to the ongoing ocean acidification.

The second chapter (**Manuscript I**) describes a newly developed high-throughput boron purification method coupled with total evaporation negative thermal ionization mass spectrometry technique to measure $\delta^{11}B$ in small samples. This technique allow us to measure a boron sample size down to < 1 ng so that we can investigate the calcifying pH for unconventional biogenic carbonates such as bivalves and coccoliths due to their low boron concentrations.

This technique is applied to a cold-water species ocean quahog, *Arctica islandica (A. islandica)* and the details are listed in Chapter 3 (**Manuscript II**). By comparing instrumental records including seawater temperature, salinity and pH to the shell boron and strontium isotopic compositions from the cultured bivalve shells, we investigated how different environmental factors could influence the boron incorporation into the

aragonite shell material and evaluated the potential application of δ^{11}B-pH in *A. islandica* in the future.

The impact of different levels of carbon dioxide to the calcification of coccolithophorid species of *Pleurochrysis carterae (P. carterae)* is examined in Chapter 4 (**Manuscript III**). Boron isotopic compositions in the coccoliths can be used to infer their internal calcifying pH. After synthesizing with other elemental and isotopic proxies and instrumental culture conditions, we can further evaluate how those geochemical proxies co-evolved with the changing culture conditions. We also evaluate the usage of different carbon species for calcification and photosynthesis in *P. carterae* at elevated dissolved inorganic carbon (DIC) concentrations. These results should provide us insight to the adaptation of coccolithophore *P. carterae* to ocean acidification.

The fifth chapter summarizes the significant findings in the previous chapters and provides potential outlooks for the applications of the high-throughput boron technique. The applications include examining the potential use of boron-pH proxy in *A. islandica,* and investigating different responses from a wider variety of marine organisms to ocean acidification. Based on better constrains of culture conditions, such as nearly constant seawater temperature and salinity while varying pH range, we can better evaluate the boron isotopic composition in bivalve shells as a pH proxy. Comparing the results of short-term and long-term pH-controlled culture experiments, one can examine the potential evolutionary responses in marine calcifiers. This may help us to interpret the geological data with respect to the changing environments in the past. Further, by extending the culture species to a boarder range to include some marine invertebrates, one can learn more about the different biological responses to elevated pCO_2.

Manuscript I has been published in Rapid Communication of Mass Spectrometry: Liu, Y.-W., S. M. Aciego, A. D. Wanamaker, and B. K. Sell (2013), A high-throughput system for boron microsublimation and isotope analysis by total evaporation thermal ionization mass spectrometry, *Rapid Commun. Mass Spectrom., 27*(15), 1705-1714.

Manuscript II has been published in Biogeoscience: Liu, Y.-W., S. M. Aciego, and A. D. Wanamaker Jr (2015), Environmental controls on the boron and strontium isotopic composition of aragonite shell material of cultured Arctica islandica, *Biogeosciences*, *12*(11), 3351-3368.

Manuscript III is in prepared and will be submit to Proceedings of the National Academy of Sciences: Liu, Y.-W., Eagle, R., Aciego, S. M., Ries, J. B., Gilmore, R., and Doss, W., Geochemical constraints on the vesicle pH of the coccolithophore *Pleurochrysis carterae* and its response to CO_2-induced ocean acidification (in prep).

I.6   References

Abbasi, T., and S. Abbasi (2011), Ocean acidification: The newest threat to the global environment, *Critical Reviews in Environmental Science and Technology*, *41*(18), 1601-1663.

Anagnostou, E., K. F. Huang, C. F. You, E. L. Sikes, and R. M. Sherrel (2012), Evaluation of boron isotope ratio as a pH proxy in the deep sea coral Desmophyllum dianthus: Evidence of physiological pH adjustment, *Earth Planet. Sci. Lett.*, *349*, 251-260.

Berglund, M., and M. E. Wieser (2011), Isotopic compositions of the elements 2009 (IUPAC Technical Report), *Pure Application of Chemistry*, *83*(2), 397-410.

Bignami, S., I. C. Enochs, D. P. Manzello, S. Sponaugle, and R. K. Cowen (2013), Ocean acidification alters the otoliths of a pantropical fish species with implications for sensory function, *Proceedings of the National Academy of Sciences*, *110*(18), 7366-7370.

Boyer, T. P., et al. (2013), World Ocean Database 2013*Rep.*, Sydney Levitus, Ed., Alexey Mishonov, Technical Ed., NOAA Atlas NESDIS 72, 209 pp., Washington, D.C.

Brown, R. E., L. D. Anderson, E. Thomas, and J. C. Zachos (2011), A core-top calibration of B/Ca in the benthic foraminifers *Nuttallides umbonifera* and *Oridorsalis umbonatus*: A proxy for Cenozoic bottom water carbonate saturation, *Earth Planet. Sci. Lett.*, *310*(3), 360-368.

Byrne, R. H., S. Mecking, R. A. Feely, and X. Liu (2010), Direct observations of basin-wide acidification of the North Pacific Ocean, *Geophys. Res. Lett.*, *37*(2).

Casareto, B. E., M. P. Niraula, H. Fujimura, and Y. Suzuki (2009), Effects of carbon dioxide on the coccolithophorid Pleurochrysis carterae in incubation experiments, *Aquatic Biology*, *7*(1-2), 59-70.

D'Olivo, J. P., M. T. McCulloch, S. M. Eggins, and J. Trotter (2014), Coral records of reef-water pH across the central Great Barrier Reef, Australia: assessing the influence of river runoff on inshore reefs, *Biogeosciences Discuss.*, *11*(7), 11443-11479.

Dahlgren, T. G., J. R. Weinberg, and K. M. Halanych (2000), Phylogeography of the ocean quahog (*Arctica islandica*): influences of paleoclimate on genetic diversity and species range, *Marine Biology*, *137*(3), 487-495.

Delille, B., et al. (2005), Response of primary production and calcification to changes of pCO_2 during experimental blooms of the coccolithophorid *Emiliania huxleyi*, *Global Biogeochem. Cycles*, *19*(2), GB2023.

Dickson, A. G. (1993), The measurement of sea water pH, *Mar. Chem.*, *44*(2), 131-142.

DOE (1994), *Handbook of methods for the analysis of the various parameters of the carbon dioxide system in sea water*, Carbon Dioxide Information and Analysis Center, Oak Ridge.

Doney, S. C., V. J. Fabry, R. A. Feely, and J. A. Kleypas (2009), Ocean Acidification: The Other CO_2 Problem, *Annual Review of Marine Science*, *1*(1), 169-192.

Douville, E., M. Paterne, G. Cabioch, P. Louvat, J. Gaillardet, A. Juillet-Leclerc, and L. Ayliffe (2010), Abrupt sea surface pH change at the end of the Younger Dryas in the central sub-equatorial Pacific inferred from boron isotope abundance in corals (*Porites*), *Biogeosciences*, *7*(8), 2445-2459.

Farmer, J. R., B. Hönisch, L. F. Robinson, and T. M. Hill (2015), Effects of seawater-pH and biomineralization on the boron isotopic composition of deep-sea bamboo corals, *Geochim. Cosmochim. Acta*, *155*, 86-106.

Feely, R. A., C. L. Sabine, K. Lee, W. Berelson, J. Kleypas, V. J. Fabry, and F. J. Millero (2004), Impact of Anthropogenic CO_2 on the $CaCO_3$ System in the Oceans, *Science*, *305*(5682), 362-366.

Feely, R. A., C. L. Sabine, J. M. Hernandez-Ayon, D. Ianson, and B. Hales (2008), Evidence for upwelling of corrosive" acidified" water onto the continental shelf, *Science*, *320*(5882), 1490-1492.

Findlay, H. S., M. A. Kendall, J. I. Spicer, and S. Widdicombe (2010), Relative influences of ocean acidification and temperature on intertidal barnacle post-larvae at the northern edge of their geographic distribution, *Estuarine, Coastal and Shelf Science*, *86*(4), 675-682.

Foster, G. L. (2008), Seawater pH, pCO_2 and $[CO_3^{2-}]$ variations in the Caribbean Sea over the last 130 kyr: A boron isotope and B/Ca study of planktic foraminifera, *Earth Planet. Sci. Lett.*, *271*(1-4), 254-266.

Foster, G. L., P. A. E. Pogge von Strandmann, and J. W. B. Rae (2010), Boron and magnesium isotopic composition of seawater, *Geochemistry, Geophysics, Geosystems*, *11*(8), Q08015.

Foster, G. L., and P. F. Sexton (2014), Enhanced carbon dioxide outgassing from the eastern equatorial Atlantic during the last glacial, *Geology*, *42*(11), 1003-1006.

Foster, L. C., A. A. Finch, N. Allison, C. Andersson, and L. J. Clarke (2008), Mg in aragonitic bivalve shells: Seasonal variations and mode of incorporation in *Arctica islandica*, *Chem. Geol.*, *254*(1), 113-119.

Frank, N., et al. (2011), Northeastern Atlantic cold-water coral reefs and climate, *Geology*, *39*(8), 743-746.

Hemming, N. G., and G. N. Hanson (1992), Boron isotopic composition and concentration in modern marine carbonates, *Geochim. Cosmochim. Acta*, *56*(1), 537-543.

Henehan, M. J., et al. (2013), Calibration of the boron isotope proxy in the planktonic foraminifera Globigerinoides ruber for use in palaeo-CO_2 reconstruction, *Earth Planet. Sci. Lett.*, *364*, 111-122.

Hofmann, G. E., J. P. Barry, P. J. Edmunds, R. D. Gates, D. A. Hutchins, T. Klinger, and M. A. Sewell (2010), The Effect of Ocean Acidification on Calcifying Organisms in Marine Ecosystems: An Organism-to-Ecosystem Perspective, *Annual Review of Ecology, Evolution, and Systematics*, *41*(1), 127-147.

Hönisch, B., N. G. Hemming, A. G. Grottoli, A. Amat, G. N. Hanson, and J. Bijma (2004), Assessing scleractinian corals as recorders for paleo-pH: Empirical calibration and vital effects, *Geochim. Cosmochim. Acta*, *68*(18), 3675-3685.

Hönisch, B., and N. G. Hemming (2005), Surface ocean pH response to variations in pCO_2 through two full glacial cycles, *Earth Planet. Sci. Lett.*, *236*(1-2), 305-314.

Hönisch, B., A. Ridgwell, D. N. Schmidt, E. Thomas, S. J. Gibbs, A. Sluijs, R. Zeebe, L. Kump, R. C. Martindale, and S. E. Greene (2012), The geological record of ocean acidification, *Science*, *335*(6072), 1058-1063.

Iglesias-Rodriguez, M. D., et al. (2008), Phytoplankton Calcification in a High-CO_2 World, *Science*, *320*(5874), 336-340.

IPCC (2013), Climate Change 2013: The Physical Science Basis. Working Group I Contribution to the IPCC 5th Assessment Report - Changes to the Underlying Scientific/Technical Assessment*Rep.*, Cambridge, United Kingdom and New York, NY, USA.

Kakihana, H., M. Kotaka, S. Satoh, M. Nomura, and M. Okamoto (1977), Fundamental studies on the ion-exchange separation of boron isotopes, *Bull. Chem. Soc. Jpn.*, *50*, 158-163.

Kleypas, J. A., R. W. Buddemeier, D. Archer, J.-P. Gattuso, C. Langdon, and B. N. Opdyke (1999), Geochemical Consequences of Increased Atmospheric Carbon Dioxide on Coral Reefs, *Science*, *284*(5411), 118-120.

Klochko, K., A. J. Kaufman, W. Yao, R. H. Byrne, and J. A. Tossell (2006), Experimental measurement of boron isotope fractionation in seawater, *Earth Planet. Sci. Lett.*, *248*(1-2), 276-285.

Krief, S., E. J. Hendy, M. Fine, R. Yam, A. Meibom, G. L. Foster, and A. Shemesh (2010), Physiological and isotopic responses of scleractinian corals to ocean acidification, *Geochim. Cosmochim. Acta*, *74*(17), 4988-5001.

Lemarchand, D., J. Gaillardet, E. Lewin, and C. J. Allegre (2000), The influence of rivers on marine boron isotopes and implications for reconstructing past ocean pH, *Nature*, *408*(6815), 951-954.

Lindberg, B., C. Berndt, and J. Mienert (2007), The Fugløy Reef at 70°N; acoustic signature, geologic, geomorphologic and oceanographic setting, *International Journal of Earth Sciences*, *96*(1), 201-213.

Liu, Y., W. Liu, Z. Peng, Y. Xiao, G. Wei, W. Sun, J. He, G. Liu, and C.-L. Chou (2009), Instability of seawater pH in the South China Sea during the mid-late Holocene: Evidence from boron isotopic composition of corals, *Geochim. Cosmochim. Acta*, *73*(5), 1264-1272.

Martinez-Boti, M. A., G. L. Foster, T. B. Chalk, E. J. Rohling, P. F. Sexton, D. J. Lunt, R. D. Pancost, M. P. S. Badger, and D. N. Schmidt (2015a), Plio-Pleistocene climate sensitivity evaluated using high-resolution CO_2 records, *Nature*, *518*(7537), 49-54.

Martinez-Boti, M. A., G. Marino, G. L. Foster, P. Ziveri, M. J. Henehan, J. W. B. Rae, P. G. Mortyn, and D. Vance (2015b), Boron isotope evidence for oceanic carbon dioxide leakage during the last deglaciation, *Nature*, *518*(7538), 219-222.

Orr, J. C., et al. (2005), Anthropogenic ocean acidification over the twenty-first century and its impact on calcifying organisms, *Nature*, *437*(7059), 681-686.

Pagani, M., D. Lemarchand, A. Spivack, and J. Gaillardet (2005), A critical evaluation of the boron isotope-pH proxy: The accuracy of ancient ocean pH estimates, *Geochim. Cosmochim. Acta*, *69*(4), 953-961.

Pelejero, C., E. Calvo, M. T. McCulloch, J. F. Marshall, M. K. Gagan, J. M. Lough, and B. N. Opdyke (2005), Preindustrial to Modern Interdecadal Variability in Coral Reef pH, *Science*, *309*(5744), 2204-2207.

Penman, D. E., B. Hönisch, E. T. Rasbury, N. G. Hemming, and H. J. Spero (2012), Boron, carbon, and oxygen isotopic composition of brachiopod shells: Intra-shell variability, controls, and potential as a paleo-pH recorder, *Chem. Geol.*

Rae, J. W. B., G. L. Foster, D. N. Schmidt, and T. Elliott (2011), Boron isotopes and B/Ca in benthic foraminifera: Proxies for the deep ocean carbonate system, *Earth Planet. Sci. Lett.*, *302*(3-4), 403-413.

Reynaud, S., N. G. Hemming, A. Juillet-Leclerc, and J.-P. Gattuso (2004), Effect of pCO_2 and temperature on the boron isotopic composition of the zooxanthellate coral *Acropora* sp., *Coral Reefs*, *23*(4), 539-546.

Reynaud, S., C. Rollion-Bard, S. Martin, R. Rolopho-Metalpa, and J.-P. Gattuso (2008), Effect of elevated pCO_2 on the boron isotopic composition into the Mediterranean scleractinian coral *Cladocora caespitosa*, in *Impacts of Acidification on Biological,*

Chemical, and Physical Systems in the Mediterranean and Black Seas, No 36 in CIESM Workshop Monographs, edited by F. Briand, pp. 71-75, Monaco.

Rickaby, R. E. M., J. Henderiks, and J. N. Young (2010), Perturbing phytoplankton: response and isotopic fractionation with changing carbonate chemistry in two coccolithophore species, *Clim. Past*, *6*(6), 771-785.

Riebesell, U., I. Zondervan, B. Rost, P. D. Tortell, R. E. Zeebe, and F. M. M. Morel (2000), Reduced calcification of marine plankton in response to increased atmospheric CO_2, *Nature*, *407*(6802), 364-367.

Ries, J. B., A. L. Cohen, and D. C. McCorkle (2009), Marine calcifiers exhibit mixed responses to CO_2-induced ocean acidification, *Geology*, *37*(12), 1131-1134.

Ries, J. B. (2011), A physicochemical framework for interpreting the biological calcification response to CO_2-induced ocean acidification, *Geochim. Cosmochim. Acta*, *75*(14), 4053-4064.

Sabine, C. L., R. A. Feely, N. Gruber, R. M. Key, K. Lee, J. L. Bullister, R. Wanninkhof, C. Wong, D. W. Wallace, and B. Tilbrook (2004), The oceanic sink for anthropogenic CO_2, *Science*, *305*(5682), 367-371.

Sanyal, A., N. G. Hemming, G. N. Hanson, and W. S. Broecker (1995), Evidence for a higher pH in the glacial ocean from boron isotopes in foraminifera, *Nature*, *373*(6511), 234-236.

Schmidt, M. W., H. J. Spero, and D. W. Lea (2004), Links between salinity variation in the Caribbean and North Atlantic thermohaline circulation, *Nature*, *428*(6979), 160-163.

Sorensen, S. P. L., and S. Palitzsch (1910), On measuring hydrogen ion concentration of sea water, *BIOCHEMISCHE ZEITSCHRIFT*, *24*, 387-415.

Trotter, J., P. Montagna, M. McCulloch, S. Silenzi, S. Reynaud, G. Mortimer, S. Martin, C. Ferrier-Pagès, J.-P. Gattuso, and R. Rodolfo-Metalpa (2011), Quantifying the pH 'vital effect' in the temperate zooxanthellate coral *Cladocora caespitosa*: Validation of the boron seawater pH proxy, *Earth Planet. Sci. Lett.*, *303*(3-4), 163-173.

Vázquez-Rodrıguez, M., F. Pérez, A. Velo, A. Ríos, and H. Mercier (2012), Observed acidification trends in North Atlantic water masses, *Biogeosciences*, *9*, 5217-5230.

Wei, G., M. T. McCulloch, G. Mortimer, W. Deng, and L. Xie (2009), Evidence for ocean acidification in the Great Barrier Reef of Australia, *Geochim. Cosmochim. Acta*, *73*(8), 2332-2346.

Wells, S. M. (1988), *Coral Reefs of the World*, UCN Conservation Monitoring Center and United Nations Environment Programme (UNEP), Gland Switzerland and Cambridge, U.K.

Yu, J., and H. Elderfield (2007), Benthic foraminiferal B/Ca ratios reflect deep water carbonate saturation state, *Earth Planet. Sci. Lett.*, *258*(1-2), 73-86.

Yu, J., H. Elderfield, and B. Hönisch (2007), B/Ca in planktonic foraminifera as a proxy for surface seawater pH, *Paleoceanography*, *22*, 17 PP.

Yu, J., H. Elderfield, and A. M. Piotrowski (2008), Seawater carbonate ion-δ^{13}C systematics and application to glacial–interglacial North Atlantic ocean circulation, *Earth Planet. Sci. Lett.*, *271*(1–4), 209-220.

Yu, J., D. J. R. Thornalley, J. W. B. Rae, and N. I. McCave (2013), Calibration and application of B/Ca, Cd/Ca, and δ^{11}B in *Neogloboquadrina pachyderma* (sinistral) to constrain CO_2 uptake in the subpolar North Atlantic during the last deglaciation, *Paleoceanography*, *28*(2), 237-252.

Chapter II   A high throughput system for boron microsublimation and isotope analysis by Total Evaporation Thermal Ionization Mass Spectrometry (TE-TIMS)

Yi-Wei Liu[1], Sarah M. Aciego[1], Alan D. Wanamaker Jr.[2], Bryan K. Sell[1]

[1.] Earth and Environmental Sciences, University of Michigan, 1100 N. University Avenue, Ann Arbor, MI 48109, USA

[2.] Department of Geological and Atmospheric Sciences, Iowa State University, Ames, Iowa, 50011, USA

II.1   Abstract

Rationale: Research on the ocean carbon cycle is vitally important due to the projected impacts of atmospheric CO_2 on global temperatures and climate change, but also on ocean chemistry. The direct influence of this CO_2 rise on the seawater pH can be evaluated from the boron isotopic composition in biogenic carbonates; however, conscientious laboratory techniques and data treatment are vital in obtaining accurate and precise results. A rapid-throughput boron purification and Total Evaporation Thermal Ionization Mass Spectrometry method was developed for high accuracy and precision boron isotopic analysis for small (ng) sample sizes.

Methods: An improved microsublimation method, in which up to 20 samples can be processed simultaneously under identical temperature conditions, was developed. Several tests have confirmed the viability of this technique. First, seawater and *Porites* coral samples were processed with H_2O_2 and the results compared with those obtained using microsublimation; second, the impact of various sublimation times was evaluated; and third, quantitative recovery was assessed using standard addition method.

Results: Microsublimation provides a valid method for the quantitative recovery and separation of boron from both major elements and organic matter under low-blank conditions. The close agreement of our results with published values validates the accuracy of the measurements. The isotopic ratio for SRM 951a boric acid isotopic standard was 4.0328±0.0054 (2 σ, n = 25). The reproducibility of boron isotopic composition for standards including AE121, IAEA B-1 and an in-house coral standard UM-CP1 were ± 0.68‰ (2 σ, n = 15), ± 1.12 ‰ (2 σ, n = 24), and ± 1.17 ‰ (2 σ, n = 14), respectively. The sample sizes were <1 ng for each measurement.

Conclusions: The developed method for preparing and measuring boron isotopic values in a variety of carbonate materials should facilitate the reconstruction of past ocean pH conditions with decadal-scale resolution.

II.2 Introduction

Boron has two naturally occurring stable isotopes, ^{10}B (19.9(7) %) and ^{11}B (80.1(7) %) (Berglund and Wieser, 2011). The distribution of these two isotopes ($\delta^{11}B$, defined as $\delta^{11}B = \left[\frac{\left(^{11}B/^{10}B\right)_{sample}}{\left(^{11}B/^{10}B\right)_{SRM\,951a}} - 1 \right] \times 1000$ (‰)) in various geological samples can be use to explore natural processes such as the extent of water-rock/soil interactions or weathering processes (Chetelat *et al.*, 2009b; Lemarchand and Gaillardet, 2006; Liu *et al.*, 2012), airborne anthropogenic emissions (Chetelat *et al.*, 2009a), clay mineral formation in soils at the soil-water-plant scale (Schmitt *et al.*, 2012), fluid transfer across tectonic subduction zones (Scambelluri and Tonarini, 2012), and seawater pH variations (Douville *et al.*, 2010; Foster, 2008; Hemming and Hanson, 1992; Hönisch and Hemming, 2005; Pelejero *et al.*, 2005).

One of the most widely applied applications of boron isotopes in climate and aqueous chemistry is in determining the historical record of pH in seawater. Because direct measurements of seawater pH prior to 1980 are sparse, the actual influence of the anthropogenic rise in atmospheric CO_2 on the pH of seawater is still largely undetermined. Reliable proxies of seawater pH during the Industrial Revolution and from recent millennia and into deep geologic time are few, but the $\delta^{11}B$ values derived from biogenic carbonates (e.g., corals, brachiopods, and foraminifera) have provided important constraints on ancient pH levels (Douville *et al.*, 2010; Pelejero *et al.*, 2005; Sanyal *et al.*, 1995).

The dominant aqueous species of boron in seawater are $B(OH)_3$ and $B(OH)_4^-$. The relative proportion of these two species in seawater is a function of pH and can be described as:

$$B(OH)_3 + H_2O \rightleftharpoons B(OH)_4^- + H^+ \qquad\qquad \text{(Eq. II.1)}$$

At low pH, boron exists as $B(OH)_3$ in solution, and, conversely, at high pH, it exists as $B(OH)_4^-$ (Hemming and Hanson, 1994). The governing reaction for isotope exchange between these two species is:

$$^{10}B(OH)_3 + {}^{11}B(OH)_4^- \rightleftharpoons {}^{11}B(OH)_3 + {}^{10}B(OH)_4^- \qquad\qquad \text{(Eq. II.2)}$$
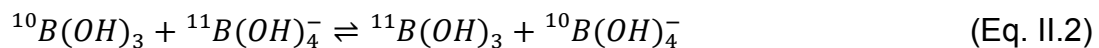
The stable isotope ^{11}B is enriched in $B(OH)_3$ compared with $B(OH)_4^-$, and the combination of equations (Eq. II.1) and (Eq. II.2) can be used to determine the distribution of the two boron species and the isotopic composition of each for a given pH. The boron isotopic composition in the ocean is relatively constant over this time period because the residence time of seawater boron is about 14 million years (Lemarchand *et al.*, 2000), and has an average seawater $\delta^{11}B$ value of 39.61 ‰ (Foster *et al.*, 2010). At low pH, $B(OH)_3$ is dominant and therefore the $\delta^{11}B$ value of $B(OH)_3$ is equal to the isotopic composition of the total dissolved boron in seawater (39.61‰). In contrast, the isotopic composition of $B(OH)_4^-$ is dominant in seawater and equal to the isotopic composition of the total dissolved boron at high pH. In addition, the $\delta^{11}B$ value

of B(OH)$_3$ is about 20 ‰ higher than that of B(OH)$_4^-$ at any pH at equilibrium, based on a constant fractionation factor (α). This boric acid-borate fractionation number was defined as $\alpha \equiv \frac{(^{11}B/^{10}B)_{Boric\ acid}}{(^{11}B/^{10}B)_{Borate}}$, and two empirical and analytical values have been suggested in seawater: (1) α = 1.0194, a theoretical result of Kakihana *et al.* (1977) that has been applied widely in paleo-reconstructions (Hönisch *et al.*, 2004; Kakihana *et al.*, 1977; Sanyal *et al.*, 1995), and (2) α = 1.0272, which was empirically obtained from Klochko *et al.* (2006) and is considered to better describe the present distribution of the two boron species in nature (Foster, 2008; Klochko *et al.*, 2006; Pagani *et al.*, 2005). During crystal growth, marine carbonates will primarily incorporate B(OH)$_4^-$ into the carbonate structure so that biogenic carbonates such as coral and foraminifera have δ^{11}B values that will coevolve with ambient seawater pH and therefore can be used to reconstruct ancient seawater pH values (Hemming and Hanson, 1992; Hönisch *et al.*, 2009; Pearson and Palmer, 1999; Pelejero *et al.*, 2005). However, due to biological adjustments to the environment, species-specific fractionation factors and transfer functions may be more appropriate than the α values described above (Anagnostou *et al.*, 2012; Hönisch *et al.*, 2004; Krief *et al.*, 2010; Rae *et al.*, 2011; Reynaud *et al.*, 2004; Reynaud *et al.*, 2008; Trotter *et al.*, 2011).

A precise and accurate measuring technique is critical because modern ocean pH changes of between 0.1 to 0.5 pH units can occur (Pelejero *et al.*, 2010), which translate into changes of δ^{11}B values of 1 to 4 ‰. Most aragonite skeletal structures have relatively low boron concentrations (Hemming and Hanson, 1992); hence an ideal analytical technique would allow small sample sizes (several ng or less) to be processed in order to produce highly resolved (annual to decadal) estimates of pH.

Four different methods have been employed to measure boron isotopes: (1) Secondary Ion Mass Spectrometry (SIMS) (Allison and Finch, 2010; Kasemann *et al.*, 2009); (2) Positive Ion Thermal Ionization Mass Spectrometry (PTIMS) (Lemarchand *et al.*, 2002; Liu *et al.*, 2009; Wei *et al.*, 2009); (3) Negative Ion Thermal Ionic Mass Spectrometry (NTIMS) (Barth, 1997; Foster *et al.*, 2006; Hemming and Hanson, 1992; 1994); and (4) Multi-collector Inductively Coupled Plasma Mass Spectrometry (MC-ICPMS) (Foster,

2008; Ni *et al.*, 2010). SIMS is an *in situ* approach that is appropriate for small sample sizes and it appears to be the most promising technique for high-resolution temporal records of pH. However, seasonal or annual variation of pCO_2 in seawater will induce changes in seawater pH of 0.2 to 0.4 units or 1.5 to 3.5 ‰ in the $\delta^{11}B$ values of carbonates (Pelejero *et al.*, 2005). Because the typical internal precision of SIMS is 1.2 ‰ (Allison and Finch, 2010), this *in situ* analytical method may be more appropriate for longer time scale paleoclimate studies or time frames with large pH variations.

PTIMS ionizes the boron as Cs_2BO_2 that is formed by mixing a Cs-bearing solution with the samples in the preparation procedure, resulting in a stable beam for measurement with low boron isotope fractionation. The combination of stable beam and low fractionation results in an analytical precision of the order of ± 0.2 ‰ (Lemarchand *et al.*, 2002). The PTIMS method requires > 250 ng of boron, purified to remove both alkali ions and organic material. Despite the large sample requirements, PTIMS has been used for coral studies (Liu *et al.*, 2009; Wei *et al.*, 2009); however, negative polarity thermal ionization is required for smaller samples. NTIMS ionizes boron as the negative ion BO_2^-, and the presence of natural matrix salts (e.g., seawater and carbonate) can increase the ionization efficiency to up to two orders of magnitude higher than that of PTIMS (Barth, 1997; Foster *et al.*, 2006; Hemming and Hanson, 1992; 1994). The higher ionization efficiency reduces the amount of sample required (~1 ng), but, because instrumental mass fractionation occurs between the dominant $^{11}BO_2^-$ and $^{10}BO_2^-$ species, triplicate or more analyses are required for accurate, precise results (Hönisch *et al.*, 2004). Therefore, the standard NTIMS approach requires 3 to 6 ng per sample. Foster *et al.* (2006) reported an improved method for small samples (<1 ng), Total Evaporation NTIMS (TE-NTIMS), which minimizes the instrumental mass fractionation and maximizes the sample signal by analyzing samples from beginning to exhaustion. Both NTIMS methods result in typical errors of < 0.5 ‰ (Foster *et al.*, 2006; Hönisch *et al.*, 2004; Pelejero *et al.*, 2005).

Recently, boron isotopic ratios have also been measured by MC-ICPMS with precision comparable with that of PTIMS on sample sizes of 15 to 30 ng (Foster, 2008; Ni *et al.*,

2010). One of the drawbacks to the MC-ICPMS method has been the long wash out time between samples required to eliminate residual boron in the sample introduction system (i.e. memory). In order to eliminate this memory effect these latest studies applied two methods: injection of ammonia gas (Al-Ammar *et al.*, 2000) and high efficiency nebulization (d-DIHEN) (Louvat *et al.*, 2010). In either case, the sample size requirements are still too large to precisely or accurately (because of blank issues) measure samples < 5 ng in size. Ni *et al.* (2010) explored a side-by-side comparison of MC-ICPMS and NTIMS techniques and determined that organic materials probably bias the boron isotopic results in NTIMS, which may explain the deviations in results between laboratories. Because boron isotope analysis by MC-ICPMS requires boron purification, and the organic materials may result in inaccurate boron measurements in TIMS, chemical treatments are required for both NTIMS and MC-ICPMS analysis.

Many methods have been reported for the purification of boron from aqueous samples, including solvent extraction, chelation, chromatographic separation, conversion into gaseous methyl borate or boron fluoride, and ion exchange/B-specific resin (Sah and Brown, 1997). The conventional method for purifying boron from alkaline matrix ions and organic materials is ion-exchange column chemistry. B-specific resin, Amberlite IRA-743, is widely used to separate boron from matrix materials (Foster, 2008; Lemarchand *et al.*, 2002; Ni *et al.*, 2010). However, the blank increases as a result of the reagents used during the column procedure and isotopic fractionation may occur in the ion-exchange process (Foster *et al.*, 2006; Hemming and Hanson, 1994). An alternative way to purify boron is the microsublimation technique, developed by Gaillardet *et al.* (2001), which separates boron without any isotope fractionation. Wang *et al.* (2010) modified the method and showed that, with small modifications to the sublimation processing, no reagents or ion-exchange resins are required in the process. Thus, microsublimation is a promising method for purification of boron (blank sensitive) samples that are extremely small (of the order of several ng).

Here we report a new approach that applies microsublimation and TE-NTIMS measurement to achieve highly precise and accurate boron isotopic analysis for small samples (boron < 1 ng). We have developed a microsublimation method modified from

those of Gaillardet *et al.* (2001) and Wang *et al.* (2010) in order to process more samples (up to 20 per hotplate) with excellent reproducibility.

II.3   Experimental Procedures

II.3.1   Laboratory conditions, reagents, and labware

All chemical separation and sample handling were performed under ISO 4 (class 10) laminar flow hoods within an ISO 7 (class 10,000) clean room of the Glaciochemistry and Isotope Geochemistry Laboratory in the Department of Earth & Environmental Sciences at the University of Michigan (Ann Arbor, MI, USA). The air supply to the clean room is purified by boron-free ultra-low-penetration air (ULPA) filters with polytetrafluoroethylene (PTFE) backing in both the clean and the machine rooms. Ultra-pure reagents were used throughout the chemistry steps: reagents (HCl, HNO_3, HF, and H_2O_2) were either Fischer Scientific Optima (Thermo Fisher Scientific, Hudson, NH, USA) or distilled in Savillex (Eden Prairie, MN, USA) DST 1000 distillation units in order to maintain ultra-low blanks. Water was first purified using a Super-Q (SQ) Millipore system (EMD Millipore Corp., Billerica, MA, USA) at 18.2 MΩ and then distilled again before use. The reagent boron blanks were all less than 1 ppb, which was measured on a Varian (Palo Alto, CA, USA) 820 MS plasma-source quadrupole mass spectrometer housed in the Element Measurement Facility at the State University of New York, Oswego (Oswego, NY, USA). With a maximum of 50 µl reagent used for each sample and 1 µl of sample loaded onto a filament, the blank introduced was lower than 1 pg for each measurement and was thus negligible.

Savillex perfluoroalkoxy (PFA) labware was cleaned in a three-step cleaning procedure: (1) submerged overnight in 7 N distilled HNO_3, (2) submerged overnight in 6 N distilled HCl, and (3) filled with distilled concentrated HNO_3 for three days; all steps performed at 90 °C. Between steps the labware beakers were triple rinsed with SQ water. After cleaning, labware was dried in a boron-free filtered air drying cabinet (ProPlastic Technology, Chandler, AZ, USA).

II.3.2 Standards and Samples

A range of elemental standard solutions was used to evaluate the success of the sublimation and mass spectrometric techniques. Solution standards included certified boric acid standards NIST SRM 951a (NIST, Gaithersburg, MD, USA) (a replacement of NIST SRM 951), AE-121 (BAM, Berlin, Germany) and a west Mediterranean seawater standard, IAEA B-1 (IAEA, Vienna, Austria). In order to assess the long-term analytical precision, we processed a large *Porites* coral sample to be used as an in-house working standard for marine aragonite carbonate (UM-CP1). The coral was live-collected off the coast at Rodriguez Key, Florida, USA in 1990. The coral was treated with sodium hypochlorite after collection and a pristine segment (approximately 2 grams) was powdered, rinsed three times with SQ water and dried at room temperature. For standard or seawater sample solutions, the samples were diluted to provide a concentration of 750 ppb boron in 1.7 N HCl. The carbonate powders were dissolved in 1.7 N HCl to a concentration of 750 ppb.

Finally, we assessed the reproducibility of this technique by measuring a series of natural seawater samples from a bivalve culture experiment in the Gulf of Maine, USA (Beirne *et al.*, 2012). Natural seawater – seasonally varying in salinity, pH and temperature – was pumped into the Darling Marine Center (Walpole, Maine, USA) from an average depth of 10 m. Samples were directly collected from the experimental tanks approximately biweekly (January 2010 to August 2010) and then were filtered through a 0.45-μm filter (Cameo^{TM} 30GN Nylon prefilter; GE Osmonics Inc., Minnetonka, MN, USA) and refrigerated at ~4 °C.

Because the Darling Marine Center pumps water in from the Damariscotta River, a tidewater estuary slightly inland from the central coastal of the Gulf of Maine, an additional seawater sample that was removed from the influences of the estuary was collected for comparison. The Gulf of Maine surface seawater sample was collected at 44°26'9.829" N, 67°26.0'18.045" W off Jonesport, Maine, on November 23, 2009. In order to assess possible factors that might affect the boron isotopic composition, it is useful to track the boron isotopic ratio in different sources (freshwater versus full marine

conditions). The collection and measurement of boron isotopic composition in seawater from the culture tanks and the open ocean environment can be used to evaluate whether the culture experiments were representative of the natural marine environment.

II.3.3   Boron separation by microsublimation

II.3.3.1   Principles

The microsublimation technique for boron purification is based on the tendency of boron to sublimate at a temperature and pressure where alkaline matrices and organic matter remain in solution or solid form (Gaillardet *et al.*, 2001). The technique design utilized uses a 5-ml conic bottom Savillex PFA vial. The vial is set upside-down so that the cap can be heated, causing the boron to sublimate and then condense onto a cooler surface at the conical point in the bottom of the vial. In the experiments of Gaillardet *et al.* (2001), the flat bottom (the cap of the vial) was heated to 60 – 65 °C for 12 hours with aluminum foil wrapped on the lower part of the device. The drawback of this design lies in the difficulty of controlling and maintaining stable and consistent heating and cooling conditions, as non-reproducible heating and cooling conditions may result in variable sample recoveries. Furthermore, this sublimation process was conducted after conventional column chemistry techniques, which may cause isotopic fractionation. Wang *et al.* (2010) modified the above technique by performing a sublimation process, which included an additional fan for cooling but did not require prior resin use. Even with these modifications, inconsistent heating conditions may still occur between different vials, especially at the conical top of the vials. Therefore, we designed and fabricated microsublimation block sets to ensure that all samples were exposed to the same thermal conditions during this process.

In this study, samples were dissolved and diluted to a concentration of about 750 ppb in 1.7 N HCl. About 20 µl was weighed and about 30 µl of standard SRM 951a was added, to evaluate the boron concentration using the standard addition technique. Another 50-µl sample solution droplet was loaded onto the cap of a 5-ml conic bottom PFA vial (Savillex). The vial was then closed firmly and placed conic-bottom-side up in our machined sublimation blocks and a cooling block placed on top (Figure II. 1). The

heating and cooling blocks are both coated in a proprietary thermoplastic material. The bottom heating blocks were machined to precisely fit the tops of the 5-ml conic beakers. Water from the in-house deionized chilled water system flows through the upper part of cooling coil block through machined channels connected by polyvinyl chloride (PVC) tubing so that the temperature can be maintained at about 23 °C. The cooling coil block rests on threaded chlorinated polyvinyl chloride (CPVC, a thermoplastic that has excellent corrosion resistance at high temperature), such that no vibration from water flow disturbs the drops. In addition to supporting the cooling block, the low thermal conductivity CPVC prevents heat transfer to the upper cooling block, is corrosion resistant, and can withstand temperatures up to 90 ºC. The coated stainless steel design of our heating blocks provides a uniform heating and cooling surfaces for the sublimation, which facilitates complete boron evaporation (Figure II. 1 (b)). In order to process large numbers of samples, we designed the heating and cooling blocks to process 10 separate samples at a time and up to 20 per hotplate.

Once sample vials had been loaded into the vials and placed on the microsublimation blocks, they were heated at 70 to 74 °C for 12 hours. The sublimate boron sample was then split in half and one part was used to test the yield using standard addition while the other half of the solution was used for isotopic analysis by TE-TIMS. To confirm the ability of our method to purify boron without organic interferences or isotopic fractionation, two additional steps were tested: H_2O_2 treatment and 20 hours sublimation time.
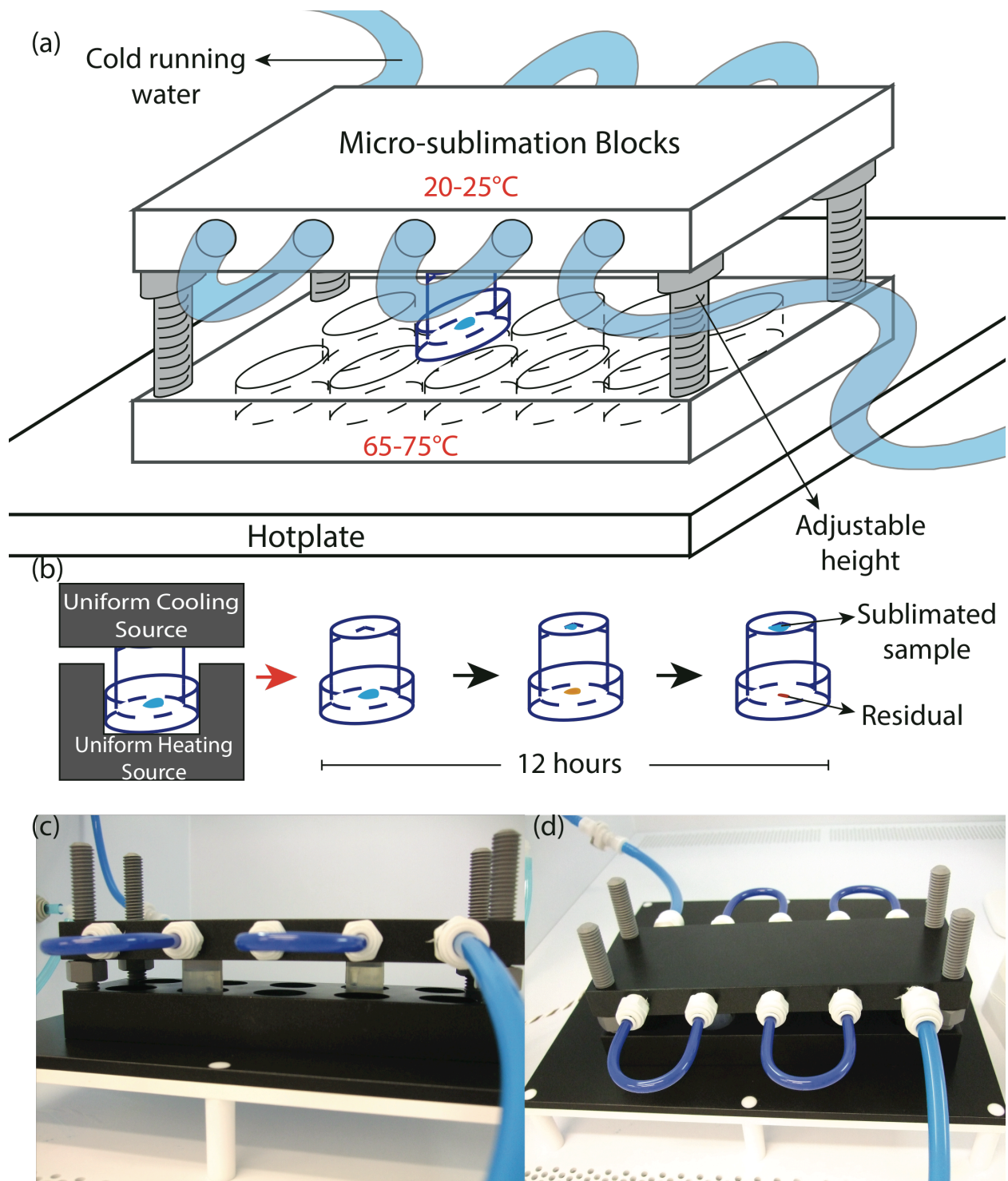
Figure II. 1 **Illustration of the microsublimation device used in this study.**
The cartoon (a) shows the generalized microsublimation design. The illustration (b) shows the uniform heating and cooling of the vial containing a sample. Samples are loaded onto the cap with 5-ml conic bottom vial in an upside-down position. After a 12-h sublimation, boron is separated and condensed at the tip of the vial. Photographs (c) and (d) are the sublimation block sets.

II.3.3.2 Assessment of organic removal: comparison with H_2O_2

In order to assess the performance of the microsublimation blocks in separating the organic matter from the boron sample solution, the in-house standard UM-CP1 and standard seawater IAEA B-1 were processed with and without hydrogen peroxide treatment prior to sublimation. For the hydrogen peroxide test, 30 % H_2O_2 and concentrated HCl were added to dissolve (carbonate) or dilute (seawater) samples to 750 ppb in 1.7 N HCl and 10 % H_2O_2 and the samples were then placed in an ultrasonic bath for two hours in closed vials. The samples then were uncapped and allowed to decompose and exsolve O_2 for one hour before being loaded onto the caps. Two sublimation periods, 12 and 20 hours, were also tested to assess quantitative sublimation of boron from an organic rich matrix (e.g., Wang *et al.* (2010)).

II.3.3.3 Quantitative recovery of boron

A standard addition method was used to quantify the recovery of the microsublimation method. SRM 951a was added to two sets of standards (UM-CP1 and IAEA B-1) before and after sublimation for each set. The samples were weighed before and after standard addition and microsublimation for concentration calculations. Sample concentrations before and after sublimation can therefore be calculated from the equations based on two end-member mixing model:

$$[B]_{before} = \frac{[B]_{SRM\ 951a} \times W_{SRM\ 951a} \times \left[(^{11}B/^{10}B)_{measured} - (^{11}B/^{10}B)_{SRM\ 951a} \right]}{W_{sample} \times \left[(^{11}B/^{10}B)_{sample} - (^{11}B/^{10}B)_{measured} \right]}$$

$$[B]_{after} = \frac{[B]_{SRM\ 951a} \times W_{SRM\ 951a} \times \left[(^{11}B/^{10}B)_{measured} - (^{11}B/^{10}B)_{SRM\ 951a} \right]}{50/45 \times W_{sample'} \times \left[(^{11}B/^{10}B)_{sample} - (^{11}B/^{10}B)_{measured} \right]}$$

$[B]_{before}$ is the boron concentration with standard added before sublimation, and $[B]_{after}$ is the boron concentration with standard added after sublimation. The boron concentration prepared for SRM 951a is 722 ppb in this study. $W_{SRM\ 951a}$, W_{sample} and $W_{sample'}$ are the weight of SRM 951a, the original sample solution and the sublimated sample solution, respectively. The $^{11}B/^{10}B$ ratios are boron isotopic ratios for SRM 951a, the target sample and the mixture solution measured in this study. The 50/45 factor in the

calculation for boron concentration after microsublimiation results from the removal of alkaline matrix and organic matter residual, which changed post-sublimation solution mass.

II.3.4   Mass spectrometry, measurement by TE-TIMS

All measurements were conducted on a TRITON Plus multicollector thermal ionization mass spectrometer (Thermo Electron Corp., San Jose, CA, USA) operating in negative mode at the Department of Earth and Environmental Sciences, University of Michigan. Daily gain calibrations were conducted to minimize instrumental uncertainty. A cold trap with liquid nitrogen was used to sustain the main high vacuum source pressure (HV source pressure) between 4×10^{-8} to 8×10^{-8} mbar, which improved the stability of the environment and reduced possible interferences from water vapor and CO_2 in the sample chamber. Venting of the mass spectrometer with ultra-high purity nitrogen gas and baking of the source between turret exchanges was also implemented to reduce interferences and pump down time.

Samples were loaded onto outgassed single Re filament at 0.8 A current. First 1 μl boron-free synthetic seawater matrix was loaded and dried to facilitate ionization efficiency. The synthetic seawater was made based on the method developed by Kester *et al.* (1967). A total evaporation method was employed in order to decrease the variability in isotopic measurements caused by different mass fractionation behavior of sample types and load sizes (Foster *et al.*, 2006). This technique also reduced the sample size, so that 1 μl of sample solution (< 1 ng boron) was loaded onto the filament following the matrix. The samples were dried down at 2 A current for 15 seconds and the filaments were flashed to a dull red color in the center of the filament (about 2.5 A). The loaded samples were then immediately placed into the source chamber, maintained at low humidity with ultra-pure nitrogen gas during sample turret changes.

The samples were preheated to 1200 mA at a rate of 100 mA/min while 600 cycles of (about 10 minutes) baseline were measured. The sample was then gradually heated to 1300 mA at a rate slower than 30 mA/min. The ^{35}Cl signal was detected when the filament reached ~800 ºC because of its lower ionization energy and was used for initial

source lenses tuning when the ^{35}Cl signal increased to about 100 mV. To assess the organic interference on mass 42 ($^{12}C^{14}N^{16}O$), mass 26 ($^{12}C^{14}N$) was also monitored with a secondary electron multiplier (SEM) in the beginning of the heating process because organic matter tends to ionize at a lower temperature than boron. The control masses were then switched to 42 ($^{10}B^{16}O^{16}O^-$) and 43 ($^{11}B^{16}O^{16}O^-$) after initial tuning of the source lenses. The sample was gradually heated (10 – 20 mA per heating cycle) and the source lenses were optimized between cycles. When the intensity of mass 43 reached 60 - 70 mV, peak centering was conducted for mass 42 and 43. The total evaporation data acquisition was started when the intensity of mass 42 reached 20 mV (~830 – 890 ℃) and the collection was terminated when the signal dropped to lower than the initial 20 mV intensity. Typical curves for SRM 951a measurement are illustrated in Figure II. 2. The detailed cup configuration and method settings are listed in Table II.1. The heating slope was 10 mA/cycle in our method, which we found allows us to achieve maximum intensity of the signal and maintain stability rather than exceed detection limits due to sudden sample exhaustion. To eliminate the interferences from different oxygen isotopic compositions when forming BO_2^-, mass 45 ($^{11}B^{16}O^{18}O^-$) was measured. The ratio of mass 45 to 43 was used to calculate the oxygen fractionation factor based on the exponential law for mass dependent fractionation, which follows the equations:

$\left(\frac{O_{18}}{O_{16}}\right)_m = \left(\frac{O_{18}}{O_{16}}\right)_n \times \left(\frac{17.9992}{15.9949}\right)^\beta$ and $\left(\frac{O_{17}}{O_{16}}\right)_m = \left(\frac{O_{17}}{O_{16}}\right)_n \times \left(\frac{16.9991}{15.9949}\right)^\beta$, where the subscription m and n represent the measured isotopic ratio and the ratio of isotope abundances in nature, respectively. The β value is the fractionation factor for the measurement. Therefore, by knowing the $\left(\frac{O_{18}}{O_{16}}\right)_m$ ratio (determined from the ratio of mass 45 to 43), we can obtain a filament-specific $^{17}O/^{16}O$ ratio and then subtract the number to correct 43/42 ($^{11}B/^{10}B$) ratios.

All the boron isotopic ratios were normalized to NIST SRM 951a standard using the δ notation as: $\delta^{11}B = \left[\frac{(^{11}B/^{10}B)_{sample}}{(^{11}B/^{10}B)_{SRM\ 951a}} - 1\right] \times 1000$ (‰).
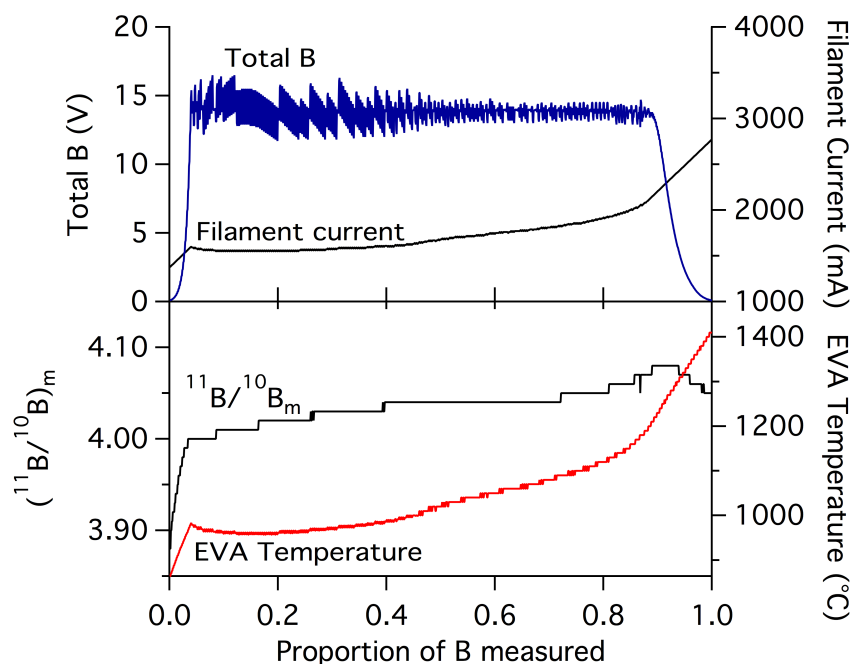
Figure II. 2   **Example ionization curves**
of the measured boron isotopic ratio, total boron intensity, filament current and filament temperature for SRM 951a by TE-NTIMS on the Thermo Scientific TRITON Plus at the Department of Earth and Environmental Sciences, University of Michigan.

Table II. 1   **Cup configurations and general settings**

Faraday Cup	Species	Other Settings
C	42	Maximum pilot signal: 14 V
H1	43	Heat Slope: 10 mA/cycle
H2	--	Intensity offset for stop: 0
H3	45	Integration time: 8.389 s

II.4   Results

All of the mean values from this study are consistent with the certified or other published values. Slightly higher averages were obtained than in published results using conventional NTIMS techniques.

The results for the boron isotope standards NIST SRM 951a, AE-121, IAEA B-1 and an in-house working standard UM-CP1 are shown in Figure II. 3 to Figure II. 5. The boron isotopic ratios for the inter-laboratory standards SRM 951a, AE-121 and IAEA B-1 reported in other studies are plotted in Figure II. 3 and Figure II. 4 for comparison (Foster *et al.*, 2006; Gonfiantini *et al.*, 2003; Hemming and Hanson, 1992; Kasemann *et*

al., 2001; Vengosh *et al.*, 1991; Vogl and Rosner, 2012). No organic signal was detected after sublimation. A total number of 25 SRM 951a samples were measured over 3 months, and the ratio of $^{11}B/^{10}B_{SRM\ 951a}$ was 4.0328 ± 0.0054 (1.35 ‰, 2 σ, n = 25). The mean $\delta^{11}B$ values of AE-121 and IAEA B-1 were 20.37 ± 0.68 ‰ (2 σ, n = 15) and 40.60 ± 1.12 ‰ (2 σ, n = 24), respectively. For the internal standard UM-CP1, the $\delta^{11}B$ value was 19.08 ± 1.17 ‰ (2 σ, n=14).

For the analysis of UM-CP1, the samples were cross-tested both with and without H_2O_2 treatment and sublimated for 12 or 20 hours. The same testing was also carried out for the IAEA B-1 seawater standard, as indicated in the last four data points in Figure II. 4 (b). These results agree well (with a similar reproducibility to the other boron isotopic standards shown above), regardless whether they were processed with H_2O_2 or had a longer sublimation time.

The calculated concentrations before and after microsublimation are 1154 ppb and 1106 ppb for UM-CP1 and 619 ppb and 633 ppb for IAEA B-1.

The $\delta^{11}B$ values of seawater from the culture experiment in the Gulf of Maine are shown in Figure II. 6. The mean $\delta^{11}B$ value was 39.31 ± 1.73 ‰ (2 σ, n = 36).
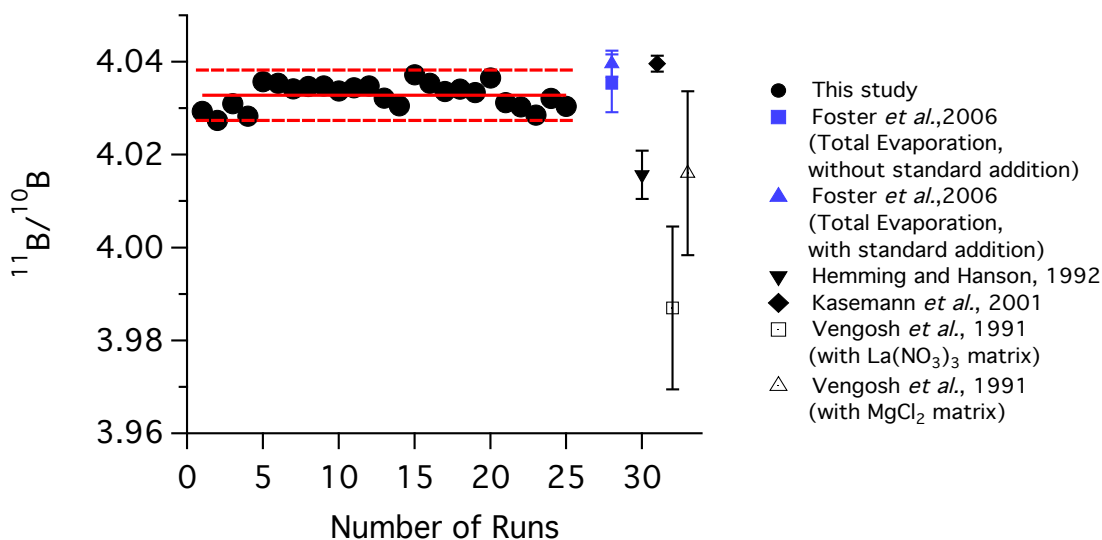
Figure II. 3 **The results of $^{11}B/^{10}B$ ratio of SRM 951a in this study.**
Data are shown with solid black circles. Solid red lines represent mean values for different data sets, with two standard deviations shown in dash red lines. Data analyzed by the NTIMS method from previous studies are listed for comparison.
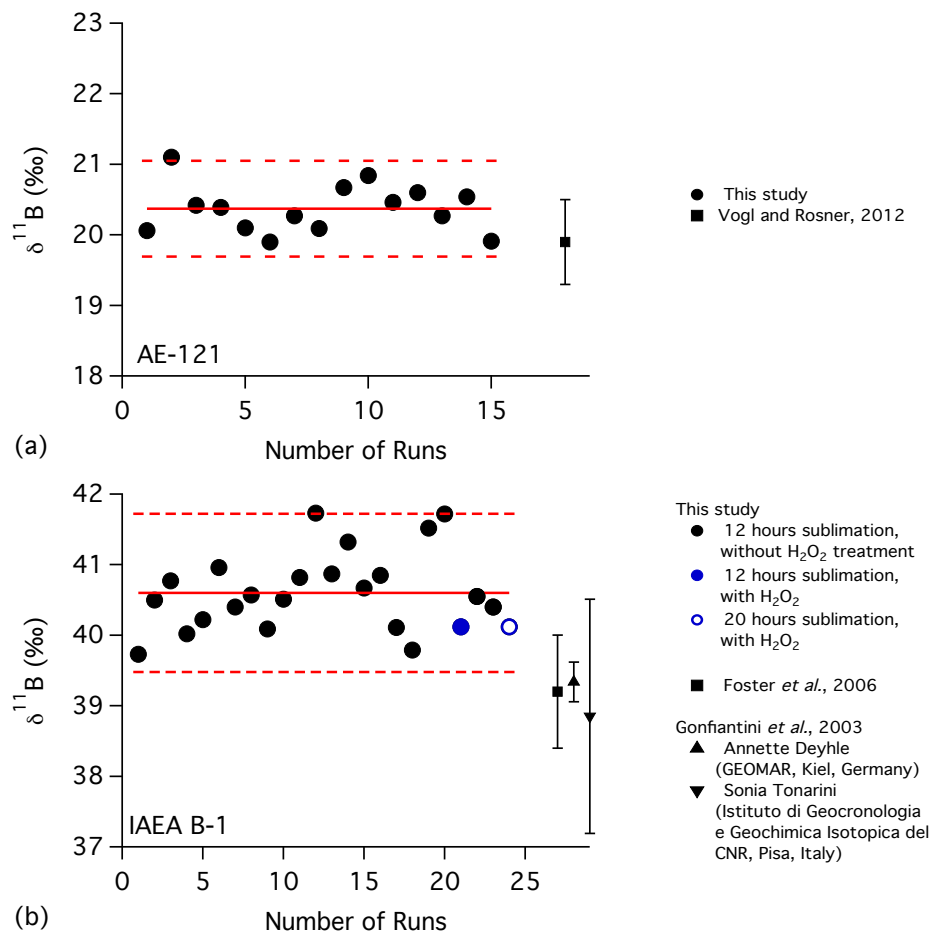
Figure II. 4   The δ^{11}B results for standards (a) AE-121 and (b) IAEA B-1.
Data analyzed by the NTIMS method from previously published literature are shown for comparison.
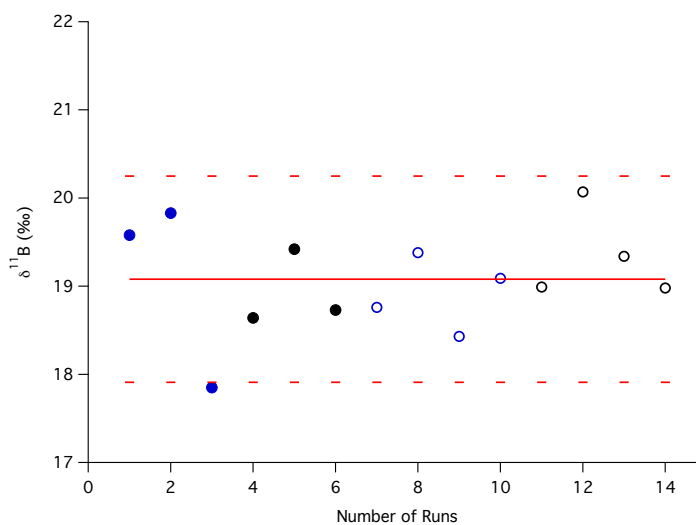
Figure II. 5   The δ^{11}B values of in-house aragonite carbonate standard UM-CP1.
Solid circles represent samples with 12-h sublimation time. Open circles represent sample with 20-h sublimation time.
Samples with H_2O_2 treatment are shown in blue.
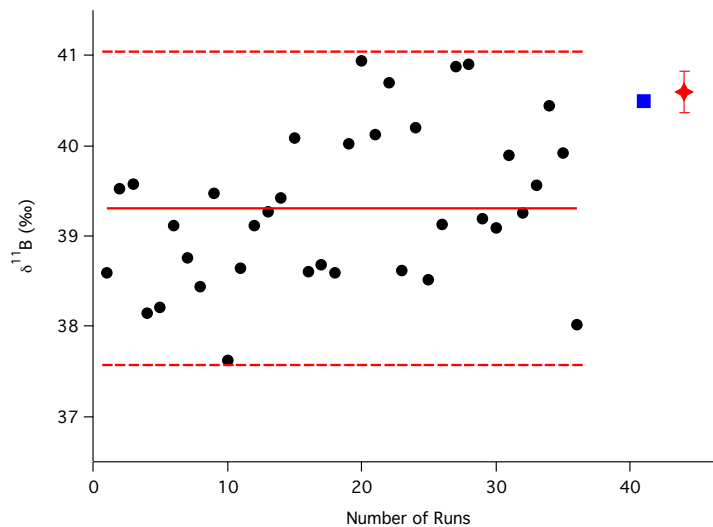
Figure II. 6　　　　**The δ^{11}B values of seawater (black circles) from the culture experiment from the Damariscotta River (Gulf of Maine).**
The δ^{11}B results from Jonesport (Gulf of Maine) seawater (blue square), and IAEA B-1, with 2 SE from Figure II. 4 (b) (red star) are plotted for comparison.

II.5　Discussion

II.5.1　Accuracy

Mass 26 was monitored at the beginning of every measurement and no signal (< 2 cps) was detected, confirming the success of microsublimation for purification from organic materials. The boron isotopic ratios measured by TIMS for SRM 951a fall within a range of 3.98 to 4.04. Our results are similar and consistent with the data from Foster *et al.* (2006), measured using the TE-NTIMS method. This indicates that our analysis can provide externally reproducible boron measurements from extremely small samples. Offsets appeared between our ^{11}B/^{10}B ratios with other non-TE-NTIMS data, which might be attributed to laboratory-specific instrumental fractionation. These differences should not affect the δ^{11}B value between laboratories because all the boron isotopic ratios were normalized to SRM 951a. Based on the results reported here for the two external standards, AE-121 and IAEA B-1, and after comparing these results with those published using both TIMS and MC-ICPMS, we conclude that accurate and reproducible δ^{11}B measurements were achieved in this study.

II.5.2 Assessment of microsublimation technique: organic removal and recovery

The results of H_2O_2 sample treatment with 12 and 20 hours are shown in Figure II. 5 and the last four data points in Figure II. 4 (b). The treatment with H_2O_2 oxidizes organic matter adhering to carbonate skeletons such that it has been widely used to eliminate the interferences from organic matter (Barker *et al.*, 2003; Ni *et al.*, 2010; Stoll *et al.*, 2012; Trotter *et al.*, 2011; Wei *et al.*, 2009). There is no trend or systematic offset between samples with different sublimation time or treatment with H_2O_2, indicating that our microsublimation method is highly suitable for recovering boron for isotopic analysis. Based on these experiments, a rapid throughput of 10 to 20 samples was achievable using a 12-hour sublimation period for 50-μl sample solutions in 5-ml conic bottom vials.

The boron concentrations of UM-CP1 and IAEA B-1 before and after sublimation are consistent with each other, with standard deviations of 3 % and 1.5 %, respectively, and yields are better than 97 %. The equivalent solution concentrations before and after microsublimation indicate the success of the purification design and the reliability of the data. For UM-CP1, the differences between the calculated solution concentration of ~750 ppb and the concentration of ~1100 ppb obtained by standard addition is due to a higher boron concentration in the powder than our initial assumption of 40 ppm. The actual boron concentration in the coral *Porites* powder UM-CP1 is about 65 ppm, measured by Varian 820 MS plasma-source quadrupole mass spectrometer.

II.5.3 Reproducibility

The combination of the warm block on the bottom and the water-cooled coil at the top provides reproducible sample processing for analysis by mass spectrometry. For a variety of standards, including boric acid, seawater and coral, a precision better than 1.4 ‰ (2 σ, n > 10) was achieved. This precision is comparable with previous TE-NTIMS measurements by Foster *et al.* (2006) and Ni *et al.* (2010) in which precisions of 1.5 ‰ for SRM 951 and 0.8 ‰ for IAEA B-1, and 1.2 ‰ for their in-house foraminifera standard, were reported, respectively. Although the precision of our method is slightly

worse than that of MC-ICPMS and P-TIMS, the sample amount required for single measurement is lower than 1 ng, which provides the potential to construct high-resolution pH records during modern times, including the Industrial Revolution, and over longer geologic timescales.

II.5.4 Boron isotopic composition of seawater for culture experiments

The preliminary results of boron isotopic composition in tank seawater from the culture experiment in the Gulf of Maine (δ^{11}B = 39.31 ‰) is about 1.3 ‰ lower than the isotopic ratio in IAEA B-1 (δ^{11}B = 40.60 ‰) and in the open ocean sample from the Gulf of Maine (δ^{11}B = 40.49 ‰). Since riverine flux is considered to be an important input to balance the global marine boron isotope budget (Lemarchand *et al.*, 2000), this offset might be attributed to the influence of river water in the Gulf of Maine with a lower boron isotopic composition. Because the absolute boron isotopic compositions in biogenic carbonate depend on not only the pH in seawater, but also the δ^{11}B value in water from which it precipitates, it is important to have seawater δ^{11}B constraints in order to verify the boron isotopic composition for culture experiments. In addition, other isotopic composition such as ^{87}Sr/^{86}Sr may be needed to clarify the water sources influencing the marine environment.

II.6 Conclusions

In this study, we developed a rapid and high-throughput microsublimation method to purify boron from alkaline matrices and organic matter. The advantage of our method is that it provides a consistent, steady heating and cooling environment for large quantity of samples. Several tests have confirmed the viability of our technique, including comparisons of results from additional H_2O_2 treatment and applying the microblimation method alone, different sublimation times, and quantitative recovery tests using standard addition (e.g., Foster *et al.* (2006)). Based on these assessments, our microsublimation technique provides a low-blank method for the quantitative recovery and separation of boron from both major elements and organic matter. No further resins or H_2O_2 treatment are required. Coupling the new microsublimation technique with the

TE-NTIMS method, a reproducibility better than 1.4 ‰ (2 σ, n > 10) was achieved for a variety of standards with a wide range of boron isotopic ratios, including boric acid standards SRM 951a and AE-121, seawater standard IAEA B-1, and an in-house coral standard UM-CP1. Furthermore, a sample size < 1 ng is required for each measurement, which is sufficient for reconstructing high-resolution geological records. The preliminary test on natural seawater showed comparable precision with measurements on standards, confirming the applicability of our high-precision boron isotopic analysis by TE-NTIMS.

II.7   Acknowledgements

II.8 References

Al-Ammar, A. S., R. K. Gupta, and R. M. Barnes (2000), Elimination of boron memory effect in inductively coupled plasma-mass spectrometry by ammonia gas injection into the spray chamber during analysis, *Spectrochimica Acta Part B: Atomic Spectroscopy*, *55*(6), 629-635.

Allison, N., and A. A. Finch (2010), $\delta^{11}B$, Sr, Mg and B in a modern Porites coral: the relationship between calcification site pH and skeletal chemistry, *Geochim. Cosmochim. Acta*, *74*(6), 1790-1800.

Anagnostou, E., K. F. Huang, C. F. You, E. L. Sikes, and R. M. Sherrel (2012), Evaluation of boron isotope ratio as a pH proxy in the deep sea coral Desmophyllum dianthus: Evidence of physiological pH adjustment, *Earth Planet. Sci. Lett.*, *349*, 251-260.

Barker, S., M. Greaves, and H. Elderfield (2003), A study of cleaning procedures used for foraminiferal Mg/Ca paleothermometry, *Geochemistry, Geophysics, Geosystems*, *4*(9).

Barth, S. (1997), Boron isotopic analysis of natural fresh and saline waters by negative thermal ionization mass spectrometry, *Chem. Geol.*, *143*(3-4), 255-261.

Beirne, E. C., A. D. Wanamaker Jr, and S. C. Feindel (2012), Experimental validation of environmental controls on the $\delta^{13}C$ of *Arctica islandica* (ocean quahog) shell carbonate, *Geochim. Cosmochim. Acta*, *84*, 395-409.

Berglund, M., and M. E. Wieser (2011), Isotopic compositions of the elements 2009 (IUPAC Technical Report), *Pure Application of Chemistry*, *83*(2), 397-410.

Chetelat, B., J. Gaillardet, and R. m. Freydier (2009a), Use of B isotopes as a tracer of anthropogenic emissions in the atmosphere of Paris, France, *Appl. Geochem.*, *24*(5), 810-820.

Chetelat, B., C. Q. Liu, J. Gaillardet, Q. L. Wang, Z. Q. Zhao, C. S. Liang, and Y. K. Xiao (2009b), Boron isotopes geochemistry of the Changjiang basin rivers, *Geochim. Cosmochim. Acta*, *73*(20), 6084-6097.

Douville, E., M. Paterne, G. Cabioch, P. Louvat, J. Gaillardet, A. Juillet-Leclerc, and L. Ayliffe (2010), Abrupt sea surface pH change at the end of the Younger Dryas in the central sub-equatorial Pacific inferred from boron isotope abundance in corals (*Porites*), *Biogeosciences*, *7*(8), 2445-2459.

Foster, G. L., Y. Ni, B. Haley, and T. Elliott (2006), Accurate and precise isotopic measurement of sub-nanogram sized samples of foraminiferal hosted boron by total evaporation NTIMS, *Chem. Geol.*, *230*(1-2), 161-174.

Foster, G. L. (2008), Seawater pH, pCO_2 and $[CO_3^{2-}]$ variations in the Caribbean Sea over the last 130 kyr: A boron isotope and B/Ca study of planktic foraminifera, *Earth Planet. Sci. Lett.*, *271*(1-4), 254-266.

Foster, G. L., P. A. E. Pogge von Strandmann, and J. W. B. Rae (2010), Boron and magnesium isotopic composition of seawater, *Geochemistry, Geophysics, Geosystems*, *11*(8), Q08015.

Gaillardet, J., D. Lemarchand, C. Göpel, and G. Manhès (2001), Evaporation and Sublimation of Boric Acid: Application for Boron Purification from Organic Rich Solutions, *Geostandards Newsletter*, *25*(1), 67-75.

Gonfiantini, R., et al. (2003), Intercomparison of Boron Isotope and Concentration Measurements. Part II: Evaluation of Results, *Geostandards Newsletter*, *27*(1), 41-57.

Hemming, N. G., and G. N. Hanson (1992), Boron isotopic composition and concentration in modern marine carbonates, *Geochim. Cosmochim. Acta*, *56*(1), 537-543.

Hemming, N. G., and G. N. Hanson (1994), A procedure for the isotopic analysis of boron by negative thermal ionization mass spectrometry, *Chem. Geol.*, *114*(1-2), 147-156.

Hönisch, B., N. G. Hemming, A. G. Grottoli, A. Amat, G. N. Hanson, and J. Bijma (2004), Assessing scleractinian corals as recorders for paleo-pH: Empirical calibration and vital effects, *Geochim. Cosmochim. Acta*, *68*(18), 3675-3685.

Hönisch, B., and N. G. Hemming (2005), Surface ocean pH response to variations in pCO_2 through two full glacial cycles, *Earth Planet. Sci. Lett.*, *236*(1-2), 305-314.

Hönisch, B., N. G. Hemming, D. Archer, M. Siddall, and J. F. McManus (2009), Atmospheric Carbon Dioxide Concentration Across the Mid-Pleistocene Transition, *Science*, *324*(5934), 1551-1554.

Kakihana, H., M. Kotaka, S. Satoh, M. Nomura, and M. Okamoto (1977), Fundamental studies on the ion-exchange separation of boron isotopes, *Bull. Chem. Soc. Jpn.*, *50*, 158-163.

Kasemann, S., A. Meixner, A. Rocholl, T. Vennemann, M. Rosner, A. K. Schmitt, and M. Wiedenbeck (2001), Boron and Oxygen Isotope Composition of Certified Reference Materials NIST SRM 610/612 and Reference Materials JB-2 and JR-2, *Geostandards Newsletter*, *25*(2-3), 405-416.

Kasemann, S. A., D. N. Schmidt, J. Bijma, and G. L. Foster (2009), In situ boron isotope analysis in marine carbonates and its application for foraminifera and palaeo-pH, *Chem. Geol.*, *260*(1-2), 138-147.

Kester, D. R., I. W. Duedall, D. N. Connors, and R. M. Pytkowicz (1967), Preparation of Artificial Seawater, *Limnology and Oceanography*, *12*(1), 176-179.

Klochko, K., A. J. Kaufman, W. Yao, R. H. Byrne, and J. A. Tossell (2006), Experimental measurement of boron isotope fractionation in seawater, *Earth Planet. Sci. Lett.*, *248*(1-2), 276-285.

Krief, S., E. J. Hendy, M. Fine, R. Yam, A. Meibom, G. L. Foster, and A. Shemesh (2010), Physiological and isotopic responses of scleractinian corals to ocean acidification, *Geochim. Cosmochim. Acta*, *74*(17), 4988-5001.

Lemarchand, D., J. Gaillardet, E. Lewin, and C. J. Allegre (2000), The influence of rivers on marine boron isotopes and implications for reconstructing past ocean pH, *Nature*, *408*(6815), 951-954.

Lemarchand, D., J. Gaillardet, C. Göpel, and G. Manhès (2002), An optimized procedure for boron separation and mass spectrometry analysis for river samples, *Chem. Geol.*, *182*(2-4), 323-334.

Lemarchand, D., and J. Gaillardet (2006), Transient features of the erosion of shales in the Mackenzie basin (Canada), evidences from boron isotopes, *Earth Planet. Sci. Lett.*, *245*(1-2), 174-189.

Liu, Y., W. Liu, Z. Peng, Y. Xiao, G. Wei, W. Sun, J. He, G. Liu, and C.-L. Chou (2009), Instability of seawater pH in the South China Sea during the mid-late Holocene: Evidence from boron isotopic composition of corals, *Geochim. Cosmochim. Acta*, *73*(5), 1264-1272.

Liu, Y.-C., C.-F. You, K.-F. Huang, R.-M. Wang, C.-H. Chung, and H.-C. Liu (2012), Boron sources and transport mechanisms in river waters collected from southwestern Taiwan: Isotopic evidence, *Journal of Asian Earth Sciences*, *58*, 16-23.

Louvat, P., J. Bouchez, and G. Paris (2010), MC-ICP-MS Isotope Measurements with Direct Injection Nebulisation (d-DIHEN): Optimisation and Application to Boron in Seawater and Carbonate Samples, *Geostandards and Geoanalytical Research*, *35*(1), 75-88.

Ni, Y., G. L. Foster, and T. Elliott (2010), The accuracy of $\delta^{11}B$ measurements of foraminifers, *Chem. Geol.*, *274*(3-4), 187-195.

Pagani, M., D. Lemarchand, A. Spivack, and J. Gaillardet (2005), A critical evaluation of the boron isotope-pH proxy: The accuracy of ancient ocean pH estimates, *Geochim. Cosmochim. Acta*, *69*(4), 953-961.

Pearson, P. N., and M. R. Palmer (1999), Middle Eocene Seawater pH and Atmospheric Carbon Dioxide Concentrations, *Science*, *284*(5421), 1824-1826.

Pelejero, C., E. Calvo, M. T. McCulloch, J. F. Marshall, M. K. Gagan, J. M. Lough, and B. N. Opdyke (2005), Preindustrial to Modern Interdecadal Variability in Coral Reef pH, *Science*, *309*(5744), 2204-2207.

Pelejero, C., E. Calvo, and O. Hoegh-Guldberg (2010), Paleo-perspectives on ocean acidification, *Trends in Ecology & Evolution*, *25*(6), 332-344.

Rae, J. W. B., G. L. Foster, D. N. Schmidt, and T. Elliott (2011), Boron isotopes and B/Ca in benthic foraminifera: Proxies for the deep ocean carbonate system, *Earth Planet. Sci. Lett.*, *302*(3-4), 403-413.

Reynaud, S., N. G. Hemming, A. Juillet-Leclerc, and J.-P. Gattuso (2004), Effect of pCO_2 and temperature on the boron isotopic composition of the zooxanthellate coral *Acropora* sp., *Coral Reefs*, *23*(4), 539-546.

Reynaud, S., C. Rollion-Bard, S. Martin, R. Rolopho-Metalpa, and J.-P. Gattuso (2008), Effect of elevated pCO_2 on the boron isotopic composition into the Mediterranean scleractinian coral *Cladocora caespitosa*, in *Impacts of Acidification on Biological, Chemical, and Physical Systems in the Mediterranean and Black Seas, No 36 in CIESM Workshop Monographs*, edited by F. Briand, pp. 71-75, Monaco.

Sah, R. N., and P. H. Brown (1997), Boron Determination-A Review of Analytical Methods, *Microchem. J.*, *56*(3), 285-304.

Sanyal, A., N. G. Hemming, G. N. Hanson, and W. S. Broecker (1995), Evidence for a higher pH in the glacial ocean from boron isotopes in foraminifera, *Nature*, *373*(6511), 234-236.

Scambelluri, M., and S. Tonarini (2012), Boron isotope evidence for shallow fluid transfer across subduction zones by serpentinized mantle, *Geology*, *40*(10), 907-910.

Schmitt, A.-D., N. Vigier, D. Lemarchand, R. Millot, P. Stille, and F. Chabaux (2012), Processes controlling the stable isotope compositions of Li, B, Mg and Ca in plants, soils and waters: A review, *Comptes Rendus Geoscience*, *344*(11-12), 704-722.

Stoll, H., G. Langer, N. Shimizu, and K. Kanamaru (2012), B/Ca in coccoliths and relationship to calcification vesicle pH and dissolved inorganic carbon concentrations, *Geochim. Cosmochim. Acta*, *80*, 143-157.

Trotter, J., P. Montagna, M. McCulloch, S. Silenzi, S. Reynaud, G. Mortimer, S. Martin, C. Ferrier-Pagès, J.-P. Gattuso, and R. Rodolfo-Metalpa (2011), Quantifying the pH 'vital effect' in the temperate zooxanthellate coral *Cladocora caespitosa*: Validation of the boron seawater pH proxy, *Earth Planet. Sci. Lett.*, *303*(3-4), 163-173.

Vengosh, A., Y. Kolodny, A. Starinsky, A. R. Chivas, and M. T. McCulloch (1991), Coprecipitation and isotopic fractionation of boron in modern biogenic carbonates, *Geochim. Cosmochim. Acta*, *55*(10), 2901-2910.

Vogl, J., and M. Rosner (2012), Production and Certification of a Unique Set of Isotope and Delta Reference Materials for Boron Isotope Determination in Geochemical, Environmental and Industrial Materials, *Geostandards and Geoanalytical Research*, *36*(2), 161-175.

Wang, B.-S., C.-F. You, K.-F. Huang, S.-F. Wu, S. K. Aggarwal, C.-H. Chung, and P.-Y. Lin (2010), Direct separation of boron from Na- and Ca-rich matrices by sublimation for stable isotope measurement by MC-ICP-MS, *Talanta*, *82*(4), 1378-1384.

Wei, G., M. T. McCulloch, G. Mortimer, W. Deng, and L. Xie (2009), Evidence for ocean acidification in the Great Barrier Reef of Australia, *Geochim. Cosmochim. Acta*, *73*(8), 2332-2346.

Chapter III Environmental Controls on the Boron and Strontium Isotopic Composition of Aragonite Shell Material of Cultured *Arctica islandica*

Y.-W. Liu[1], S. M. Aciego[1] and A. D. Wanamaker Jr.[2]

1. Department of Earth and Environmental Sciences, University of Michigan, 1100 N. University Avenue, Ann Arbor, MI 48109-1005, USA

2. Department of Geological and Atmosphere Sciences, Iowa State University, Room 12, Science I, Ames, IA 50011-3212, USA

III.1 Abstract

Ocean acidification, the decrease in ocean pH associated with increasing atmospheric CO_2, is likely to impact marine organisms, particularly those that produce carbonate skeletons or shells. Therefore, it is important to investigate how environmental factors (seawater pH, temperature and salinity) influence the chemical compositions in biogenic carbonates. In this study we report the first high-resolution strontium ($^{87}Sr/^{86}Sr$ and $\delta^{88/86}Sr$) and boron ($\delta^{11}B$) isotopic values in the aragonite shell of cultured *Arctica islandica* (*A. islandica*). The $^{87}Sr/^{86}Sr$ ratios from both tank water and shell samples show ratios nearly identical to the open ocean, which suggests that the shell material reflects ambient ocean chemistry without terrestrial influence. The ^{84}Sr-^{87}Sr double-spike-resolved shell $\delta^{88/86}Sr$ and Sr concentration data show no resolvable change

throughout the culture period and reflect no theoretical kinetic mass fractionation throughout the experiment despite a temperature change of more than 15 °C. The δ^{11}B records from the experiment show at least a 5 ‰ increase through the 29-week culture season (January 2010 – August 2010), with low values from the beginning to week 19 and higher values thereafter. The larger range in δ^{11}B in this experiment compared to predictions based on other carbonate organisms (2 – 3 ‰) suggests that a species-specific fractionation factor may be required. A significant correlation between the ΔpH (pH$_{shell}$-pH$_{sw}$) and seawater pH (pH$_{sw}$) was observed (R^2 = 0.35), where the pH$_{shell}$ is the calcification pH of the shell calculated from boron isotopic composition. This negative correlation suggests that *A. islandica* partly regulates the pH of the extrapallial fluid. However, this proposed mechanism only explains approximately 35 % of the variance in the δ^{11}B data. Instead, a rapid rise in δ^{11}B of the shell material after week 19, during the summer, suggests that the boron uptake changes when a thermal threshold of > 13 °C is reached.

III.2 Introduction

Since the onset of the Industrial Revolution (ca. AD 1750) the global ocean has absorbed approximately 30 % of the emitted anthropogenic carbon dioxide (CO_2) causing ocean acidification (IPCC, 2013). The ecological effects from lowering the pH of the surface ocean on marine organisms, especially those which calcify, will likely be substantial (Doney *et al.*, 2009; Hofmann *et al.*, 2010; Orr *et al.*, 2005), highly variable among taxa (Kroeker *et al.*, 2010; Riebesell *et al.*, 2013), and extend throughout the global ocean (Feely *et al.*, 2004; Orr *et al.*, 2005). Furthermore, anthropogenic CO_2 is not evenly distributed among the ocean basins. In particular, the North Atlantic Ocean stores about 23 % of anthropogenic CO_2 despite representing only 15 % of the global ocean area (Sabine *et al.*, 2004). Consequently, the North Atlantic Basin, compared to other regions, might be more susceptible to ocean acidification. *In situ* measurements of surface ocean pH are rare prior to about 1990 (Byrne *et al.*, 2010; Dore *et al.*, 2009), however, instrumental data show that the surface global ocean pH has decreased by approximately 0.05 pH units in the last 20 – 25 years (IPCC, 2013). Time-series data from the North Pacific and the North Atlantic oceans indicate that the surface ocean pH

has been changing between -0.0015 and -0.0024 pH units per year (IPCC, 2013; Vázquez-Rodrıguez *et al.*, 2012).

This global rise in atmospheric CO_2 has resulted in changes in surface ocean pH and shows a projected persistence in the near future. Therefore, proxy records from the geologic record sensitive to oceanic carbon dynamics are highly desired to place modern pH trends into context (e.g., Hönisch et al., 2012). Biogenic proxy archives calcifying within the surface waters of the global oceans have the unique potential to reveal spatial and temporal patterns and trends in pH using boron isotopes (e.g., Anagnostou et al., 2012; Shinjo et al., 2013). However, in the dynamic coastal regions of the global ocean, local and regional processes have the potential to complicate the boron-pH proxy (described in detail below). Freshwater mixing has the potential to change (1) temperature, salinity, and pH; (2) nutrient availability and productivity leading to changes in pH; and (3) local seawater boron isotopic composition. Additionally, potential species-specific biological effects that occur during calcification need to be evaluated. Here we apply multiple isotope systems to evaluate the boron-pH proxy in the northern North Atlantic coastal and shelf-dwelling marine bivalve *Arctica islandica* (*A. islandica*) exposed to ambient conditions. We use radiogenic strontium isotopes to assess terrestrial river water influence on seawater and shell geochemistry for elements with long residence times in coastal water, such as boron. We utilize stable strontium isotopes from shell material to evaluate the potential impacts of growth rates during biomineralization.

III.2.1 Boron isotopes as pH indicators in biogenic carbonates

Boron has two natural stable isotopes, [10]B and [11]B, which comprise 19.9(7) % and 80.1(7) % of total boron, respectively (Berglund and Wieser, 2011). The dominant aqueous species of boron in seawater are $B(OH)_3$ and $B(OH)_4^-$. The relative proportion of these two species in an aqueous environment is a function of pH with the following relationship:

$$B(OH)_3 + H_2O \rightleftharpoons B(OH)_4^- + H^+ \qquad\qquad \text{(Eq. III.1)}$$

At low pH, boron exists as $B(OH)_3$ in solution, conversely, at high pH, boron exists as $B(OH)_4^-$. The governing reaction for isotope exchange between these two species is

$$^{10}B(OH)_3 + {}^{11}B(OH)_4^- \rightleftharpoons {}^{11}B(OH)_3 + {}^{10}B(OH)_4^- \qquad \text{(Eq. III.2)}$$
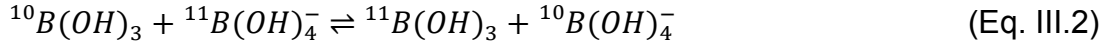
The stable isotope ^{11}B is enriched in $B(OH)_3$ compared to $B(OH)_4^-$, and the combination of equations (Eq. III.1) and (Eq. III.2) can be used to determine the distribution of the two boron species and the isotopic composition of each for a given pH. The isotopic composition of boron is generally reported as

$$\delta^{11}B = \left[\frac{\left({}^{11}B/{}^{10}B\right)_{sample}}{\left({}^{11}B/{}^{10}B\right)_{SRM\ 951a}} - 1 \right] \times 1000\ (\text{‰}) \qquad \text{(Eq. III.3)}$$

where SRM 951a is the internationally recognized boron isotope standard. Because the residence time of seawater boron is approximately 14 million years (Lemarchand *et al.*, 2000), boron isotopic composition in the open ocean is considered constant over this time period, with an average seawater $\delta^{11}B$ value of 39.61 ‰ (Foster *et al.*, 2010). Therefore, $\delta^{11}B$ has the following relationship: at low pH, the isotopic composition of $B(OH)_3$ is equal to the isotopic composition of the total dissolved boron (39.61 ‰). In contrast, at high pH, the isotopic composition of $B(OH)_4^-$ is equal to the isotopic composition of the total dissolved boron. Therefore the $\delta^{11}B$ is enriched in $B(OH)_3$ by about 20 ‰ with respect to $B(OH)_4^-$ at any equilibrium pH based on a constant fractionation factor.

During growth, it is assumed that marine carbonates primarily incorporate $B(OH)_4^-$ into the carbonate structure. Building on these relationships, seawater pH dictates the amount of $B(OH)_4^-$ in seawater and thus the isotopic composition of boron in marine carbonates. The possibility of trigonal $B(OH)_3$ incorporation in carbonates, especially in calcite, is still under debate (Klochko *et al.*, 2009; Rollion-Bard *et al.*, 2011a); however after thorough calibration in targeted marine carbonate species, the $\delta^{11}B$ to pH transfer function can be applied. Changes in the $\delta^{11}B$ composition of shell carbonates are based on the equation

$$pH = pK_b - \log \left(\frac{\delta^{11}B_{sw} - \delta^{11}B_{carbonate}}{\alpha \delta^{11}B_{carbonate} - \delta^{11}B_{sw} + 1000(\alpha - 1)} \right) \qquad \text{(Eq. III.4)}$$

where pK_b is the pK value for boric acid at a given temperature and salinity, and is
8.5975 at 25 °C and 35 PSU salinity (DOE, 1994), $\delta^{11}B_{sw}$ is the isotopic composition of
seawater, and α is the equilibrium isotopic fractionation factor between boric acid and

borate ion, $\left(\alpha \equiv \frac{\left({}^{11}B / {}^{10}B \right)_{B(OH)_3}}{\left({}^{11}B / {}^{10}B \right)_{B(OH)_4^-}} \right)$. Of these variables, only the seawater composition can

be considered known and constant for all geographic locations and carbonate-
precipitating species. Temperature, salinity and the fractionation factor must be
estimated. Two empirical and analytical values of α are suggested for seawater: (1) α =
1.0194, a theoretical result of Kakihana *et al.* (1977), which has been applied widely on
paleo-reconstructions (Hönisch *et al.*, 2004; Sanyal *et al.*, 1995); and (2) α = 1.0272,
which was empirically obtained from Klochko *et al.* (2006) and is considered to better
describe the distribution of the two boron species in nature today (Foster, 2008; Rollion-
Bard and Erez, 2010; Rollion-Bard *et al.*, 2011b). Recent work of Nir *et al.* (2015), using
reverse osmosis membranes under controlled pH, also suggests a higher fractionation
factor than the theoretical result from Kakihana *et al.* (1977). However, due to the ability
of calcifying organisms to buffer their own local environments, species-specific
fractionation factors and transfer functions are likely more appropriate than theoretical α
values (Anagnostou *et al.*, 2012; Hönisch *et al.*, 2004; Krief *et al.*, 2010; Rae *et al.*,
2011; Reynaud *et al.*, 2004; Reynaud *et al.*, 2008; Trotter *et al.*, 2011). Thus far, the pH-
δ^{11}B relationship has been tested extensively on some biogenic marine carbonates,
primarily foraminifera and coral records, with broad success (Anagnostou *et al.*, 2012;
Henehan *et al.*, 2013; Hönisch *et al.*, 2004; Ni *et al.*, 2007; Rae *et al.*, 2011; Reynaud *et
al.*, 2004); a few measurements have been made on calcite shells (Heinemann *et al.*,
2012; Penman *et al.*, 2012), but no published data exist for aragonitic bivalves.

As indicated earlier, one of the primary assumptions in applying the boron isotope/pH
proxy technique is that the boron isotopic composition of the seawater from which the
biogenic carbonates form remains constant. Therefore, in order to use such a proxy to

understand pH changes through the geological past, a technique is required to evaluate variability in local seawater geochemistry.

III.2.2   Radiogenic strontium isotopes as a water mass tracer

To evaluate the potential impacts of freshwater on local or regional ocean chemistry, it is necessary to differentiate sources that influence the chemical composition of the target water mass. This is especially important in coastal regions where freshwater input from river, surface runoff and/or groundwater mix with seawater often modifying both physical (e.g., temperature, salinity and/or turbidity) and chemical (e.g., nutrients, trace metal and/or isotopic compositions) conditions. Even for isotopic systems with long residence times in seawater (including boron), observations indicate that large fluxes of freshwater can cause substantial variations in coastal environments where conservative mixing behavior is generally assumed but not always achieved (Chung *et al.*, 2009; D'Olivo *et al.*, 2014; Huang and You, 2007; Huang *et al.*, 2011; Widerlund and Andersson, 2006).

Radiogenic strontium has successfully been used to trace unique water masses. There are four naturally occurring isotopes of strontium: ^{84}Sr, ^{86}Sr, ^{87}Sr and ^{88}Sr, with the only radiogenic isotope being ^{87}Sr, which decays from ^{87}Rb. Therefore, the ^{87}Sr/^{86}Sr ratio is widely used to trace provenance in geological studies (Aarons *et al.*, 2013; Bataille and Bowen, 2012; Huang and You, 2007; Jahn *et al.*, 2001). Because the residence time of Sr in seawater is more than 4 million years, shorter but comparable to the residence time of boron (Broecker, 1963; Goldberg, 1963), ^{87}Sr/^{86}Sr is considered spatially homogeneous in seawater at any instant of geological time. However, in coastal areas, radiogenic Sr isotopes vary as inputs from continental sources are released from terrestrial sediments to freshwater and then exported to the open ocean (Huang *et al.*, 2011). The variability in ^{87}Sr/^{86}Sr ratios in natural archives on seasonal and annual timescales has been used as a proxy for quantitatively evaluating proportions of different water mass sources in coastal regions (Huang *et al.*, 2011). The similarity of residence times of Sr and B in the ocean, and potential large differences between ocean and terrestrial isotopic compositions, suggests that the radiogenic strontium

composition of shell material can be used to determine if there is a potential offset between local seawater and open-ocean B isotopic composition.

Prior studies have shown that bivalve shells record both ambient seawater composition and mixing of water sources in the ambient seawater. Widerlund and Andersson (2006) developed a two-endmember mixing model of terrestrial fluvial water and seawater radiogenic Sr in the Baltic Sea and compared the modern bivalve $^{87}Sr/^{86}Sr$ inferred salinity across the Baltic Sea from inland to the Atlantic coast to the *in situ* measurements of water salinity. Their results indicate conservative characteristics of $^{87}Sr/^{86}Sr$ vs. salinity in the Baltic Sea. Maurer *et al.* (2012) also measured the $^{87}Sr/^{86}Sr$ ratio in a freshwater bivalve species: the Sr isotopic ratios recorded in the shells, in both early and late ontogeny ages, agreed with local water samples, indicating their usefulness in investigating the effects of anthropogenic contamination in rivers.

III.2.3 Stable strontium isotopes in biogenic carbonates

In addition to $^{87}Sr/^{86}Sr$, the stable isotopes of Sr ($\delta^{88/86}Sr$, the deviation in $^{88}Sr/^{86}Sr$ of a sample relative to a standard given in parts per mil) in natural archives can serve as a means to evaluate potential vital effects linked to growth rates and metabolic processes, although the applicability is less well established and still controversial. Previously reported $\delta^{88/86}Sr$ values of coral, foraminifera and coccolithophores from the literature show ^{88}Sr depleted results compared to the $\delta^{88/86}Sr$ value in seawater, which suggest the lighter ^{86}Sr is preferentially incorporated into biogenic carbonates (Böhm *et al.*, 2012; Fietzke and Eisenhauer, 2006; Krabbenhöft *et al.*, 2010; Rüggeberg *et al.*, 2008; Stevenson *et al.*, 2014). If the fractionation of stable Sr isotopes in precipitated biogenic carbonates is dominated by kinetic isotope effects and not under equilibrium conditions, the $\delta^{88/86}Sr$ ratio would likely have a strong correlation with precipitation temperature and/or precipitation rate. As an environmental proxy, $^{88}Sr/^{86}Sr$ in both deep sea and tropical corals has been reported as a temperature proxy (Fietzke and Eisenhauer, 2006; Rüggeberg et al., 2008). However, more recent, higher precision work, has indicated either a null relationship (foraminifera) or negative relationship (coccolithophore) between $\delta^{88/86}Sr$ and ambient seawater temperature, suggesting

growth rate controls the uptake of Sr isotopes into biogenic carbonates (Böhm *et al.*, 2012; Stevenson *et al.*, 2014). Although stable strontium applications are in their infancy, the potential for vital effects, such as growth rates, impacting stable Sr incorporation indicates it could be useful for assessing vital effects during calcification in bivalve archives.

III.2.4 The Biogenic Archive *Arctica islandica*

The long-lived bivalve mollusk *A. islandica*, common in the shelf seas of the temperate to sub-polar North Atlantic Ocean, is an excellent high-resolution marine archive with a huge potential for monitoring pH as well as other seawater properties (for a recent review, see Schöne, 2013). This stationary benthic clam lives in water depths ranging from ~10 m to as deep as 500 m and thrives in full marine conditions yet can also tolerate salinities as low as 28 PSU for short time intervals (Merrill and Ropes, 1968; Nicol, 1951). *Arctica islandica* lives within the sediment and extends its relatively short siphons into the main water column, exchanging water to feed and remove waste. Weidman (1995) demonstrated that the geochemical signature in the shell material reflects that of the ambient water conditions and not pore water. *Arctica islandica* is highly suitable for environmental and ocean studies because (1) *A. islandica* is extremely long-lived – up to 5 centuries (Butler *et al.*, 2013; Schöne *et al.*, 2005; Wanamaker Jr. *et al.*, 2008a); (2) it produces annual growth increments in its shell (Jones, 1980); (3) regional increment series can be crossdated, demonstrating a common response to environmental forcing(s) (Schöne *et al.*, 2003); (4) fossil shells can be crossdated and floating shell chronologies can be constructed after radiocarbon dating (Scourse *et al.*, 2006); (5) live-caught shells can be crossdated with fossil shells to assemble very long, absolutely dated growth records (Butler *et al.*, 2009; Butler *et al.*, 2011; Marchitto *et al.*, 2000); (6) master shell chronologies can be created that are as statistically robust as tree ring chronologies (Butler *et al.*, 2010); (7) it precipitates its aragonite shell in oxygen isotope equilibrium with ambient seawater (Weidman *et al.*, 1994); and (8) the geochemical signature (e.g., ^{14}C, $\delta^{18}O$, $\delta^{13}C$) from shell material has been used to reconstruct ocean circulation, hydrographic changes, seasonal changes in ocean conditions, and ecosystem dynamics (Butler *et al.*, 2009; Schöne *et al.*, 2005;

Schöne *et al.*, 2011a; Scourse *et al.*, 2012; Wanamaker Jr. *et al.*, 2008a; Wanamaker Jr. *et al.*, 2008b; Wanamaker Jr. *et al.*, 2009; Wanamaker Jr. *et al.*, 2011; Wanamaker Jr. *et al.*, 2012; Weidman and Jones, 1993; Weidman *et al.*, 1994; Witbaard and Bergman, 2003). Despite the potential as environmental proxies, applications of non-traditional isotopic systems (δ^{11}B and $\delta^{88/86}$Sr) that have the capacity to reveal additional oceanographic and environmental information have not been explored fully.

III.3 Methods

III.3.1 Sample preparation

Living shells from the Gulf of Maine (GoM) were collected from Jonesport, Maine, USA on 21 November 2009 with a commercial quahog-fishing vessel, F. V. *Three of A Kind*. The live-caught animals were then transported to the Darling Marine Center (University of Maine) in Walpole, Maine, USA, for the culture experiment. Seawater was pumped from the Damariscotta River estuary from ~10 m and delivered to the flowing seawater laboratories. The shells were reared in flow-through seawater tanks without filtration, in which the temperature, salinity and seawater pH were monitored *in situ* concurrently and continuously (Figure III. 1 (d)). The pH of the culture seawater was also measured a total of 7 times with a highly accurate Metrohm handheld pH meter (± 0.003 units). Additional details of the culture conditions are given in Beirne *et al.* (2012). Tank seawater was sampled biweekly throughout the culture period and filtered through a 0.45 μm filter. Two additional samples, one from the Gulf of Maine surface seawater and one from auxiliary water flow pumped into the culture tanks, were also sampled to evaluate if the culture experiment was representative of the natural marine environment. Boron isotopic data from seawater samples during the experiment were previously measured and published by Liu *et al.* (2013).

Shell subsamples were collected at Iowa State University via a Dremel hand drill, with 10 intervals throughout the 8-month culturing (Figure III. 1 (c)). Based on the calcein staining (see Beirne et al., 2012, for details) and natural marking on the external shell, the timing of the winter (January – March), spring (March – May), and summer (May –

August) growing seasons were evident (Figure III. 1 (a) – (c)). These markings were used to establish growth rates during each season as well as to provide temporal controls on the sampled shell material. The instrumental data and shell growth-rates have been published by Beirne *et al.* (2012), and the average seawater salinity, temperature, and pH for shell record comparison are summarized in Table III. 1.

The boron and strontium concentrations in *A. islandica* shells are about 10 and 1000 ppm, respectively (Zhang, 2009); 1 mg of shell material, after cleaning (details noted below), is required for B (Liu *et al.*, 2013) and Sr (Stevenson *et al.*, 2014) isotopic measurements. Because shell growth rates differ throughout the year, and throughout ontogeny (Beirne *et al.*, 2012), we have one subsample from January to March, but we have four subsamples from March to May and five subsamples from May to August.

The subsample cleaning procedure was modified from Barker *et al.* (2003). In summary, coral and shell powders were first cleaned with Super-Q (SQ) water (Millipore, > 18.2 MΩ) in an ultrasonic bath 3 times and the suspension solution was extracted after centrifuging. Samples were then treated with 10 % H_2O_2 at room temperature overnight to remove organic particles embedded in skeletons. The samples were rinsed with SQ water, 0.001 N HNO_3 and SQ water again. After drying at 60 °C, samples were weighed and then dissolved in ~1.7 N HCl with a boron concentration equal to about 750 ppb.

Seawater samples were diluted to [B] = ~750 ppb in 1.7 N HCl for boron measurements. Because the strontium concentration in seawater is about 9 ppm, the residual after sublimation (see below) is not enough for strontium isotope measurements. Therefore, for strontium isotope analysis of seawater, an additional 100 μl of seawater sample was dried and redissolved in concentrated HNO_3 3 times and brought into solution in 7 N HNO_3 for column chemistry. Spiked samples were mixed to have a sample to spike ratio of 1:1, with at least 600 ng of sample Sr in solution prior to preconditioning steps.

Separation of the boron and strontium elemental fractions was achieved using a combination of microsublimation (Liu *et al.*, 2013) and elemental specific ion exchange resin. Briefly, < 50 μl of sample solution was loaded in the cap of a conic-bottom vial in an up-side-down position and put into the high-throughput system. After 12 hours of

sublimation at 70 – 74 °C, the purified boron sample solution is condensed and collected on the conic tip. To further improve the reproducibility for carbonate samples, an extra 2 µl of 30 % H_2O_2 was added to the purified solution (~ 90 % of the volume before sublimation) for all the runs after 23 April 2014. The sample solution was left stagnant in the vial, and the cap of the conic vial was then loosened for 2 hours to reduce the organic levels and to liberate oxygen gas. The microsublimation method only extracts boron from the sample solution; therefore, the residual on the cap of the vials is reserved for Sr separation and analysis.

All measurements were conducted on a Thermo Fisher Triton PLUS multicollector thermal ionization mass spectrometer operating in positive ion mode for strontium isotope analysis and negative ion mode for boron isotope analysis at the Glaciochemistry and Isotope Geochemistry Lab (GIGL) at the Department of Earth and Environmental Sciences, University of Michigan.
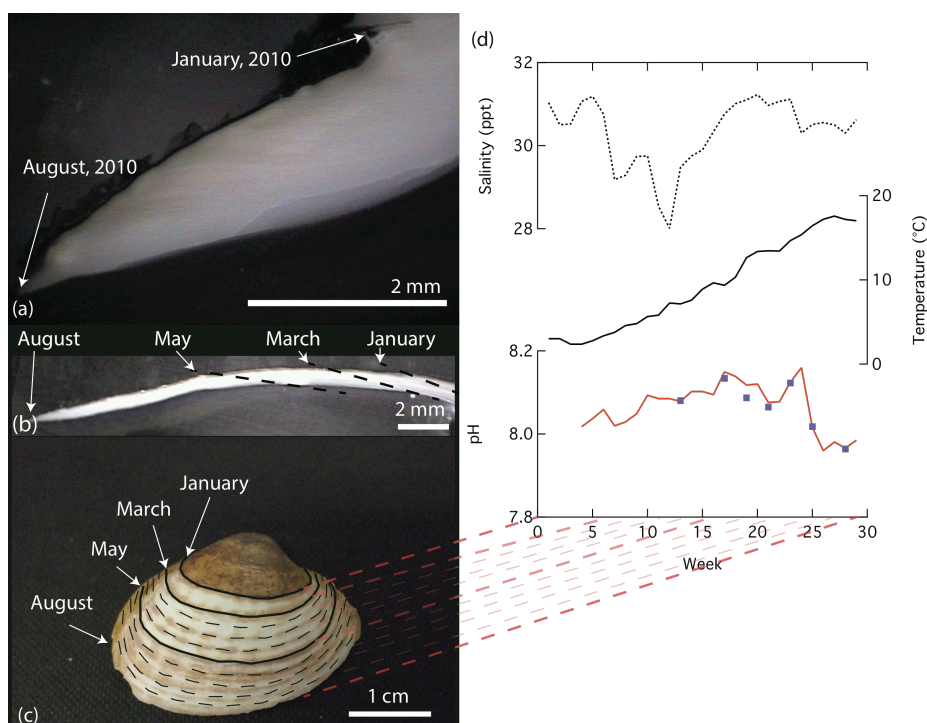
Figure III. 1   **Photos of (a) adult and (b) (c) juvenile *A. islandica* from the culture experiment.**
External marks on the shell or calcein marks in the cross section were used to constrain shell growth. (d) shows the corresponding *in situ* measurements of tank water salinity, temperature and pH during the 31-week culture experiment. The juvenile shells were sampled in 10 intervals for this study (c). Note that because the growth rates differ during the season, each interval represents different time durations (c) and (d).

Table III. 1   Summary of *in situ* instrumental data of tank seawater salinity, temperature, and pH during culture season

Week number (dates)	Salinity (PSU)[1]	Average to subsampling interval[3]	Temperature (°C)[1]	Average to subsampling interval[3]	pH[1]	Average to subsampling interval[3]	Predicted δ^{11}B with α = 1.0260[2]	Predicted δ^{11}B with α = 1.0272[2]
1 (1/17 - 1/23)	31.036		3.029		--		--	--
2 (1/24 - 1/30)	30.508		3.030		--		--	--
3 (1/31 - 2/6)	30.520		2.375		--		--	--
4 (2/7 - 2/13)	31.066	30.608 ± 0.683	2.369	2.960 ± 0.511	8.018	8.033 ±0.019	15.84	14.79
5 (2/14 - 2/20)	31.186		2.776		8.037		16.00	14.95
6 (2/21 - 2/27)	30.755		3.367		8.059		16.18	15.14
7 (2/28 - 3/6)	29.183		3.774		8.019		15.90	14.85
8 (3/7 - 3/13)	29.288		4.596		8.029		16.03	14.99
9 (3/14 - 3/19 (3/20))	29.743	29.516 ± 0.322	4.800	4.698 ± 0.145	8.049	8.039 ± 0.014	16.20	15.16
10 (3/21 - 3/27)	29.751		5.646		8.094		16.59	15.57
11 (3/28 - 4/3)	28.547	29.149 ± 0.851	5.825	5.735 ± 0.127	8.085	8.089 ± 0.006	16.49	15.47
12 (4/4 - 4/10)	28.011		7.252		8.085		16.60	15.58
13 (4/11 (4/14) - 4/17)	29.478	28.745 ± 1.037	7.158	7.205 ± 0.066	8.078	8.082 ± 0.005	16.61	15.59
14 (4/18 - 4/24)	29.751		7.594		8.102		16.85	15.84
15 (4/25 - 5/1)	29.902	29.827 ± 0.107	8.898	8.246 ±0.922	8.102	8.102 ± 0.000	16.99	15.99
16 (5/2 - 5/8)	30.335		9.662		8.095		17.03	16.03
17 (5/9 - 5/15)	30.762	30.702 ± 0.341	9.364	9.784 ± 0.494	8.150	8.128 ± 0.029	17.48	16.50
18 (5/16 - 5/22)	31.008		10.328		8.139		17.51	16.53
19 (5/23-5/29)	31.102		12.653		8.118		17.59	16.61
20 (5/30-6/5)	31.227	31.099 ± 0.129	13.385	13.170 ± 0.450	8.120	8.105 ± 0.025	17.69	16.72
21 (6/6-6/12)	30.969		13.472		8.076		17.30	16.31
22 (6/13-6/19)	31.067		13.427		8.078		17.32	16.33
23 (6/20-6/26)	31.115	30.829 ± 0.454	14.676	14.494 ± 0.989	8.125	8.121 ± 0.041	17.88	16.91
24 (6/27-7/3)	30.306		15.380		8.159		18.24	17.30
25 (7/4-7/10)	30.508		16.445		8.015		17.07	16.08
26 (7/11-7/17)	30.555	30.521 ± 0.030	17.209	17.076 ± 0.577	7.960	7.985 ± 0.028	16.71	15.70
27 (7/18-7/24)	30.500		17.576		7.981		16.91	15.90
28 (7/25-7/31)	30.305	30.466 ± 0.227	17.188	17.107 ± 0.115	7.966	7.976 ± 0.013	16.75	15.73
29 (8/1-8/5)	30.626		17.026		7.985		16.89	15.89

1.   Data from Beirne *et al.* (2012)

2.   Calculation based on Eq. III.2, where $\alpha \equiv \frac{(^{11}B/^{10}B)_{B(OH)_3}}{(^{11}B/^{10}B)_{B(OH)_4^-}}$ and $pK_b = -log\left(exp\left(\frac{-8966.90-2890.53S^{\frac{1}{2}}-77.942S+1.728S^{\frac{3}{2}}-0.0996S^2}{T}\right.\right.$ $\left.\left. + 148.0248 + 137.1942S^{\frac{1}{2}} + 1.62142S - \left(24.4344 + 25.085S^{\frac{1}{2}} + 0.2474S\right)\ln T + 0.053105S^{\frac{1}{2}}T\right)\right)$ (DOE, 1994).

3.   ± Standard deviation (σ) of the data

III.3.2 Radiogenic and Stable Strontium Isotope analysis

III.3.2.1 General

The residuals of carbonate samples after sublimation were redissolved in concentrated HNO_3 to [Sr] = ~10 ppm, which is approximately the same Sr concentration in seawater. A small aliquot of sample was spiked with our ^{84}Sr-^{87}Sr double-spike solution. Both unspiked normal sample and spiked mixture sample solutions were then dried down 3 times and then dissolved in 7 N HNO_3 for Sr column chemistry. In order to separate strontium element from the matrix, samples were passed through a 50 – 100 µm Sr-spec resin (Eichrom), and 0.035 N HNO_3 was used to elute Sr after using 7 N HNO_3 to elute the others. The eluted Sr aliquots were refluxed with 30 % H_2O_2 overnight, dried, and finally dissolved in concentrated HNO_3 for loading (Liu, 2010).

For radiogenic isotopic measurements, 100 – 200 ng of Sr sample was loaded onto outgassed Re filaments with TaF_5 activator solution. Each sample was heated to an intensity of ~8 V ^{88}Sr. A total of 400 cycles of data were collected for each measurement to determine the Sr isotopic ratios with within run precision better than 10 ppm (2 SE). Mass 84 – 86 were detected with five Faraday cups positioned from L1 to H3, respectively, with ^{85}Rb measured in the center cup. The long-term reproducibility of $^{87}Sr/^{86}Sr$ for SRM987 Sr standard was 0.710268 ± 21 (2 σ, n = 140) from the time of Triton installation in January 2012 to April 2014. In May 2014, problems associated with the H3 Faraday cup resulted in change to a ^{86}Sr-centered cup configuration (June to October 2014). After H3 cup replacement, the ^{85}Rb-centered cup configuration was established again. The new SRM987 $^{87}Sr/^{86}Sr$ average value is 0.719246 ± 13 (2 σ, n = 42) for data collected after June 2014 (for both cup configurations) and sample data were normalized based on this new SRM987 standard ratio. The reported $^{87}Sr/^{86}Sr$ data in this study were all normalized to SRM987 = 0.710250 for inter-laboratory comparisons.

III.3.2.2 Double spike (84-87) Sr

High precision $^{88}Sr/^{86}Sr$ isotopic compositions are measured by double spike (DS); measurements by DS remove instrumental mass bias associated with thermal ionization during sample runs. The double-spike method was first developed in the 1960s: Dodson (1963) outlined a methodology for determining the unknown mass discrimination factor directly if the sample is mixed with a double spike, consisting of an enriched mixture of two stable isotopes. Later, Krogh (1964) worked out a graphical method for a spike enriched in both ^{84}Sr and ^{86}Sr. Finally, Long (1966) showed that the correction factor for mass discrimination can be calculated by using three elements and depends on the fractional abundances in the normal and spike elements. A simpler expression was then published by Boelrijk (1968). These pioneering studies founded the basis of the Sr double-spike method, and Sr double spikes have already been successfully used to determine the Sr isotopic composition of the early solar system (Patchett, 1980a; 1980b). Optimal spike compositions are determined using a 3-D data reduction method (Galer, 1999). The choice of isotope ratios used in the equations, the mathematical formulation to solve for the mass discrimination factor ε and the influence of the spike-to-sample ratio in the mixture should be taken into consideration. With the addition of "tuning" with IAPSO (International Association for Physical Sciences of the Oceans) seawater standards (Krabbenhöft *et al.*, 2009), this double-spike method could produce more precise true isotopic compositions in an unknown sample solution.

A ^{84}Sr-^{87}Sr double-spike solution was prepared at GIGL at the University of Michigan following the method from Liu (2010). The optimal value of the spike depends on the angle of two planes, defined by normal sample (N) fractionation line and spike point and mixture (M) fractionation line and spike point, respectively (Figure III. 2), expressed as θ here. Because all the measured points have their own errors, when the angle between these two planes approximates a right angle, the intersected area reaches a minimum and, thus, the N-M-S line will be defined precisely (Figure III. 2 (b)). Therefore, by checking different portions of spike mixing with normal sample (Qs), mathematically, the distribution of θ to spike composition can be derived (Figure III. 2 (c)). For our ^{84}Sr-^{87}Sr double spike with an $^{84}Sr/^{87}Sr$ ratio of 0.8679, the optimal Qs is about 0.5, which makes

the two planes perpendicular to each other. Within a range of Qs = 0.45 – 0.55, θ is still in a range of ± 2 degree, which supports a tolerance of spiking samples with a slight deviation from a 1:1 sample to spike ratio. The stable Sr data were reported as $\delta^{88/86}Sr$, which was defined as:

$$\delta^{88/86}Sr = \left[\frac{(^{88}Sr/^{86}Sr)_{sample}}{(^{88}Sr/^{86}Sr)_{SRM\,987}} - 1\right] \times 1000 \; (‰) \qquad \text{(Eq. III.5)}$$

In this study, a Python script was applied to evaluate true normal values of the shells. We assumed the measured isotopic ratios of normal sample and spiked mixture would follow exponential law, and the equations of each ^{87}Sr-based isotopic ratio for both normal and mixture sample could be stated. After inputting the known isotopic composition of the spike, the true value of each isotope concentration can be solved using a least squares minimization of the residual of the non-linear equations.

For the spiked sample solution, 200 – 250 ng of Sr samples was loaded onto outgassed Re filaments with TaF_5 activator solution and run the same as the unspiked samples described in the previous section. The deconvolved $\delta^{88/86}Sr$ values for seawater standard IAPSO 141 and the inter-laboratory coral standard JCp-1 are 0.390 ± 16 ‰ (2 σ, n = 4) and 0.144 ± 26 ‰ (2 σ, n = 3), respectively. According to Krabbenhöft *et al.* (2009), using the IAPSO seawater standard to fine-tune the Sr double-spike composition provides an optimal $\delta^{88/86}Sr$ result. Here we used the same technique and obtained a compatible $\delta^{88/86}Sr$ value for the IAPSO seawater standard to the reported values from Krabbenhöft *et al.* (2009). However, due to the H3 cup deficiency, the deconvolved $\delta^{88/86}Sr$ value of inter-laboratory carbonate standard JCp-1 is about 0.05 ‰ lighter than the reported values between April 2014 and June 2014. This offset was fixed, with the alternate cup configuration and replacement of H3 cup, after June 2014 and new values of IAPSO = 0.365 ± 73 ‰ (2 σ, n = 4) and JCp-1 = 0.195 ± 21 ‰ (2 σ, n = 4) (Figure III. 3) were obtained.
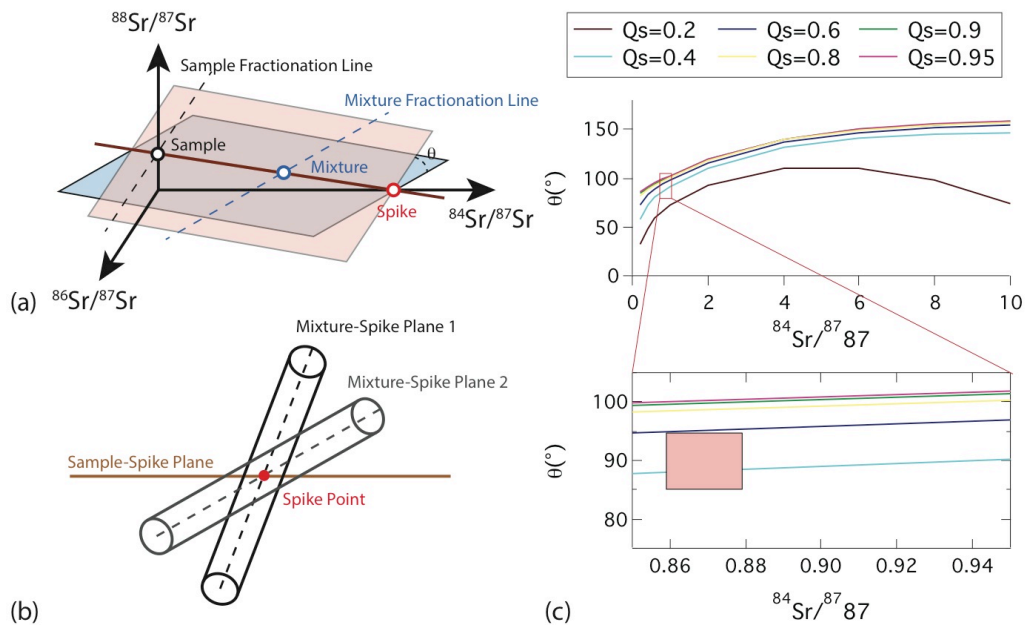
Figure III. 2 The illustrations of (a) the 84-87 Sr double-spike method, (b) how the angle between mixture-spike plane and sample-spike plane can influence the precision of the deconvolved result, and (c) the optimal sample-spike ratio in our study.
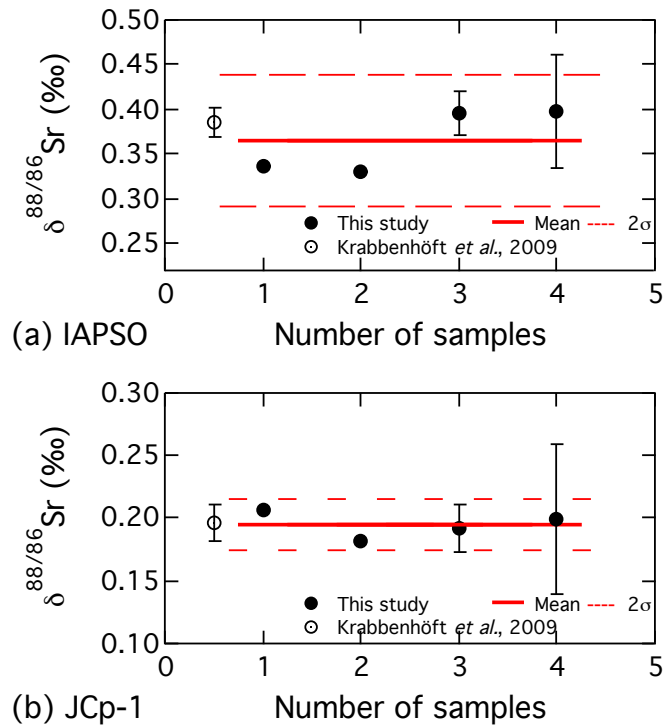
Figure III. 3 Stable Sr results for (a) seawater standard IAPSO and (b) inter-laboratory biogenic carbonate standards JCp-1.

III.3.3 Boron Isotope Analysis

The procedure used for obtaining B isotopic compositions by total evaporation (TE) is described in Liu *et al.* (2013). In summary, 1 µl of boron-free synthetic seawater matrix was loaded onto outgassed single Re filament at 0.8 A current, followed by 1 µl of sample solution with 30 seconds of waiting between the two steps. Samples were then dried down at 2 A current for 10 seconds and then the filaments were flashed to a dull red color in the center of the filament (about 2.5 A) and ready for analysis. Data collection was initiated when the intensity of mass 42 reached 20 mV, and terminated after the signal dropped lower than the initial 20 mV.

The long-term reproducibility (18 months) of $^{11}B/^{10}B$ for boric acid standard SRM (standard reference material) 951a is 4.0332 ± 0.0064 (2 σ, n = 97) before treated with 30 % H_2O_2 and is 4.0316 ± 0.0084 (2 σ, n = 19) after the extra treatment. The precisions of $\delta^{11}B$ for seawater and biogenic carbonate standards without addition of peroxide are 40.46 ± 1.29 ‰ (2 σ, n = 54) and 24.94 ± 2.35 ‰ (2 σ, n = 39) for IAEA B-1 and JCp-1, respectively; and 41.70 ± 1.13 ‰ (2 σ, n = 8) and 24.93 ± 1.83 ‰ (2 σ, n = 18) for IAEA B-1 and JCp-1, respectively, with H_2O_2 treatment (Figure III.4).
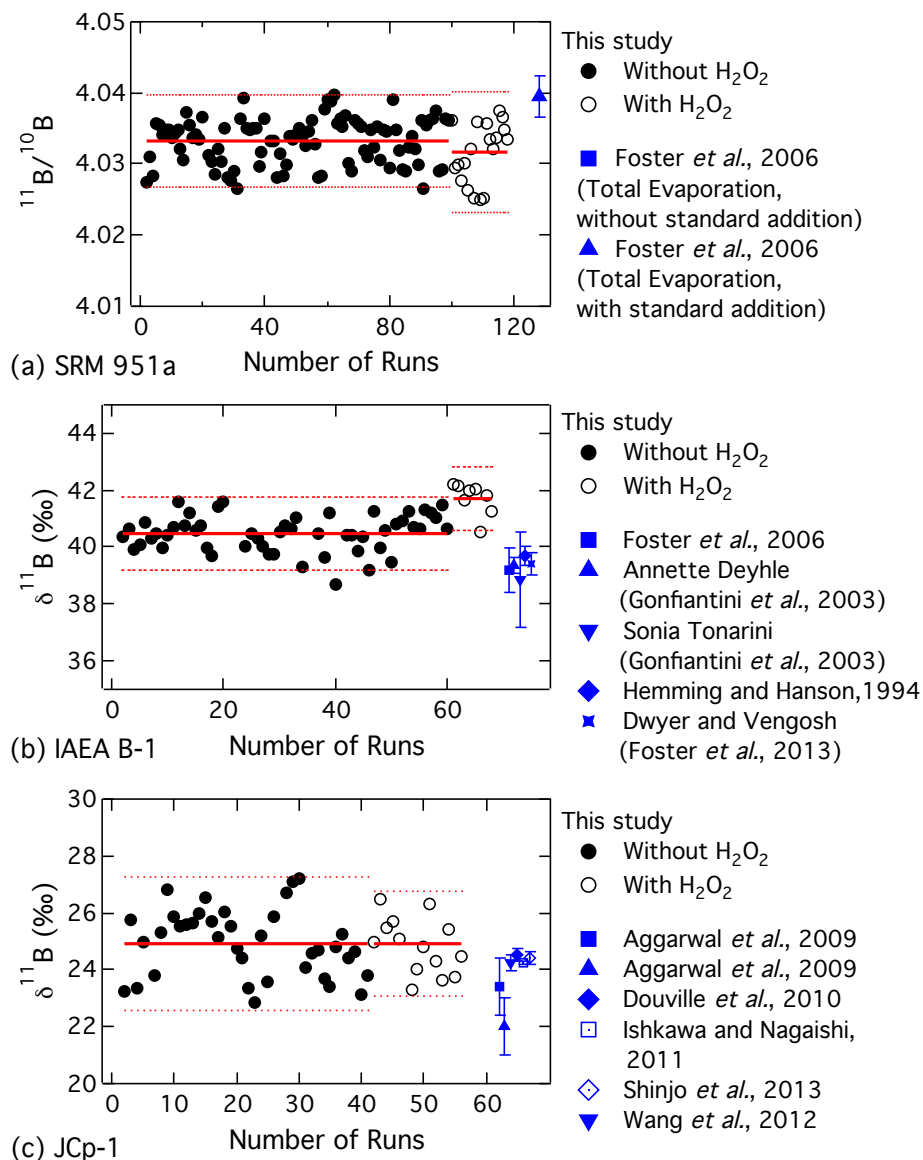
Figure III. 4   Long-term precision of (A) boric acid standard SRM 951a, (B) seawater standard IAEA B-1, and (C) inter-laboratory carbonate standard JCp-1.

III.4 Results

The *in situ* seawater salinity, temperature and pH results are summarized in Table III. 1. To compare the instrumental data to the shell records, the instrumental results were averaged with respect to the subsampling intervals. The seawater and shell results are summarized in Table III. 2 and Table III. 3, respectively.

Table III. 2   Summary of seawater data

Sample ID	Week	^{87}Sr/^{86}Sr (2 SE)	δ^{11}B (‰)
Tank A 031710	9	0.709182(4)	38.48
Tank A 041810	14	0.709192(5)	39.41
Tank A 050810	16	0.709183(4)	39.47
Tank A 052210	18	0.709186(4)	38.04
Tank A 081610	31	0.709188(4)	38.10
Tank B 031910	9	0.709185(4)	39.31
			39.97
			38.50
			40.59
			38.51
			40.10
			39.45
			40.33
			39.81
			37.91
Flow A 021410	5	0.709184(4)	39.00
Flow A 070510	25	0.709188(4)	38.65
Flow A 072210	27	0.709187(4)	38.33
			39.36
			38.57
			38.48
			38.40
			39.02
			40.77
			40.78
Flow #2 013010	2	0.709180(4)	37.51
			38.53
			39.01
			39.91
			40.83
			40.01
			39.08
			38.98
			39.78
			39.14
Flow #2 022710	6	0.709189(4)	39.16
Aux.	33	0.709182(5)	36.93
GoM 112309	33	0.709177(4)	40.38

Table III. 3 **Summary of shell data**

Sample ID	Week number	$^{87}Sr/^{86}Sr$ (2 SE)	$\delta^{88/86}Sr$ (‰)	[Sr] (ppm)	$\delta^{11}B$ (‰)	Average growth rate (mm/week)[1]	pH_{shell}[2]	ΔpH[3]	2σ for calculated pH[4]
A101JV-8	22	--	--	--	20.32	--	8.419	0.298	0.22
A101JV-9	24.8	--	--	--	23.34	--	8.595	0.610	0.10
A102JV-1	4	0.709181 (7)	0.132	1403	15.68	0.27	8.139	0.105	0.11
A102JV-2	8.5	0.709210 (10)	0.151	1282	14.94		8.020	-0.019	0.08
A102JV-3	10.5	0.709181 (10)	0.158	1422	14.28	0.53	7.898	-0.191	0.42
A102JV-4	12.5	0.709157 (15)	0.112	1452	--				
A102JV-5	14.5	0.709201 (7)	0.118	1435	13.77		7.756	-0.346	0.15
A102JV-6	16.4	0.709194 (12)	0.124	1319	13.65		7.705	-0.423	0.14
A102JV-7	19.2	0.709169 (13)	0.154	1474	16.80	0.65	8.132	0.028	0.10
A102JV-8	22	0.709170 (5)	0.099	1558	18.04		8.236	0.115	0.13
A102JV-9	24.8	0.709178 (6)	0.112	1491	20.23		8.382	0.397	0.02
A102JV-10	27.6	0.709184 (6)	0.097	--	21.93		8.502	0.527	0.02
A103JV-1	4	--	--	--	16.57	0.24	8.242	0.209	0.25
A103JV-2	8.5	--	--	--	16.57		8.225	0.186	0.25
A103JV-3	10.5	0.709191 (7)	--	--	18.41	0.51	8.389	0.300	0.03
A103JV-4	12.5	0.709187 (5)	--	--	16.04		8.138	0.056	0.17
A103JV-5	14.5	0.709195 (9)	--	--	16.28		8.145	0.043	0.11
A103JV-6	16.4	0.709204 (15)	--	--	17.71		8.265	0.138	0.13
A103JV-7	19.2	--	--	--	16.57		8.108	0.003	0.06
A103JV-8	22	0.709188 (6)	--	--	17.45	0.61	8.182	0.061	0.24
A103JV-9	24.8	0.709182(5)	--	--	19.21		8.305	0.319	0.07
A103JV-10	27.6	0.709182 (5)	--	--	25.12		8.708	0.733	0.22
A105JV-1	4	0.709178 (6)	0.227	1414	14.53	0.24	7.970	-0.064	0.53
A105JV-2	8.5	0.709191 (7)	0.255	1534	13.75		7.802	-0.237	0.39
A105JV-3	10.5	0.709183 (6)	0.251	1482	12.22	0.60	7.175	-0.914	0.76
A105JV-4	12.5	0.709184 (5)	0.263	1453	17.15		8.257	0.176	0.21
A105JV-5	14.5	0.709175 (7)	0.216	1521	14.59		7.916	-0.186	0.25
A105JV-6	16.4	0.709179 (6)	0.273	2559	11.09		--	--	0.30
A105JV-7	19.2	0.709183 (5)	0.296	2048	12.52		7.272	-0.833	0.33
A105JV-8	22	0.709163 (5)	0.230	2204	17.41	0.68	8.178	0.057	0.17
A105JV-9	24.8	0.709186 (6)	0.234	1850	19.43		8.322	0.337	0.09
A105JV-10	27.6	0.709177 (6)	0.238	1795	22.11		8.514	0.539	0.23

[1.] Data from Beirne (2011)

[2.] pH_{shell} was calculated with Eq. 4, in situ temperature and salinity data was used to determine pK_b and $\alpha = 1.0272$ was used.

[3.] ΔpH (pH_{shell}-pH_{sw})

[4.] Propagation error determined from within run standard deviation of shell $\delta^{11}B$ (duplication or triplication of the same sample solution).

III.4.1 $^{87}Sr/^{86}Sr$ and $\delta^{88/86}Sr$

III.4.1.1 $^{87}Sr/^{86}Sr$

The $^{87}Sr/^{86}Sr$ ratios of seawater range from 0.709177 to 0.709192, with an average of 0.709185 ± 8 (2 σ, n = 13). There is no distinguishable difference between samples from offshore Gulf of Maine seawater, auxiliary flow and tank waters (Figure III.5 (a)). For shell carbonate, the $^{87}Sr/^{86}Sr$ ratios range from 0.709163 to 0.709210, with an average of 0.709183 ± 23 (2 σ, n = 27). Both the seawater and shell $^{87}Sr/^{86}Sr$ are identical to the mean seawater values (Figure III. 5 (a) and (b)). Because all the radiogenic Sr results are identical within error, there is no impact from seawater salinity, seawater temperature or pH.
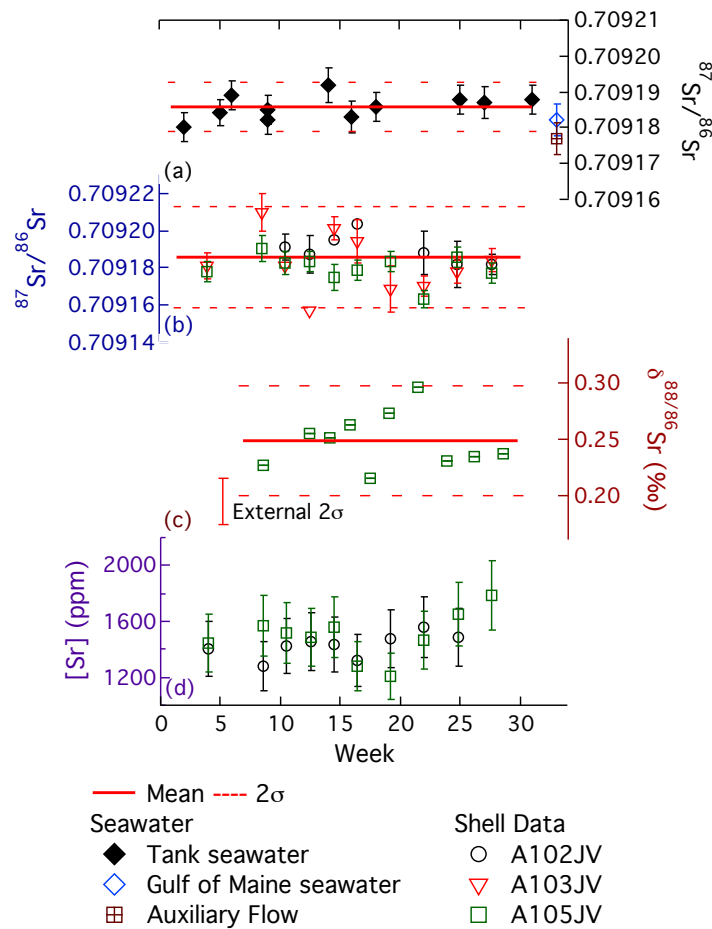
Figure III. 5   **GoM $^{87}Sr/^{86}Sr$ data**
for (a) seawater samples and (b) shell samples and the double-spike-deconvolved (c) $\delta^{88/86}Sr$ values and (d) Sr concentrations for the juvenile shell.

III.4.1.2 $\delta^{88/86}Sr$

Two sets of shell samples, A103JV and A105JV, were spiked for stable Sr measurements. However, due to the defect of H3 cup, the A103JV double-spike results are underestimated and are not listed. The deconvolved $\delta^{88/86}$Sr for A105JV and Sr concentration values for both of A103JV and A105JV from high-resolution shell records are shown in Figure III. 5 (c) and (d), respectively. The $\delta^{88/86}$Sr values range from 0.215 to 0.296 ‰ with an average of 0.248 ± 48 ‰ (2 σ, n = 10) and the concentration ranges from 1200 – 1800 ppm. Considering analytical uncertainty, no distinctive differences or trend for either Sr concentration or stable Sr isotopic compositions in the shells is observed throughout the culture season. Similarly, no significant correlation can be found between stable Sr isotopes or Sr concentrations with any measured ambient seawater conditions.

## III.4.2 Boron isotopic composition (δ^{11}B) in ambient seawater the shell and aragonite shell

Boron isotopic compositions of 11 tank water samples are from 37.51 ‰ to 47.83 ‰, and the average for 36 sample runs is 39.20 ± 1.73 ‰. The δ^{11}B values for additional seawater samples from the offshore Gulf of Maine and the auxiliary flow to the culture tanks are 36.93 ‰ and 40.38 ‰, respectively (Figure III. 6 (a)) (Liu *et al.*, 2013). Similar to what has been observed from radiogenic Sr data in seawater, the boron isotopic composition of our culture seawater is invariant and identical to the open-ocean composition reported by Foster *et al.* (2010).

High-resolution boron isotopic composition records from four juvenile shells (A101JV, A102JV, A103JV and A105JV) show nearly identical patterns and trends throughout the experiment. The shell δ^{11}B values range from 11.09 to 18.81 ‰ before week 19 and from 17.41 to 25.12 ‰ after week 19 (Figure III. 6 (b)). Compared to seawater temperature and average shell growth rates in three growth seasons, we found a distinct rise in δ^{11}B for temperatures over ~13 °C. However, this rapid change in δ^{11}B did not correlate to the rapid change in shell growth during the culture period.

In order to evaluate the pH dependency of the $\delta^{11}B$, Eq. III.4 is used. Based on *in situ* temperature, salinity and pH measurements throughout the culture experiment, we calculated the predicted range in $\delta^{11}B$ of the *A. islandica* shell with α = 1.0272, which was empirically obtained from Klochko *et al.* (2006) and is considered to better describe the distribution of the two boron species in the natural system (Foster, 2008; Rollion-Bard and Erez, 2010; Rollion-Bard *et al.*, 2011b) (Figure III. 6 (b)). Another prediction line calculated based on an independently derived fractionation factor from Nir *et al.* (2015) is also shown for reference (Figure III. 6 (b)). The predictions suggest a slight increase in $\delta^{11}B$ throughout the culture season, primarily due to more than a 15 °C temperature increase. A 0.2 pH unit drop, observed between week 24 and 26, should have decreased the $\delta^{11}B$ value by about 2 ‰ even with the large temperature change. Most of the shell $\delta^{11}B$ data followed the two prediction lines before week 19, with some of the data lower than the predictions. After week 19, the $\delta^{11}B$ data deviate significantly and trend toward higher $\delta^{11}B$ values. Duplications on different individual shells all show the same trend.

We also calculated shell pH (pH_{shell}) with α = 1.0272 based on average tank water $\delta^{11}B$, shell $\delta^{11}B$ and the corresponding average seawater temperature and salinity values. The results show a significant negative relationship between ΔpH and pH_{sw} (R^2 = 0.35; p-value ≤ 0.001) (Figure III. 7).
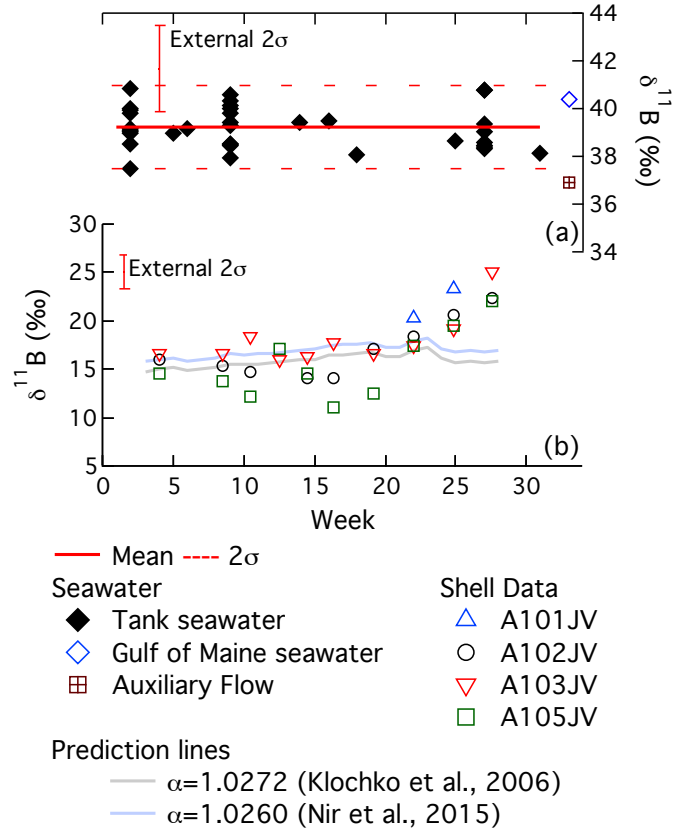
Figure III. 6   **GoM boron data**

for (a) seawater samples and (b) shell samples. Two prediction lines listed were calculated based on our instrumental culture seawater pH, temperature, and salinity data, and two boron fractionation factors: α = 1.0272 (Klochko *et al.*, 2006) and α = 1.0260 (Nir *et al.*, 2015), where $\alpha \equiv \frac{\left(^{11}B/^{10}B\right)_{B(OH)_3}}{\left(^{11}B/^{10}B\right)_{B(OH)_4^-}}$. Equation Eq. III.4 was used for the calculation.
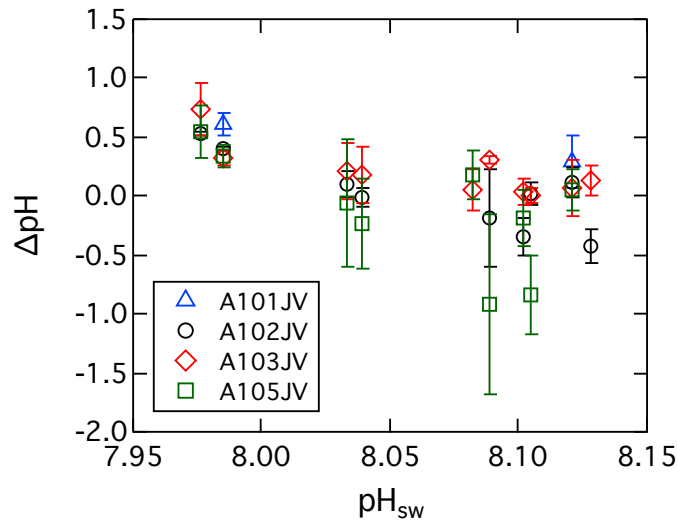
Figure III. 7   **The calculated pH discrepancy (ΔpH = pH_shell - pH_sw)**

shows a statistically significant negative relationship to pH_{sw} ($R^2 = 0.35$; p-value ≤ 0.001). The negative correlation supports the argument that *A. islandica* regulate their EPF pH for calcification. The shell calcification pH (pH_{shell}) were calculated based on in situ water temperature α = 1.0272 (Klochko *et al.*, 2006).

III.5 Discussion

III.5.1 Radiogenic Sr isotope incorporation into *A. islandica*

In this study, we measured the radiogenic Sr isotope ratios in seawater to estimate the source water contributions to the culture site, which is situated within the Damariscotta River estuary. The ^{87}Sr/^{86}Sr ratios in cultured seawater showed identical values to the open surface seawater ratio. Bedrock types in the Gulf of Maine coastal region are dominated by late Proterozoic and lower Paleozoic sedimentary rocks (Osberg *et al.*, 1985), which would provide a terrestrial source with high ^{87}Sr/^{86}Sr values. Considering rock type, age and freshwater flux, a recent model of ^{87}Sr/^{86}Sr for flux-weighted catchment water suggests the ^{87}Sr/^{86}Sr value to be in a range of 0.7099 – 0.7145 (Bataille and Bowen, 2012). If river fluxes influence the Sr isotopic composition of coastal seawater, the value should be enriched in ^{87}Sr, driving the ^{87}Sr/^{86}Sr higher than the current seawater ratio. Therefore, the Sr isotopic results suggest a negligible amount of terrestrial input into the culture site at the Darling Marine Center.

The mean ^{87}Sr/^{86}Sr ratio in the shell is consistent with the isotopic composition in the culture seawater, but with a relatively larger variation between individual shell samples. Therefore, incorporation of radiogenic Sr ratios into the shells occurs without measurable fractionation and reflects the isotopic composition of ambient seawater. Although the shell ^{87}Sr/^{86}Sr values have a larger standard deviation compared to the seawater values, they are within the range of the long-term precision of Triton plus at the Department of Earth and Environmental Sciences, University of Michigan (see Sect. III.3.2.1). The high content of calcium in carbonate samples, which cannot be fully separated using Sr-specific ion exchange column chemistry, may contribute to the larger variation of shell ^{87}Sr/^{86}Sr compared to seawater.

III.5.2 Stable Sr isotope incorporation into *A. islandica*, and Sr concentrations

In this study we observed no statistically significant correlation of $\delta^{88/86}$Sr or Sr concentrations with respect to seawater temperature. The stable Sr isotopic composition of some biogenic carbonates has been suggested to reflect ambient seawater temperature due to mass-dependent kinetic fractionation, in which the relative mass difference of the isotopes involved accounts for the inverse correlation to the ion mass in a kinetic fractionation process (Fietzke and Eisenhauer, 2006; Rüggeberg *et al.*, 2008). However, more recent work has shown no relationship between seawater temperature and $\delta^{88/86}$Sr values from various biogenic archives (Böhm *et al.*, 2012; Raddatz *et al.*, 2013; Stevenson *et al.*, 2014; Vollstaedt *et al.*, 2014). Our results support the argument that a simple temperature-dependent kinetic effect is not the primary control on $\delta^{88/86}$Sr in the aragonite shell of *A. islandica*. The temperature range in the experiment is over 15 °C (2.4 – 17.6 °C) and growth rate more than doubled (0.24 – 0.68 mm/week) during the experiment, which could result in over 1.5 ‰ change in $\delta^{88/86}$Sr if *A. islandica* incorporated ^{88}Sr/^{86}Sr similarly as noted by the Stevenson *et al.* (2014) study on coccolithophores. The lack of a consistent relationship between $\delta^{88/86}$Sr and temperature or shell growth rates during the experiment indicates that $\delta^{88/86}$Sr is not controlled by these factors. Thus, it is likely that $\delta^{88/86}$Sr records derived from *A. islandica* shells reflect ambient seawater conditions and could be a potential archive for studying the global Sr cycle in the context of chemical weathering (Krabbenhöft *et al.*, 2010; Raddatz *et al.*, 2013; Vollstaedt *et al.*, 2014). More work is needed to fully evaluate this potential proxy.

Our deconvolved shell Sr concentrations show no resolvable relationship with the seawater temperature, despite a possible physiological control on Sr uptake into bivalve shell material. In general, co-precipitation of Sr to Ca in aragonite decreases with temperature increases due to a declining distribution coefficient, which has been both measured and derived theoretically (Dietzel *et al.*, 2004). The negative correlation between skeletal Sr/Ca ratios observed in some massive corals with ambient seawater temperature has been widely established and applied to reconstruct paleo-seawater

temperature (Beck *et al.*, 1992; Corrège, 2006; de Villiers, 1999; McCulloch *et al.*, 1994; McCulloch *et al.*, 1996; Shen *et al.*, 1996; Weber, 1973; Yan *et al.*, 2013; Yu *et al.*, 2005). However, these relationships may be biased by the influence from symbionts causing an apparent vital effect (Böhm *et al.*, 2012; Cohen *et al.*, 2002; Cohen *et al.*, 2006; Stevenson *et al.*, 2014) or by ontogenetic age, grow rates, metabolic activity related to temperature and/or salinity (Purton *et al.*, 1999). Schöne *et al.* (2011b) observed a strong physiological regulation to Sr/Ca and Mg/Ca on ontogenetically old adult *A. islandica* records. The metal to calcium ratio (Me/Ca) increased with shell age when the annual increment widths were below 30 – 200 µm. However, Schöne *et al.* (2013) concluded that the faster-growing juvenile portion of the shells showed a weak relationship between Me/Ca and ambient temperature and results from different specimens were variable. Schöne *et al.* (2013) proposed that pronounced vital effects may control the trace metal uptake in juvenile shells. Our results are also consistent with the study of Schöne *et al.* (2011b), where the juvenile portion of the two *A. islandica* shells with annual growth increments larger than 750 µm, showed no obvious relationship between Me/Ca ratios and growth rates.

III.5.3 Controls on δ^{11}B in *A. islandica* and an evaluation of the proxy archive as a seawater pH indicator

The range in measured shell δ^{11}B values lies between the prediction lines (Figure III. 6 (b)), which suggest that the shell boron content generally reflects the ambient seawater conditions. However, our data do not consistently follow either prediction line. Previous studies on foraminifera have shown offsets between different genera and the empirical δ^{11}B-pH relationship of α = 1.0194 (Hönisch and Hemming, 2004). The inconsistency between shell δ^{11}B and either prediction is therefore strong evidence that a species-specific fractionation factor is required for bivalves.

The offsets between our shell data with the predicted trends (Figure III. 6 (b)) are likely from vital effects during biomineralization. Previous studies suggested a range of fractionation factors might be applied, and an additional constant offset might better describe the empirical δ^{11}B-pH relationship (Anagnostou *et al.*, 2012; Hönisch *et al.*,

73

2004; Rae *et al.*, 2011). Therefore, a species-specific offset may account for the smaller variations before week 19, where many of the results are below the prediction lines and have a negative ΔpH value. In this study, because the temperature and salinity were highly variable and pH changes were relatively small, we cannot determine a precise δ^{11}B-pH shell transfer function for *A. islandica*. However, the total variation throughout the experiment is about 10 ‰, and has an obvious trend after week 19, suggesting non-pH-related controls on boron incorporation in the shell.

Rollion-Bard and Erez (2010) and Trotter *et al.* (2011) evaluated vital effects in corals and foraminifera, and the potential use of the δ^{11}B-pH relationship in such biogenic carbonates. They observed a pH offset between calcifying fluid and ambient seawater, and this pH discrepancy (ΔpH) increases with decreasing ambient seawater pH (pH_{sw}). As the environment becomes more acidic, marine calcifiers likely adjust their internal microenvironment during calcification, resulting in larger ΔpH values than expected. Under careful culture conditions, species-specific ΔpH-pH_{sw} relationships can be developed and, after calibration, the corresponding ambient seawater pH can be determined.

It has been argued that bivalves have the ability to regulate their inner shell fluid chemistry, more specifically the extrapallial fluid (EPF), to achieve a carbonate saturation state in order to facilitate biomineralization (Crenshaw, 1980). Stemmer (2013) observed pH gradients between the inner shell surface and the outer mantle epithelium (OME) of *A. islandica* via an *in situ* pH microscopy method. During a short-term monitoring, Stemmer (2013) also observed the measured pH rose rapidly as the probe approached the OME. They concluded this elevation was due to active proton uptake by the epithelium. This result suggests a pH self-regulation occurs for *A. islandica* shell precipitation, and the shell will record the regulated calcification pH in the carbonate shell.

The calculated ΔpH shows a statistically significant negative relationship to pH_{sw} (R^2 = 0.35; p-value ≤ 0.001) (Figure III. 7). The inverse correlation supports the argument that *A. islandica* regulate their EPF pH for calcification. However, only 35 % of the variability

can be explained by ΔpH, which indicates that the pH regulation in the EPF is likely not the prevailing factor. Instead, we found a rapid increase of the shell δ^{11}B when temperature increased over 13 °C (Figure III. 8 (a)). This rapid change in boron isotopic composition can be explained with respect to two factors: (1) a growth-rate-controlled vital effect, or (2) a temperature-controlled vital effect.

Herfort *et al.* (2008) suggested that carbonate species are the limiting factor in coral calcium precipitation rather than calcium: when ambient seawater temperature increases $[CO_2]_{aq}$ decreases and leads to a rising $[CO_3^{2-}]$ and calcification rate. The rapid growth rate change is likely related to spring bloom. Our data show no statistically significant correlation between shell δ^{11}B and shell growth rates, indicating shell growth is not causing the boron isotope deviation in the culture experiment (Figure III. 8b). Therefore, the associated change in shell δ^{11}B with elevated seawater temperatures and the lack of correlation with shell growth rates to the shell δ^{11}B deviation after week 19 cannot be explained by a temperature-controlled growth/precipitation effect.

Alternatively, a proton removal mechanism via Ca^{2+}-ATPase from the site of calcification has been proposed. This mechanism raises the pH of the calcification solution (Dissard *et al.*, 2012; Rollion-Bard *et al.*, 2011b). In this scenario, the activity of the enzyme is enhanced when a certain temperature has been reached, accelerating the proton removal process and resulting in a higher boron isotopic composition in the calcification solution with respect to the elevated pH. We suggest that there may be a temperature threshold of the boron incorporation into the shell aragonite of *A. islandica*. This proposed threshold may be related to the upper-end thermal tolerance of *A. islandica*, which is generally a cold water species. For example, below 13 °C, the δ^{11}B values closely matched the predicted model of Klochko et al. (2006), supporting the assumption that borate is the dominant species incorporated into the shell. Thus, we suggest that shell-derived δ^{11}B in *A. islandica* reflect the ambient seawater pH at temperatures below ~13 °C. At temperatures above 13 °C the utility of shell δ^{11}B values as a pH indicator is questionable and likely unreliable. We suggest that the thermal tolerance of *A. islandica* was exceeded in the summer growing season in the culture conditions, causing biological stress on the animals.
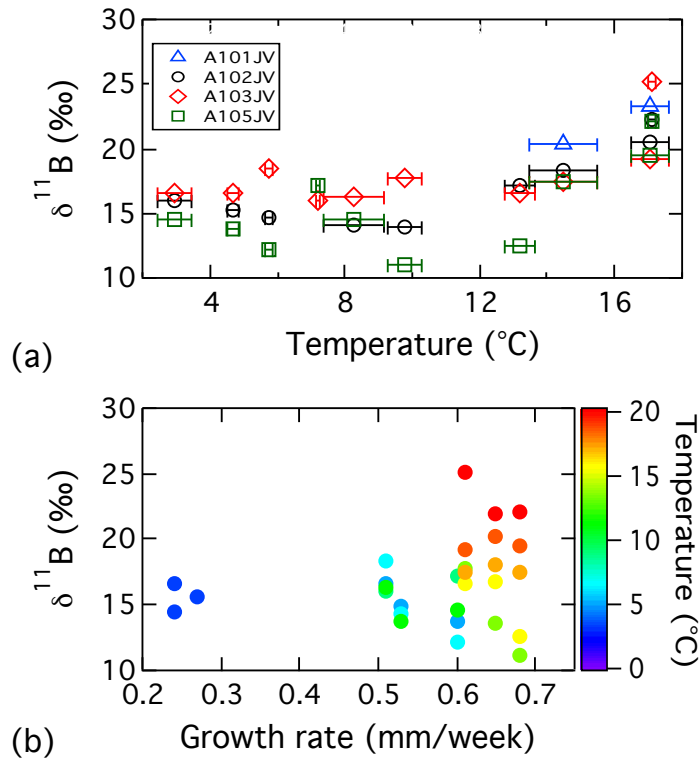
Figure III. 8 The comparisons between the shell δ¹¹B and (a) the corresponding culture water temperature and (b) the growth rates for individual shells.

Colors shown in (b) represent the temperature corresponded to each data point, with low temperatures in blue to high temperatures in red.

III.6 Conclusions

Here we examined the radiogenic and stable isotopic composition of strontium and the stable isotopic composition of boron recorded in the aragonitic shell material of cultured *A. islandica* with *in situ* seawater temperature, salinity and pH measurements. Both seawater and shell $^{87}Sr/^{86}Sr$ show identical values to the mean global seawater composition, suggesting there is trivial influence from local continental runoff. Shell $\delta^{88/86}Sr$ and Sr concentration values during the culture season were not influenced by seawater temperature or calcification rates. These results suggest that well-preserved subfossil specimens may be used to determine the past isotopic composition ($^{87}Sr/^{86}Sr$ and $\delta^{88/86}Sr$) of seawater.

The boron isotope results from the cultured aragonite *A. islandica* shells are generally within the range of two prediction lines utilizing previously published fractionation

factors. Although, to first order, these results indicate that the shell $\delta^{11}B$ values reflect ambient conditions, substantial variability unrelated to pH changes was noted. The 5 – 8 ‰ increase in shell $\delta^{11}B$ values is larger than theoretical predictions based on *in situ* seawater temperature, salinity, pH and conventional boron fractionation factors for corals and foraminifera. A species-specific $\delta^{11}B$-pH transfer function is recommended for bivalve species because of their inherent ability to self regulate calcifying fluids. The statistically significant relationship (R^2 = 0.35) between ΔpH and pH_{sw} indicates that *A. islandica* does regulate the EPF pH during calcification, but self-regulation is not the primary control on shell $\delta^{11}B$. The largest increase in shell $\delta^{11}B$ values was observed after crossing an apparent temperature threshold at 13 °C, suggesting a possible influence from biological processes. To better evaluate the potential of $\delta^{11}B$ as a seawater pH indicator in *A. islandica* shell material, a pH-controlled culture experiment with a large pH range (0.4 – 0.6 units) and with limited seawater temperature and salinity variation is needed.

III.7 Acknowledgements

III.8 References

Aarons, S. M., S. M. Aciego, and J. D. Gleason (2013), Variable HfSrNd radiogenic isotopic compositions in a Saharan dust storm over the Atlantic: Implications for dust flux to oceans, ice sheets and the terrestrial biosphere, *Chem. Geol.*, *349–350*, 18-26.

Anagnostou, E., K. F. Huang, C. F. You, E. L. Sikes, and R. M. Sherrel (2012), Evaluation of boron isotope ratio as a pH proxy in the deep sea coral Desmophyllum dianthus: Evidence of physiological pH adjustment, *Earth Planet. Sci. Lett.*, *349*, 251-260.

Barker, S., M. Greaves, and H. Elderfield (2003), A study of cleaning procedures used for foraminiferal Mg/Ca paleothermometry, *Geochemistry, Geophysics, Geosystems*, *4*(9).

Bataille, C. P., and G. J. Bowen (2012), Mapping $^{87}Sr/^{86}Sr$ variations in bedrock and water for large scale provenance studies, *Chem. Geol.*, *304–305*, 39-52.

Beck, J. W., R. L. Edwards, E. Ito, F. W. Taylor, J. Recy, F. Rougerie, P. Joannot, and C. Henin (1992), Sea-Surface Temperature from Coral Skeletal Strontium/Calcium Ratios, *Science*, *257*(5070), 644-647.

Beirne, E. C. (2011), Pursuing a proxy for carbon cycling in the temperate North Atlantic: Investigation of the utility of *Arctica islandica* shell carbonate to millennial-scale dissolved inorganic carbon reconstructions, MS thesis, 193 pp, Iowa State University, Graduate Theses and Dissertations. Paper 10124., Ames.

Beirne, E. C., A. D. Wanamaker Jr, and S. C. Feindel (2012), Experimental validation of environmental controls on the $\delta^{13}C$ of *Arctica islandica* (ocean quahog) shell carbonate, *Geochim. Cosmochim. Acta*, *84*, 395-409.

Berglund, M., and M. E. Wieser (2011), Isotopic compositions of the elements 2009 (IUPAC Technical Report), *Pure Application of Chemistry*, *83*(2), 397-410.

Boelrijk, N. A. I. M. (1968), A general formula for "double" isotope dilution analysis, *Chemical Geology*, *3*(4), 323-325.

Böhm, F., A. Eisenhauer, J. Tang, M. Dietzel, A. Krabbenhöft, B. Kisakürek, and C. Horn (2012), Strontium isotope fractionation of planktic foraminifera and inorganic calcite, *Geochim. Cosmochim. Acta*, *93*, 300-314.

Broecker, W. S. (1963), Radioisotopes and large-scale oceanic mixing*Rep.*, 88-108 pp, New York: Interscience.

Butler, P. G., J. D. Scourse, C. A. Richardson, A. D. Wanamaker Jr, C. L. Bryant, and J. D. Bennell (2009), Continuous marine radiocarbon reservoir calibration and the ^{13}C

Suess effect in the Irish Sea: Results from the first multi-centennial shell-based marine master chronology, *Earth Planet. Sci. Lett.*, *279*(3), 230-241.

Butler, P. G., C. A. Richardson, J. D. Scourse, A. D. Wanamaker Jr, T. M. Shammon, and J. D. Bennell (2010), Marine climate in the Irish Sea: analysis of a 489-year marine master chronology derived from growth increments in the shell of the clam *Arctica islandica*, *Quaternary Science Reviews*, *29*(13-14), 1614-1632.

Butler, P. G., A. D. Wanamaker, Jr., J. D. Scourse, C. A. Richardson, and D. J. Reynolds (2011), Long-term stability of $\delta^{13}C$ with respect to biological age in the aragonite shell of mature specimens of the bivalve mollusk *Arctica islandica*, *Palaeogeography, Palaeoclimatology, Palaeoecology*, *302*(1-2), 21-30.

Butler, P. G., A. D. Wanamaker Jr, J. D. Scourse, C. A. Richardson, and D. J. Reynolds (2013), Variability of marine climate on the North Icelandic Shelf in a 1357-year proxy archive based on growth increments in the bivalve Arctica islandica, *Palaeogeography, Palaeoclimatology, Palaeoecology*, *373*, 141-151.

Byrne, R. H., S. Mecking, R. A. Feely, and X. Liu (2010), Direct observations of basin-wide acidification of the North Pacific Ocean, *Geophys. Res. Lett.*, *37*(2).

Chung, C.-H., C.-F. You, and H.-Y. Chu (2009), Weathering sources in the Gaoping (Kaoping) river catchments, southwestern Taiwan: Insights from major elements, Sr isotopes, and rare earth elements, *Journal of Marine Systems*, *76*(4), 433-443.

Cohen, A. L., K. E. Owens, G. D. Layne, and N. Shimizu (2002), The Effect of Algal Symbionts on the Accuracy of Sr/Ca Paleotemperatures from Coral, *Science*, *296*(5566), 331-333.

Cohen, A. L., G. A. Gaetani, T. Lundälv, B. H. Corliss, and R. Y. George (2006), Compositional variability in a cold-water scleractinian, *Lophelia pertusa*: New insights into "vital effects", *Geochemistry, Geophysics, Geosystems*, *7*(12), Q12004.

Corrège, T. (2006), Sea surface temperature and salinity reconstruction from coral geochemical tracers, *Palaeogeography, Palaeoclimatology, Palaeoecology*, *232*(2–4), 408-428.

Crenshaw, M. A. (1980), *Mechanisms of shell formation and dissolution*, 115-132 pp., Plenum, New York.

D'Olivo, J. P., M. T. McCulloch, S. M. Eggins, and J. Trotter (2014), Coral records of reef-water pH across the central Great Barrier Reef, Australia: assessing the influence of river runoff on inshore reefs, *Biogeosciences Discuss.*, *11*(7), 11443-11479.

de Villiers, S. (1999), Seawater strontium and Sr/Ca variability in the Atlantic and Pacific oceans, *Earth Planet. Sci. Lett.*, *171*(4), 623-634.

Dietzel, M., N. Gussone, and A. Eisenhauer (2004), Co-precipitation of Sr^{2+} and Ba^{2+} with aragonite by membrane diffusion of CO_2 between 10 and 50 °C, *Chem. Geol.*, *203*(1–2), 139-151.

Dissard, D., E. Douville, S. Reynaud, A. Juillet-Leclerc, P. Montagna, P. Louvat, and M. McCulloch (2012), Light and temperature effects on delta $\delta^{11}B$ and B/Ca ratios of the zooxanthellate coral *Acropora* sp.: results from culturing experiments, *Biogeosciences*, *9*(11), 4589-4605.

Dodson, M. H. (1963), A theoretical study of the use of internal standards for precise isotopic analysis by the surface ionization technique: Part I-General first-order algebraic solutions, *Journal of Physics E: Scientific Instruments*, *40*, 289-295.

DOE (1994), *Handbook of methods for the analysis of the various parameters of the carbon dioxide system in sea water*, Carbon Dioxide Information and Analysis Center, Oak Ridge.

Doney, S. C., V. J. Fabry, R. A. Feely, and J. A. Kleypas (2009), Ocean Acidification: The Other CO_2 Problem, *Annual Review of Marine Science*, *1*(1), 169-192.

Dore, J. E., R. Lukas, D. W. Sadler, M. J. Church, and D. M. Karl (2009), Physical and Biogeochemical Modulation of Ocean Acidification in the Central North Pacific, *Proc. Natl. Acad. Sci. U. S. A.*, *106*(30), 12235-12240.

Feely, R. A., C. L. Sabine, K. Lee, W. Berelson, J. Kleypas, V. J. Fabry, and F. J. Millero (2004), Impact of Anthropogenic CO_2 on the $CaCO_3$ System in the Oceans, *Science*, *305*(5682), 362-366.

Fietzke, J., and A. Eisenhauer (2006), Determination of temperature-dependent stable strontium isotope ($^{88}Sr/^{86}Sr$) fractionation via bracketing standard MC-ICP-MS, *Geochemistry, Geophysics, Geosystems*, *7*(8), Q08009.

Foster, G. L. (2008), Seawater pH, pCO_2 and $[CO_3^{2-}]$ variations in the Caribbean Sea over the last 130 kyr: A boron isotope and B/Ca study of planktic foraminifera, *Earth Planet. Sci. Lett.*, *271*(1-4), 254-266.

Foster, G. L., P. A. E. Pogge von Strandmann, and J. W. B. Rae (2010), Boron and magnesium isotopic composition of seawater, *Geochemistry, Geophysics, Geosystems*, *11*(8), Q08015.

Galer, S. J. G. (1999), Optimal double and triple spiking for high precision lead isotopic measurement, *Chem. Geol.*, *157*(3-4), 255-274.

Goldberg, E. D. (1963), The oceans as a chemical system*Rep.*, 3-25 pp, New York: Interscience.

Heinemann, A., J. Fietzke, F. Melzner, F. Böhm, J. Thomsen, D. Garbe-Schönberg, and A. Eisenhauer (2012), Conditions of *Mytilus edulis* extracellular body fluids and shell

composition in a pH-treatment experiment: Acid-base status, trace elements and $\delta^{11}B$, *Geochemistry, Geophysics, Geosystems*, *13*(1).

Henehan, M. J., et al. (2013), Calibration of the boron isotope proxy in the planktonic foraminifera Globigerinoides ruber for use in palaeo-CO_2 reconstruction, *Earth Planet. Sci. Lett.*, *364*, 111-122.

Herfort, L., B. Thake, and I. Taubner (2008), BICARBONATE STIMULATION OF CALCIFICATION AND PHOTOSYNTHESIS IN TWO HERMATYPIC CORALS, *Journal of Phycology*, *44*(1), 91-98.

Hofmann, G. E., J. P. Barry, P. J. Edmunds, R. D. Gates, D. A. Hutchins, T. Klinger, and M. A. Sewell (2010), The Effect of Ocean Acidification on Calcifying Organisms in Marine Ecosystems: An Organism-to-Ecosystem Perspective, *Annual Review of Ecology, Evolution, and Systematics*, *41*(1), 127-147.

Hönisch, B., and N. G. Hemming (2004), Ground-truthing the boron isotope-paleo-pH proxy in planktonic foraminifera shells: Partial dissolution and shell size effects, *Paleoceanography*, *19*(4).

Hönisch, B., N. G. Hemming, A. G. Grottoli, A. Amat, G. N. Hanson, and J. Bijma (2004), Assessing scleractinian corals as recorders for paleo-pH: Empirical calibration and vital effects, *Geochim. Cosmochim. Acta*, *68*(18), 3675-3685.

Hönisch, B., A. Ridgwell, D. N. Schmidt, E. Thomas, S. J. Gibbs, A. Sluijs, R. Zeebe, L. Kump, R. C. Martindale, and S. E. Greene (2012), The geological record of ocean acidification, *Science*, *335*(6072), 1058-1063.

Huang, K.-F., and C.-F. You (2007), Tracing freshwater plume migration in the estuary after a typhoon event using Sr isotopic ratios, *Geophys. Res. Lett.*, *34*.

Huang, K.-F., C.-F. You, C.-H. Chung, and I.-T. Lin (2011), Nonhomogeneous seawater Sr isotopic composition in the coastal oceans: A novel tool for tracing water masses and submarine groundwater discharge, *Geochemistry, Geophysics, Geosystems*, *12*(5), Q05002.

IPCC (2013), Climate Change 2013: The Physical Science Basis. Working Group I Contribution to the IPCC 5th Assessment Report - Changes to the Underlying Scientific/Technical Assessment*Rep.*, Cambridge, United Kingdom and New York, NY, USA.

Jahn, B.-m., S. Gallet, and J. Han (2001), Geochemistry of the Xining, Xifeng and Jixian sections, Loess Plateau of China: eolian dust provenance and paleosol evolution during the last 140 ka, *Chemical Geology*, *178*(1-4), 71-94.

Jones, D. S. (1980), Annual Cycle of Shell Growth Increment Formation in Two Continental Shelf Bivalves and its Paleoecologic Significance, *Paleobiology*, *6*(3), 331-340.

Kakihana, H., M. Kotaka, S. Satoh, M. Nomura, and M. Okamoto (1977), Fundamental studies on the ion-exchange separation of boron isotopes, *Bull. Chem. Soc. Jpn.*, *50*, 158-163.

Klochko, K., A. J. Kaufman, W. Yao, R. H. Byrne, and J. A. Tossell (2006), Experimental measurement of boron isotope fractionation in seawater, *Earth Planet. Sci. Lett.*, *248*(1-2), 276-285.

Klochko, K., G. D. Cody, J. A. Tossell, P. Dera, and A. J. Kaufman (2009), Re-evaluating boron speciation in biogenic calcite and aragonite using ^{11}B MAS NMR, *Geochim. Cosmochim. Acta*, *73*(7), 1890-1900.

Krabbenhöft, A., J. Fietzke, A. Eisenhauer, V. Liebetrau, F. Bohm, and H. Vollstaedt (2009), Determination of radiogenic and stable strontium isotope ratios ($^{87}Sr/^{86}Sr$; $\delta^{88/86}Sr$) by thermal ionization mass spectrometry applying an $^{87}Sr/^{84}Sr$ double spike, *J. Anal. At. Spectrom.*, *24*(9), 1267-1271.

Krabbenhöft, A., et al. (2010), Constraining the marine strontium budget with natural strontium isotope fractionations ($^{87}Sr/^{86}Sr*$, $\delta^{88/86}Sr$) of carbonates, hydrothermal solutions and river waters, *Geochim. Cosmochim. Acta*, *74*(14), 4097-4109.

Krief, S., E. J. Hendy, M. Fine, R. Yam, A. Meibom, G. L. Foster, and A. Shemesh (2010), Physiological and isotopic responses of scleractinian corals to ocean acidification, *Geochim. Cosmochim. Acta*, *74*(17), 4988-5001.

Kroeker, K. J., R. L. Kordas, R. N. Crim, and G. G. Singh (2010), Meta-analysis reveals negative yet variable effects of ocean acidification on marine organisms, *Ecology Letters*, *13*(11), 1419-1434.

Krogh, T. E. (1964), Strontium isotope variation and whole-rock rubidium-strontium studies in the Grenville province of Ontario, Massachusetts Institute of Technology, Cambridge.

Lemarchand, D., J. Gaillardet, E. Lewin, and C. J. Allegre (2000), The influence of rivers on marine boron isotopes and implications for reconstructing past ocean pH, *Nature*, *408*(6815), 951-954.

Liu, Y.-W. (2010), Natural variation of Sr isotopes in coral Porites collected from Nanwan Bay, southern tip of Taiwan, 1-78 pp, National Taiwan University, Taipei.

Liu, Y.-W., S. M. Aciego, A. D. Wanamaker, and B. K. Sell (2013), A high-throughput system for boron microsublimation and isotope analysis by total evaporation thermal ionization mass spectrometry, *Rapid Commun. Mass Spectrom.*, *27*(15), 1705-1714.

Long, L. E. (1966), Isotope dilution analysis of common and radiogenic strontium using84Sr-enriched spike, *Earth and Planetary Science Letters*, *1*(5), 289-292.

Marchitto, T. M., G. A. Jones, G. A. Goodfriend, and C. R. Weidman (2000), Precise Temporal Correlation of Holocene Mollusk Shells Using Sclerochronology, *Quaternary Research*, *53*(2), 236-246.

Maurer, A.-F., S. J. G. Galer, C. Knipper, L. Beierlein, E. V. Nunn, D. Peters, T. Tütken, K. W. Alt, and B. R. Schöne (2012), Bioavailable ^{87}Sr/^{86}Sr in different environmental samples — Effects of anthropogenic contamination and implications for isoscapes in past migration studies, *Sci. Total Environ.*, *433*, 216-229.

McCulloch, M. T., M. K. Gagan, G. E. Mortimer, A. R. Chivas, and P. J. Isdale (1994), A high-resolution Sr/Ca and δ^{18}O coral record from the Great Barrier Reef, Australia, and the 1982-1983 El Niño, *Geochim. Cosmochim. Acta*, *58*(12), 2747-2754.

McCulloch, M. T., G. Mortimer, T. Esat, L. Xianhua, B. Pillans, and J. Chappell (1996), High resolution windows into early Holocene climate: Sr/Ca coral records from the Huon Peninsula, *Earth Planet. Sci. Lett.*, *138*(1-4), 169-178.

Merrill, A., and J. W. Ropes (1968), The general distribution of the surf clam and ocean quahog *Spisula-solidissima Arctica-islandica*, *Journal of shellfish research*, *59*, 40-45.

Ni, Y., G. L. Foster, T. Bailey, T. Elliott, D. N. Schmidt, P. Pearson, B. Haley, and C. Coath (2007), A core top assessment of proxies for the ocean carbonate system in surface-dwelling foraminifers, *Paleoceanography*, *22*(3).

Nicol, D. (1951), Recent species of the veneroid pelecypod *Arctica*, *Journal of the Washington Academy of sciences*, *41*(3), 102-106.

Nir, O., A. Vengosh, J. S. Harkness, G. S. Dwyer, and O. Lahav (2015), Direct measurement of the boron isotope fractionation factor: Reducing the uncertainty in reconstructing ocean paleo-pH, *Earth Planet. Sci. Lett.*, *414*, 1-5.

Orr, J. C., et al. (2005), Anthropogenic ocean acidification over the twenty-first century and its impact on calcifying organisms, *Nature*, *437*(7059), 681-686.

Osberg, P. H., A. M. Hussey, and G. M. Boone (1985), Bedrock geologic map of Maine, Maine Geological Sruvay, Geologic Map Esries BGMM.

Patchett, P. J. (1980a), Sr isotopic fractionation in Allende chondrules: A reflection of solar nebular processes, *Earth and Planetary Science Letters*, *50*(1), 181-188.

Patchett, P. J. (1980b), Sr isotopic fractionation in Ca-Al inclusions from the Allende meteorite, *Nature*, *283*(5746), 438-441.

Penman, D. E., B. Hönisch, E. T. Rasbury, N. G. Hemming, and H. J. Spero (2012), Boron, carbon, and oxygen isotopic composition of brachiopod shells: Intra-shell variability, controls, and potential as a paleo-pH recorder, *Chem. Geol.*

Purton, L. M. A., G. A. Shields, M. D. Brasier, and G. W. Grime (1999), Metabolism controls Sr/Ca ratios in fossil aragonitic mollusks, *Geology*, *27*(12), 1083-1086.

Raddatz, J., et al. (2013), Stable Sr-isotope, Sr/Ca, Mg/Ca, Li/Ca and Mg/Li ratios in the scleractinian cold-water coral Lophelia pertusa, *Chem. Geol.*, *352*(0), 143-152.

Rae, J. W. B., G. L. Foster, D. N. Schmidt, and T. Elliott (2011), Boron isotopes and B/Ca in benthic foraminifera: Proxies for the deep ocean carbonate system, *Earth Planet. Sci. Lett.*, *302*(3-4), 403-413.

Reynaud, S., N. G. Hemming, A. Juillet-Leclerc, and J.-P. Gattuso (2004), Effect of pCO_2 and temperature on the boron isotopic composition of the zooxanthellate coral *Acropora* sp., *Coral Reefs*, *23*(4), 539-546.

Reynaud, S., C. Rollion-Bard, S. Martin, R. Rolopho-Metalpa, and J.-P. Gattuso (2008), Effect of elevated pCO_2 on the boron isotopic composition into the Mediterranean scleractinian coral *Cladocora caespitosa*, in *Impacts of Acidification on Biological, Chemical, and Physical Systems in the Mediterranean and Black Seas, No 36 in CIESM Workshop Monographs*, edited by F. Briand, pp. 71-75, Monaco.

Riebesell, U., J.-P. Gattuso, T. Thingstad, and J. Middelburg (2013), Preface" Arctic ocean acidification: pelagic ecosystem and biogeochemical responses during a mesocosm study", *Biogeosciences*, *10*(8), 5619-5626.

Rollion-Bard, C., and J. Erez (2010), Intra-shell boron isotope ratios in the symbiont-bearing benthic foraminiferan *Amphistegina lobifera*: Implications for $\delta^{11}B$ vital effects and paleo-pH reconstructions, *Geochim. Cosmochim. Acta*, *74*(5), 1530-1536.

Rollion-Bard, C., D. Blamart, J. Trebosc, G. Tricot, A. Mussi, and J.-P. Cuif (2011a), Boron isotopes as pH proxy: A new look at boron speciation in deep-sea corals using ^{11}B MAS NMR and EELS, *Geochim. Cosmochim. Acta*, *75*(4), 1003-1012.

Rollion-Bard, C., M. Chaussidon, and C. France-Lanord (2011b), Biological control of internal pH in scleractinian corals: Implications on paleo-pH and paleo-temperature reconstructions, *Comptes Rendus Geoscience*, *343*(6), 397-405.

Rüggeberg, A., J. Fietzke, V. Liebetrau, A. Eisenhauer, W.-C. Dullo, and A. Freiwald (2008), Stable strontium isotopes ($\delta^{88/86}Sr$) in cold-water corals — A new proxy for reconstruction of intermediate ocean water temperatures, *Earth Planet. Sci. Lett.*, *269*(3–4), 570-575.

Sabine, C. L., R. A. Feely, N. Gruber, R. M. Key, K. Lee, J. L. Bullister, R. Wanninkhof, C. Wong, D. W. Wallace, and B. Tilbrook (2004), The oceanic sink for anthropogenic CO_2, *Science*, *305*(5682), 367-371.

Sanyal, A., N. G. Hemming, G. N. Hanson, and W. S. Broecker (1995), Evidence for a higher pH in the glacial ocean from boron isotopes in foraminifera, *Nature*, *373*(6511), 234-236.

Schöne, B. R., W. Oschmann, J. Rössler, A. D. F. Castro, S. D. Houk, I. Kröncke, W. Dreyer, R. Janssen, H. Rumohr, and E. Dunca (2003), North Atlantic Oscillation dynamics recorded in shells of a long-lived bivalve mollusk, *Geology*, *31*(12), 1037-1040.

Schöne, B. R., J. Fiebig, M. Pfeiffer, R. Gleβ, J. Hickson, A. L. A. Johnson, W. Dreyer, and W. Oschmann (2005), Climate records from a bivalved *Methuselah* (*Arctica islandica*, Mollusca; Iceland), *Palaeogeography, Palaeoclimatology, Palaeoecology*, *228*(1-2), 130-148.

Schöne, B. R., A. D. Wanamaker Jr, J. Fiebig, J. Thébault, and K. Kreutz (2011a), Annually resolved δ^{13}C shell chronologies of long-lived bivalve mollusks (*Arctica islandica*) reveal oceanic carbon dynamics in the temperate North Atlantic during recent centuries, *Palaeogeography, Palaeoclimatology, Palaeoecology*, *302*(1), 31-42.

Schöne, B. R., Z. Zhang, P. Radermacher, J. Thébault, D. E. Jacob, E. V. Nunn, and A.-F. Maurer (2011b), Sr/Ca and Mg/Ca ratios of ontogenetically old, long-lived bivalve shells (*Arctica islandica*) and their function as paleotemperature proxies, *Palaeogeography, Palaeoclimatology, Palaeoecology*, *302*(1), 52-64.

Schöne, B. R., P. Radermacher, Z. Zhang, and D. E. Jacob (2013), Crystal fabrics and element impurities (Sr/Ca, Mg/Ca, and Ba/Ca) in shells of *Arctica islandica*-Implications for paleoclimate reconstructions, *Palaeogeography, Palaeoclimatology, Palaeoecology*, *373*, 50-59.

Scourse, J. D., C. Richardson, G. Forsythe, I. Harris, J. Heinemeier, N. Fraser, K. Briffa, and P. Jones (2006), First cross-matched floating chronology from the marine fossil record: data from growth lines of the long-lived bivalve mollusc *Arctica islandica*, *The Holocene*, *16*(7), 967-974.

Scourse, J. D., A. D. Wanamaker, Jr., C. R. Weidman, J. Heinemeier, P. J. Reimer, P. G. Butler, R. Witbaard, and C. A. Richardson (2012), The marine radiocarbon bomb pulse across the temperate North Atlantic: a compilation of Delta^{14}C time histories from *Arctica islandica* growth increments, *Radiocarbon*, *54*(2), 165-186.

Shen, C.-C., T. Lee, C.-Y. Chen, C.-H. Wang, C.-F. Dai, and L.-A. Li (1996), The calibration of D[Sr/Ca] versus sea surface temperature relationship for Porites corals, *Geochim. Cosmochim. Acta*, *60*(20), 3849-3858.

Shinjo, R., R. Asami, K.-F. Huang, C.-F. You, and Y. Iryu (2013), Ocean acidification trend in the tropical North Pacific since the mid-20th century reconstructed from a coral archive, *Marine Geology*, *342*, 58-64.

Stemmer, K. (2013), Shell formation and microstucture of the ocean quahog Arctica islandica: Does ocean acidification matter?, 143 pp, Staats- und Universitaetsbibliothek Bremen, Bremen.

Stevenson, E. I., M. Hermoso, R. E. M. Rickaby, J. J. Tyler, F. Minoletti, I. J. Parkinson, F. Mokadem, and K. W. Burton (2014), Controls on stable strontium isotope fractionation in coccolithophores with implications for the marine Sr cycle, *Geochim. Cosmochim. Acta*, *128*, 225-235.

Trotter, J., P. Montagna, M. McCulloch, S. Silenzi, S. Reynaud, G. Mortimer, S. Martin, C. Ferrier-Pagès, J.-P. Gattuso, and R. Rodolfo-Metalpa (2011), Quantifying the pH 'vital effect' in the temperate zooxanthellate coral *Cladocora caespitosa*: Validation of the boron seawater pH proxy, *Earth Planet. Sci. Lett.*, *303*(3-4), 163-173.

Vázquez-Rodrıguez, M., F. Pérez, A. Velo, A. Ríos, and H. Mercier (2012), Observed acidification trends in North Atlantic water masses, *Biogeosciences*, *9*, 5217-5230.

Vollstaedt, H., et al. (2014), The Phanerozoic $\delta^{88/86}$Sr record of seawater: New constraints on past changes in oceanic carbonate fluxes, *Geochim. Cosmochim. Acta*, *128*, 249-265.

Wanamaker Jr., A. D., J. Heinemeier, J. D. Scourse, C. A. Richardson, P. G. Butler, J. Eiríksson, and K. L. Knudsen (2008a), Very long-lived mollusks confirm 17th century AD tephra-based radiocarbon reservoir ages for north Icelandic shelf waters, *Radiocarbon*, *50*(3), 399-412.

Wanamaker Jr., A. D., K. J. Kreutz, B. R. Schöne, N. Pettigrew, H. W. Borns, D. S. Introne, D. Belknap, K. A. Maasch, and S. Feindel (2008b), Coupled North Atlantic slope water forcing on Gulf of Maine temperatures over the past millennium, *Climate Dynamics*, *31*(2-3), 183-194.

Wanamaker Jr., A. D., K. J. Kreutz, B. R. Schöne, K. A. Maasch, A. J. Pershing, H. W. Borns, D. S. Introne, and S. Feindel (2009), A late Holocene paleo-productivity record in the western Gulf of Maine, USA, inferred from growth histories of the long-lived ocean quahog (*Arctica islandica*), *International Journal of Earth Sciences*, *98*(1), 19-29.

Wanamaker Jr., A. D., K. J. Kreutz, B. R. Schöne, and D. S. Introne (2011), Gulf of Maine shells reveal changes in seawater temperature seasonality during the Medieval Climate Anomaly and the Little Ice Age, *Palaeogeography, Palaeoclimatology, Palaeoecology*, *302*(1-2), 43-51.

Wanamaker Jr., A. D., P. G. Butler, J. D. Scourse, J. Heinemeier, J. Eiríksson, K. L. Knudsen, and C. A. Richardson (2012), Surface changes in the North Atlantic meridional overturning circulation during the last millennium, *Nature Communications*, *3*(899).

Weber, J. N. (1973), Incorporation of strontium into reef coral skeletal carbonate, *Geochim. Cosmochim. Acta*, *37*(9), 2173-2190.

Weidman, C. R., and G. A. Jones (1993), A Shell-Derived Time History of Bomb ^{14}C on Georges Bank and Its Labrador Sea Implications, *Journal of Geophysical Research*, *98*(C8), 14,577-514,588.

Weidman, C. R., G. A. Jones, and L. Lohman (1994), The long-lived mollusc *Arctica islandica*: A new paleoceanographic tool for the reconstruction of bottom temperatures for the continental shelves of the northern North Atlantic Ocean, *Journal of Geophysical Research*, *99*(C9), 18,305-318,314.

Weidman, C. R. (1995), Development and Application of the Mollusc *Arctica Islandica* as a Paleoceanographic Tool for the North Atlantic Ocean, Cambridge.

Widerlund, A., and P. S. Andersson (2006), Strontium isotopic composition of modern and Holocene mollusc shells as a palaeosalinity indicator for the Baltic Sea, *Chem. Geol.*, *232*(1-2), 54-66.

Witbaard, R., and M. J. N. Bergman (2003), The distribution and population structure of the bivalve *Arctica islandica L.* in the North Sea: what possible factors are involved?, *Journal of Sea Research*, *50*(1), 11-25.

Yan, H., D. Shao, Y. Wang, and L. Sun (2013), Sr/Ca profile of long-lived Tridacna gigas bivalves from South China Sea: A new high-resolution SST proxy, *Geochim. Cosmochim. Acta*, *112*, 52-65.

Yu, K.-F., J.-X. Zhao, G.-J. Wei, X.-R. Cheng, T.-G. Chen, T. Felis, P.-X. Wang, and T.-S. Liu (2005), $\delta^{18}O$, Sr/Ca and Mg/Ca records of Porites lutea corals from Leizhou Peninsula, northern South China Sea, and their applicability as paleoclimatic indicators, *Palaeogeography, Palaeoclimatology, Palaeoecology*, *218*(1-2), 57-73.

Zhang, Z. (2009), Geochemical properties of shells of *Arctica islandica* (Bivalvia)- implications for environmental and climatic change, 109 pp, Frankfurt.

Chapter IV Geochemical constraints on the vesicle pH of the coccolithophore *Pleurochrysis carterae* and its response to CO$_2$-induced ocean acidification

Yi-Wei Liu[1, *], Rob Eagle[2], Sarah M. Aciego[1], Justin B. Ries[3], Rosaleen Gilmore[2], and Whitney Doss[2, 4]

1. Department of Earth and Environmental Sciences, University of Michigan, 1100 N. University Avenue, Ann Arbor, MI 48109-1005, USA

2. Department of Earth, Planetary, and Space Sciences, University of California, Los Angeles, 595 Charles Young Drive East, Los Angeles, CA 90095-1567, USA

3. Department of Marine and Environmental Sciences, Marine Science Center, Northeastern University, Nahant, MA 01908, USA

4. Institute of Arctic and Alpine Research, University of Colorado, 1560 30th street, Boulder, CO 80303, USA

IV.1 Abstract

Coccolithophorid algae is one of the most important marine calcifying organisms and play an important role in carbon sequestration, therefore it is crucial to understand the potential impacts form CO$_2$-induced ocean acidification on coccolithophore. Here we used multiple geochemical approaches to constrain the potential impacts from ocean

acidification to phytoplankton coccolithophore species *Pleurochrysis carterae* (*P. carterae*) to investigate its adaptation ability to the changing envrironment. A CO_2 addition culture experiments was conducted, and culture water temperature, salinity, dissolve inorganic carbon (DIC) and alkalinity were monitored to deconvolve the carbonate system in different treatments. Our coccolith particulate inorganic carbon (PIC) and particulate organic carbon (POC) results suggest this coccolithophore species would not change their photosynthesis to calcification strategies with respect to decreasing ambient seawater pH. Coccolith boron isotopic composition indicates *P. carterae* would regulate their internal pH for calcification and therefore it is insensitive to ocean acidification. We also observe positive correlations between carbon isotopic composition in PIC and POC, suggesting that there is a shared internal inorganic carbon pool for both calcification and photosynthetic processes. In addition, we observed that the $\delta^{13}C$ became more depleted in ^{13}C under low pH. This result indicates that *P. carterae* might change the uptake of inorganic carbon species from HCO_3^- to CO_2. Therefore, in a more acidic environment, they would have more CO_2 available for calcification and photosynthesis. Our study suggests the ability for *P. carterae* to adapt to ocean acidification and therefore this species could potentially store more carbon and be used as a biofuel in the elevated atmospheric CO_2 future.

IV.2 Introduction

One impact of anthropogenic CO_2 is ocean acidification: decreasing seawater pH will reduce the carbonate saturation state and could potentially dissolve the carbonate shells or skeletons of calcifying organisms and/or inhibit growth of their carbonate structures (Anthony *et al.*, 2008; Bednarsek *et al.*, 2012; Talmage and Gobler, 2010). However, it has also been suggested that calcifying organisms will adapt to a more acidic environment by changing production of organic and inorganic carbon (Delille *et al.*, 2005; Krief *et al.*, 2010) or self-regulate the pH of their calcifying fluid (Allison *et al.*, 2014; Ries, 2011; Trotter *et al.*, 2011). Previous culture experiment studies suggest that organisms have mixed calcification responses to different pCO_2 treatments, with some species increasing their calcification in a more acidic environment by pumping H^+ from

their calcifying solution, or by the preferential uptake of HCO_3^- for calcification (Ries *et al.*, 2009). These mixed responses show the complexity of ocean acidification impacts and therefore it is crucial to investigate organisms that play strong roles in the carbon cycle in order to make predictions about ocean ecosystem response to anthropogenic CO_2. In particular, we need to understand the mechanism for survival and adaptation of marine calcifiers in the ocean: (1) the biological strategy for using additional CO_2: either increased photosynthesis or calcification or both, (2) the internal pH regulation required for higher calcification, and (3) their utilization of different dissolved carbon species. Here we address these questions for the marine calcifier coccolithophore *Pleurochrysis cartarae*.

Coccolithophore is a unicellular flagellate species with the ability to produce external calcify plates (coccoliths) that cover their surface. The distribution of coccolithophore in the ocean ranges from tropical to sub-polar (Balestra *et al.*, 2004; Winter *et al.*, 1994). It is one of the most important marine calcifiers in the ocean, accounting for almost half of $CaCO_3$ production (Moheimani *et al.*, 2012; Westbroek *et al.*, 1989). Therefore, the adaptation of coccolithophore to different pCO_2 level is important for evaluating potential carbon sequestration in ocean sediments.

Pleurochrysis carterae (P. carterae) is a motile species coccolithophore with only a single layer of coccoliths that cover the surface of individual cells. The coccoliths are normally oval shaped, composed of a base of organics and rim of calcite. In the temperature range 23 to 28 °C, typical *P. carterae* $CaCO_3$ content and lipid contents are ~12 % and ~22.5 % of the total dry weight, respectively (Moheimani, 2005). Different from the well studied coccolithophore species *Emilianian huxleyi (E. huxleyi)*, which do not possess any organic base-plate scale associated with the mature coccolith, *P. carterae* has a relatively high organic content and therefore has the potential to fix carbon in the organic lipid content, which can be extracted as a liquid biofuel (Moheimani and Borowitzka, 2006; Moheimani *et al.*, 2012; Rahbari, 2009). Because these phytoplankton store carbon both organically and inorganically, large scale culturing of *P. carterae* may be a carbon sequestration solution to combat increasing atmospheric anthropogenic CO_2 (Moheimani *et al.*, 2012; Rahbari, 2009). Therefore,

more studies are required to investigate how this particular species responds to increasing pCO_2 concentration.

In order to understand the inorganic carbon uptake mechanisms of *P. carterae* and further evaluate the potential in carbon sequestration, culture experiments have been undertaken to compare the responses of this species to other coccolithophores, including *E. huxleyi*. *Emilianian huxleyi* is widely studied for their use of carbon species in photosynthesis and calcification and many of the studies suggest HCO_3^- is the primary source of inorganic carbon for calcification and might also play an important role for photosynthesis (Bach *et al.*, 2013; Buitenhuis *et al.*, 1999; Dong *et al.*, 1993; Herfort *et al.*, 2002; Nimer *et al.*, 1992; Nimer and Merrett, 1992; Paasche, 1964). Due to different organic and inorganic growth patterns with respect to elevated pCO_2 under fixed and dynamic pH environments it has been suggested that *P. carterae* uses the CO_2 species for both calcification and photosynthesis (Moheimani and Borowitzka, 2011). However, there is no direct evidence to support this hypothesis as of yet.

We cultured *P. carterae* under differing pCO_2 (and pH) conditions. We assess their photosynthetic and calcification response to the changing available of CO_2 using their PIC/POC ratio, their ability to regulate their internal pH and subsequently their calcification using boron isotopes as a pH proxy, and their carbon species utilization using traditional stable isotopes.

IV.3 Results and Discussion

The carbonate chemistry of the culture experiment is plotted in Figure S. 1. We observed a rise in pH in the last week of culturing, especially for the strain 874, with the highest pH (pH = 9) found in the 750 ppmv pCO_2 treatments. This change in growth medium pH agrees with previous studies, where *P. carterae* raised the growth medium pH to 9 during their logarithmic growth period in small-scale culture experiments (Crenshaw, 1965; Moheimani, 2005). In larger-scale outdoor raceway experiments, the pH was shown to be as high as pH 11 depending on the health of the coccolithophores, sometimes with a pH diurnal variation to a peak high in the daytime and a drop back to

baseline in dark periods (Moheimani, 2005; Moheimani and Borowitzka, 2006; 2011; Moheimani et al., 2012). These results suggest that P. carterae might occasionally change their ambient seawater pH and this might correlate with the balance between calcification and photosynthesis (Moheimani, 2005). For the purpose of evaluating the effects of different pCO_2 concentration, we compare all the data to the average of the background seawater pH (pH_{sw}), excluding the high pH spike at the end of the experiment.

IV.3.1 PIC/POC: No distinctive change in photosynthetic and calcification response to the changing available of CO_2

The particulate organic carbon (POC) content and particulate inorganic carbon (PIC) content range from 43 % to 57 % and 8 % to 30 % of the organic and inorganic dry weights, respectively (Figure IV. 1 (a)). The PIC/POC ratios are between 0.18 and 0.69. We find no distinguishable trend in either PIC or POC content, or the PIC/POC ratio (Figure IV. 1 (b)).

The lack of correlation in PIC, POC, and PIC/POC as a function of ambient seawater pH, or pH_{sw} (see discussion below), suggests that P. carterae does not change growth strategy with increasing pCO_2. Similar results have been reported from Casareto et al. (2009) and Seki et al. (1995). Casareto et al. (2009) found that both of the inorganic and organic production increased compare to initial doping of coccolithophore cells and suggest the decreasing in the PIC/POC ratio after 7 days was due to the higher magnitude of POC production compare to that in the initial condition. They proposed that biological processes such as photosynthesis or organic carbon production are more important than physic-chemical reactions in determining calcification and dissolution of P. carterae. However, both studies from Seki et al. (1995) and Casareto et al. (2009) show no differences in the PIC/POC ratios within the pCO_2 range of our study. Additionally, the carbonate chemistry in this culture experiment suggests that the seawater pH changed from 8.36 to 7.99 with extraction and addition of CO_2. The consistent PIC/POC results under different pCO_2 treatments indicate that both organic and inorganic growth in P. carterae is insensitive to pH decline within this pH range.

Based on SEM examination, we do not find obvious a size change at the single coccolith scale or coccolithophorid sphere. We find no clear change in the coccolith scale thickness either. However, we do find malformation of the cocolith scales when the pH is below 8.08. Blocky coccoliths are observed, indicating partial dissolution or remineralization on the surface (Table S.1). However, increasing DIC may enhance both calcification and photosynthesis in *P. carterae* by providing more inorganic carbon source so that the balance between calcification and dissolution results in similar PIC/POC results even under low pH treatments.
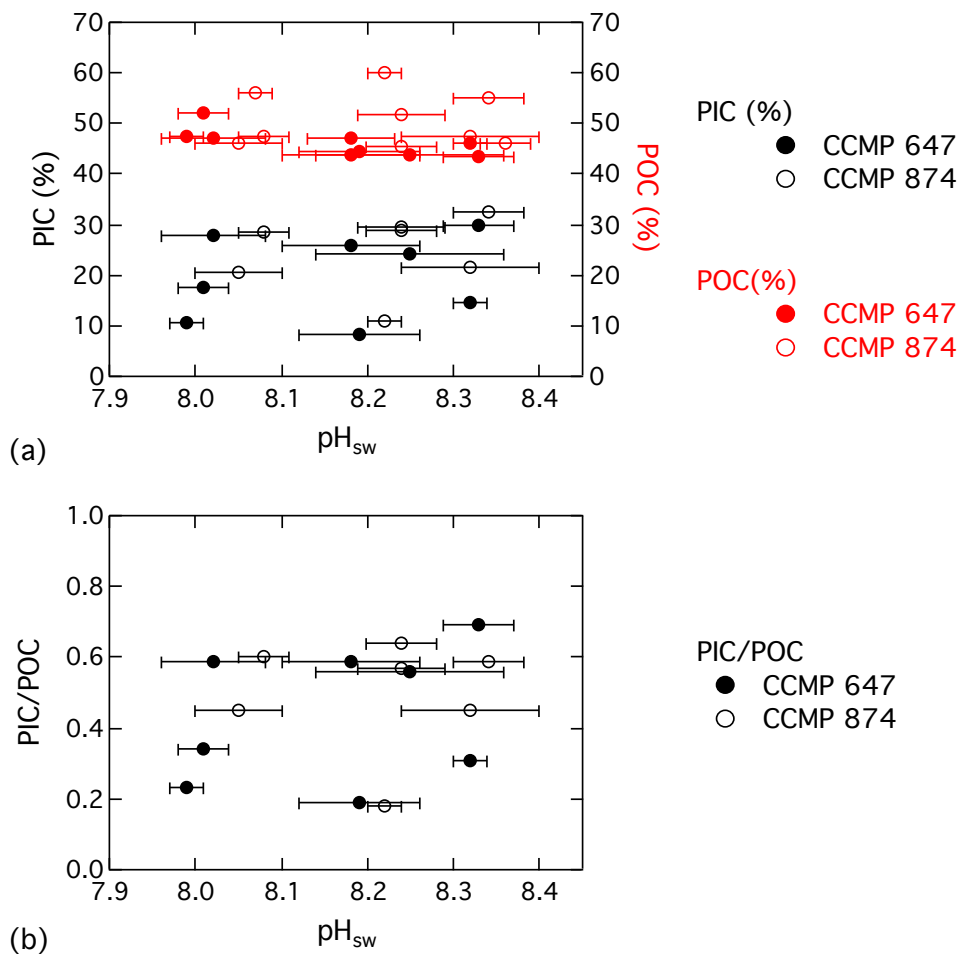
Figure IV. 1 The (a) particulate inorganic carbon (PIC) content in weight percent of inorganic sample dry weight and particulate organic carbon (POC) content in weight percent of organic sample dry weight, and (b) the PIC/POC ratio as a function of ambient seawater pH.

IV.3.2 δ^{11}B as a vesicle pH indicator: Internal pH regulation in coccolithophore species *P. carterae*

Here we use stable isotopes of boron to assess internal pH regulation. The boron isotopic composition of the growth medium synthetic seawater has an average value of 0.74 ± 1.43 ‰ (n = 23, 2 σ), about 39 ‰ lower than natural seawater. There are two dominated boron species in seawater, with boric acid ($B(OH)_3$) most abundant at low pH and borate ($B(OH)_4^-$) dominant at high pH. Because ^{11}B is enriched in $B(OH)_3$ compared to $B(OH)_4^-$, and the relative proportion of these two species in the aqueous environment is a function of pH, the δ^{11}B in $B(OH)_4^-$ should be pH dependent, and increasingly fractionate from seawater δ^{11}B as the pH decreases (Hemming and Hanson, 1992). Assuming only $B(OH)_4^-$ is incorporated into carbonate and there is no vital effect, coccolith samples record the boron isotopic composition fractionated from the synthetic seawater boron isotope baseline.

The δ^{11}B of cultured coccoliths ranges from -15 ‰ to -25 ‰, which is in a reasonable range for the δ^{11}B in $B(OH)_4^-$ with pH between 8 to 8.5 in synthetic seawater. However, there is no correlation between coccolith δ^{11}B and ambient seawater pH (Figure S. 2). Marine calcifiers likely regulate their internal pH for calcification (Allison *et al.*, 2014; Ries, 2011; Trotter *et al.*, 2011), therefore we also calculate the pH difference between coccolithophore calcifying pH, hereafter referred to as vesicle pH, and the ambient seawater pH (ΔpH = pH$_{vesicle}$ - pH$_{sw}$). We find a negative correlation between ΔpH and pH$_{sw}$ (R^2 = 0.43), neglecting one data point with a large error bar that is likely an outlier in this study.

Although there is no correlation between coccolith δ^{11}B and ambient seawater pH, there is a correlation between ΔpH and pH$_{sw}$. It has been suggested that many marine calcifying organisms raise the pH at calcification sites to achieve carbonate saturation for $CaCO_3$ calcification (Allison *et al.*, 2014; Ries, 2011; Trotter *et al.*, 2011). This pH up-regulation can also be triggered by other environmental factors (e.g., certain temperature thresholds) (Liu *et al.*, 2015). Therefore, the pH$_{vesicle}$ is not sensitive to

changing pH_{sw}, instead, ΔpH reflects the responses of calcifying organisms to ocean acidification. The strong correlation between ΔpH and pH_{sw} in this study indicates that the coccolithophore species *P. carterae* raises the calcification pH for calcite coccolith precipitation.

The fact of pH-regulation in the cell can also support the observation of constant PIC/POC ratio. Ariovich and Pienaar (1979) demonstrated that coccolith production is a fairly rapid process by decalcifying the cells to appear naked through dissolution. After they placed the cells back to medium with normal pH (8 – 8.3) and exposed to light, after 12 hours a completely new set of coccoliths cover the entire cell. Our boron isotopic results suggest that even under more acidic conditions coccolithophore regulate their vesicle pH to be more alkaline than the external environment so that calcification is not affected by ambient pH. Therefore rapid precipitation can overcome the coccolith dissolution we observed from SEM images for low pH treatments.
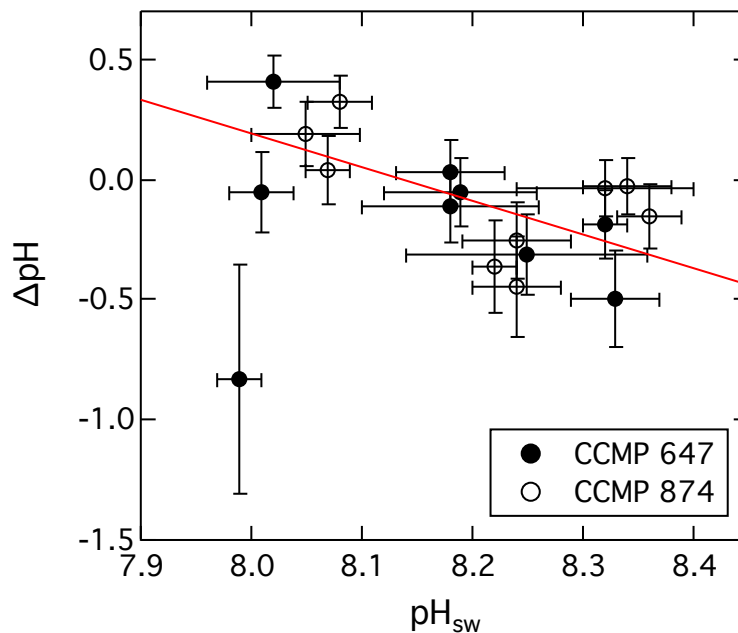
Figure IV. 2 **The pH offset between coccolith calcification site and ambient seawater (ΔpH) plotted with respect to the ambient seawater pH**
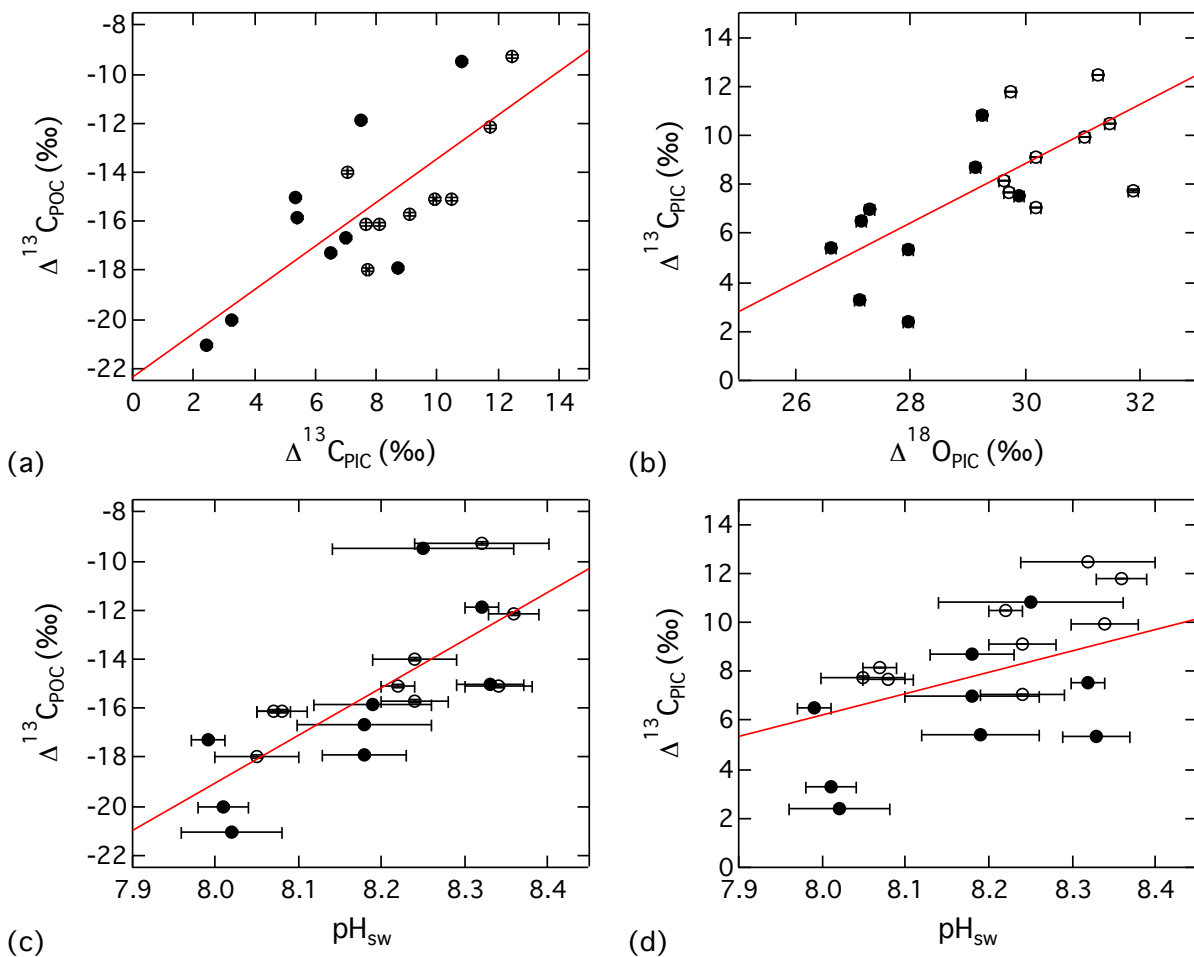
IV.3.3 Stable carbon and oxygen isotopic composition in organic and inorganic portion of *P. carterae*: switch mode from HCO_3^- to CO_2 for calcification and photosynthesis

The $\delta^{13}C_{PIC}$ and $\delta^{13}C_{POC}$ range from -25 ‰ to 5 ‰ and from -45 ‰ to -20 ‰, respectively. The addition of compressed CO_2 gas resulted in very depleted $\delta^{13}C$ values in the 280 ppmv and 750 ppmv treatments; therefore, a calibrated $\Delta^{13}C$ value is calculated for all the measurements, with $\Delta^{13}C$ is defined as the offset from the corresponding $\delta^{13}C_{DIC}$. The calculated $\Delta^{13}C_{PIC}$ and $\Delta^{13}C_{POC}$ range from 2 ‰ to 13 ‰ and -22 ‰ to -8 ‰, respectively. Both the $\Delta^{13}C_{PIC}$ and $\Delta^{13}C_{POC}$ values decrease with decreasing pH_{sw} (Figure IV. 3 (c) and (d)). The offset between $\Delta^{13}C_{PIC}$ and $\Delta^{13}C_{POC}$ under different treatments are constant, with the organic carbon isotopic composition about 25 ‰ lighter than the inorganic carbon isotopic composition. There is a positive correlation between the $\Delta^{13}C_{PIC}$ and $\Delta^{13}C_{POC}$ values ($R^2 = 0.58$, $p < 0.001$) (Figure IV. 3 (a)). Comparison of the carbon isotopic compositions to medium pH results in a negative correlation ($R^2 = 0.58$) between $\Delta^{13}C_{POC}$ and seawater pH and a weaker negative correlation between $\Delta^{13}C_{PIC}$ and seawater pH. The coccolith $\delta^{18}O$ ($\delta^{18}O_{PIC}$) values range from -4.5 ‰ to -0.5 ‰. After normalizing to the corresponding culture medium $\delta^{18}O$, the calibrated $\Delta^{18}O_{PIC}$ ($\Delta^{18}O_{PIC} = \delta^{18}O_{PIC} - \delta^{18}O_{sw}$; VPDB) values range from 26 ‰ to 32 ‰. A positive correlation between $\Delta^{18}O_{PIC}$ and $\Delta^{13}C_{PIC}$ was found, with $R^2 = 0.52$ (Figure IV. 3 (b)).

The strong lineation between $\Delta^{13}C_{PIC}$ and $\Delta^{13}C_{POC}$ with changing pH_{sw} indicates that carbon isotopic fractionation in both PIC and POC, with respect to different pCO_2 conditions, are driven by the same mechanism and the responses are tightly linked. The positive correlation implies the carbon source for calcification and photosynthesis primarily is derived from the same internal pool. However, both $\Delta^{13}C_{PIC}$ and $\Delta^{13}C_{POC}$ became lighter with decreasing pH (increasing DIC), suggesting the carbon source for the internal pool changed: more CO_2 was actively pumped into the cell membrane instead of HCO_3^-. In this study, the overall fractionation of inorganic and organic carbon from low pH to high pH was about 10 ‰. As Zeebe and Wolf-Gladrow (2001) have

shown, the $\delta^{13}C$ in $CO_{2(aq)}$ is about 9 ‰ lower than that in HCO_3^- at equilibrium under the same $\delta^{13}C_{DIC}$ at 25 °C and 35 psu, which supports the idea that at low pH, CO_2 will be the primary carbonate species for both calcification and photosynthesis. Instead of having an active CO_2 pump, the ^{13}C depletion can also be explained with by less selective uptake between CO_2 and HCO_3^- under high DIC environment. In either case, more ^{13}C depleted inorganic carbon is incorporated into the internal pool for calcification and photosynthesis of *P. carterae* and causes a negative correlation of $\Delta^{13}C_{PIC}$ to pH_{sw} and $\Delta^{13}C_{POC}$ to pH_{sw}.

The carbonate species is then redistributed in the ^{13}C-depleted internal medium and utilized for calcification and photosynthesis. Because the two processes use inorganic carbon from this internal pool, the inorganic and organic carbon isotopic composition should fractionate from the common pool in the same way. Therefore, we observe a constant offset between $\Delta^{13}C_{PIC}$ and $\Delta^{13}C_{POC}$ under different pCO_2 treatments. The stable oxygen isotopic composition in coccolithophore *P. carterae* also supports the existence of an internal pool for calcification. In a closed system, the isotopic composition of both $CaCO_3$ precipitation and the residual solution will follow Rayleigh equations and become lighter as more $CaCO_3$ precipitates. Although the inorganic carbon uptake changes under different pCO_2 treatments, the changing carbonate species barely changes the oxygen isotopic composition owing to the abundance of water in the pool. An internal Rayleigh distillation then results in a depletion of the oxygen isotopic composition in the precipitated $CaCO_3$.

Figure IV. 3 The comparisons between (a) organic and inorganic carbon isotopic composition and (b) inorganic carbon and oxygen isotopic compositions, and organic and inorganic carbon isotopic composition as a function of ambient seawater pH (c) (d).
The

IV.3.4 Potential mechanism for the adaptation of coccolithophore *P. carterae* to increasing CO_2

We propose a carbon uptake model for *P. carterae*. In general, the coccolithophore has an internal pool for both calcification and photosynthesis. The preferential uptake of light isotopes for photosynthesis results in an ~25 ‰ offset between organic carbon isotopic composition and inorganic carbon isotopic composition in the coccoliths. When the ambient seawater pH decreases, indicating an increasing DIC concentration in the seawater, the active pumping of dissolved CO_2 species instead of HCO_3^-, or a less selective of inorganic carbonate species results in ^{13}C depletion in the internal pool and

hence decreases both $\delta^{13}C_{PIC}$ and $\delta^{13}C_{POC}$. Because the coccolithophore *P. carterae* up-regulates internal pH for calcification, decreasing ambient pH does not affect the calcification of *P. carterae*. The increasing DIC concentration under lower ambient pH results in inorganic carbon saturation for both photosynthesis and calcification in *P. carterae* and therefore maintaining or even enhancing those processes. Therefore rapid production of coccoliths compromises the dissolution from the surface so that the PIC/POC ratio does not change with decreasing ambient seawater pH.

Although the lowest pH in this culture experiment was no lower than 7.9, our results suggest that the coccolithophore species *P. carterae* adapts to an acidified environment by changing the inorganic carbon uptake mode for both photosynthesis and calcification. Our results also suggest that not all marine calcifiers are sensitive to ocean acidification, and some marine calcifying organisms may act as bioremediators to ocean acidification. Our result show opposite response of the coccolithophore species *P. carterae* from the expectation that the growth of marine calcifying organisms will be inhibited by ocean acidification. More studies are required to examine the differing biological response to decreasing seawater pH in marine calcifying organisms.

IV.4 Methods

Two strains of coccolithophore species *Pleurochtrysis carterae*, CCMP 647 and CCMP 874, were cultured in synthetic seawater medium made from commercial seasalt (Instant Ocean (Atkinson; Marulla and O'Toole, 2005a; b)) from 13 December 2011 to 8 January 2012 (CCMP 647) and 11 January 2012 to 28 January 2012 (CCMP 874) at the University of North Carolina-Chapel Hill. Each strain was split into nine individual treatments with triplicates targeting 280, 400 and 750 ppmv pCO_2 using CO_2 bubbling. The three pCO_2 levels were designed to mimic atmospheric carbon dioxide concentrations before the industrial revolution, current atmospheric conditions and future projections. The depleted pCO_2 level, ~280 ppmv, was achieved by mixing pure CO_2 and CO_2-free compressed gases, the ~400 ppmv pCO_2 was bubbled with ambient airflow, and the enriched pCO_2 level, ~750 ppmv, was achieved by mixing ambient air and pure CO_2 compressed gas. The cultures were maintained at stable temperature (25

°C) and salinity (32 psu) on a 16-8 hour light-dark cycle in 10-gallon boxes with the same initial dose of coccolithophore cells (~400 ± 40 cell/L). Seawater temperature, salinity, pH, alkalinity, and DIC were monitored once a week and alkalinity and DIC measurements were used to calculate carbon system speciation with the program CO2SYS. Coccoliths were harvested after three weeks for strain CCMP 647 and two weeks for strain CCMP 874. About 10 – 15 generations of coccolithophorid growth were expected to ensure the adaptation to the treated environments. The coccolithophore were filtered, cleaned and stored in ethanol to prevent organic growth or dissolution.

Samples were cleaned and prepared for chemical analysis under class 10 laminar flow hoods in a class 10,000 clean room in the Glaciochemistry and Isotope Geochemistry Laboratory, Department of Earth and Environmental Sciences, University of Michigan. About 10 µl of the coccolith-ethonal mixture was extracted and dried directly for SEM examination. Coccolith samples were then rinsed with Super-Q (SQ) water (Millipore, > 18.2 MΩ) three times and then split into three splits, with about 1 – 1.5 mg of dry samples for total carbon, 0.5 – 1 mg of dry samples for total organic carbon and at least 2 mg of dry samples for inorganic carbon and oxygen isotopes, trace elements, boron and strontium isotopes measurements. Sample splits for total organic carbon were treated with 2 % HCl to remove calcium carbonate overnight, the dissolved solutions were pipetted after centrifuging followed by rinsing three times with SQ water. Samples for inorganic elemental and isotopic measurements were treated with 10 % H_2O_2 overnight. After centrifuging and removal of suspended solution, samples were then rinsed with SQ water, 0.001 N HNO_3 and SQ water again to prevent recoil of organics or dusts onto the samples. About 30 – 100 ng of clean samples were prepared for inorganic $\delta^{13}C$ and $\delta^{18}O$; over 1 mg of clean samples were dissolved into 1.7 N HCl for targeted [B] = ~750 ppb. Ten µl of the sample solution were split into a new beaker, dried at 30 °C and redissolved into concentrated HNO_3 and dried at 30 °C again to transform to nitric form for trace element analysis. The sample solutions were treated with 10 µl of concentrated HNO_3 and 10 µl of 30 % H_2O_2 seven times to remove any residual organic material.

Total carbon was analyzed using a Costech ECS 4010 elemental analyzer hosted in the Oceanography and Marine Geology Laboratory in the Department of Earth and Environmental Sciences at the University of Michigan. Samples were weighed and wrapped in tin foil capsules for combustion. Acetanilide standard was used to calibrate carbon responses with respect to the sample weight and the reproducibility of the weight percent is 70.83 ± 1.08 % (1 σ, n = 6).

Total organic carbon content and $\delta^{13}C$ were performed at the University of Michigan Stable Isotope Laboratory on a Costech ECS 4010 elemental analyzer coupled to the inlet of a Finnigan Delta V Plus mass spectrometer operating in continuous flow mode. About 200 to 600 µg of organic samples were weighed in tin foil capsules. Acetanilide standard was used to calibrate organic carbon weight percent, and additional IAEA 600 Caffeine and IAEA-CJ-6 Sucrose standards were used to calibrate the organic $\delta^{13}C$ values. The reproducibility for Acetanillide carbon weight percent is 71.26 ± 0.95 % (1 σ, n = 11) and the precision for the organic $\delta^{13}C$ values are -33.75 ± 0.07 ‰, -27.77 ± 0.06 ‰ and -10.45 ± 0.05 ‰ for Acitanillide, IAEA 600 Caffeine and IAEA-CJ-6 Sucrose standards, respectively.

The $\delta^{13}C$ and $\delta^{18}O$ in coccolilth calcite were analyzed by Finnigan MAT Kiel IV preparation device coupled directly to the inlet of a Finnigan MAT 253 triple collector isotope ratio mass spectrometer hosted in the Stable Isotope Laboratory in the Department of Earth and Environmental Sciences at the University of Michigan. The precisions of measurements were monitored with NBS 19 standard ($\delta^{13}C$ = 1.96 ± 0.07 ‰ and $\delta^{18}O$ = -2.24 ± 0.07 ‰; 1 σ, n = 10). The culture seawater oxygen isotopes were analyzed by Picarro L2120-i Cavity Ringdown Spectrometer equipped with the A0211 high-precision vaporizer, autosampler and ChemCorrect software in the University of Michigan Water Isotopes Lab. The water $\delta^{18}O$ values were calibrated to VSMOW/VSLAP using three internal laboratory standards and the typical analytical precision is better than 0.1 ‰. To calculate the $\Delta^{18}O_{PIC}$ ($\Delta^{18}O_{PIC} = \delta^{18}O_{PIC} - \delta^{18}O_{sw}$) values, the water $\delta^{18}O$ values were converted to VPDB scale with the relationship: $\delta^{18}O_{VPDB} = 0.97001 \times \delta^{18}O_{VSMOW} - 29.99$ (‰) (Brand *et al.*, 2014; Coplen *et al.*, 2002).

All coccolith δ^{13}C and δ^{16}O results are reported relative to the VPDB (Vienna Pee Dee

Belemnite) standard $\left(\delta^{13}C = \left[\frac{(^{13}C/^{12}C)_{sample}}{(^{13}C/^{12}C)_{VPDB}} - 1 \right] \times 1000 \; (\text{‰}); \; \delta^{18}O = \left[\frac{(^{18}O/^{16}O)_{sample}}{(^{18}O/^{16}O)_{VPDB}} - \right.$

$\left. 1 \right] \times 1000 \; (\text{‰}) \right)$. Weight percent particulate inorganic carbon was calculated by

subtracting organic carbon weight from the total carbon weight and dividing by the total

inorganic weight. The PIC/POC ratios were then obtained from the ratio of particulate

inorganic weight percent to particulate organic weight percent.

Boron isotopes were examined in this study to determine the calcification pH of the

coccolithophore. Both culture seawater and coccolith samples were measured followed

the method from Liu *et al.* (2013). Boron isotopic analysis were conducted a Thermo

Fisher Triton PLUS multicollector thermal ionization mass spectrometer operating in

negative ion mode for boron isotope analysis at the Glaciochemistry and Isotope

Geochemistry Lab (GIGL) at the Department of Earth and Environmental Sciences,

University of Michigan. Boron isotopic composition in seawater and coccolith samples

were reported as δ^{11}B, where $\delta^{11}B = \left[\frac{(^{11}B/^{10}B)_{sample}}{(^{11}B/^{10}B)_{SRM\ 951a}} - 1 \right] \times 1000 \; (\text{‰})$, with ^{11}B/^{10}B for

boric acid standard SRM 951a is 4.0345 ± 0.0084 (2 σ, n = 24). The reproducibility (2 σ)

of δ^{11}B in seawater and carbonate samples are 1.13 and 1.83 ‰, respectively (Liu *et al.*,

2015). A δ^{11}B-pH transfer equation was used to calculate coccolithophore vesicle pH:

$$pH = pK_b - \log \left(\frac{\delta^{11}B_{sw} - \delta^{11}B_{carbonate}}{\alpha\delta^{11}B_{carbonate} - \delta^{11}B_{sw} + 1000(\alpha-1)} \right) \qquad \text{(Eq. IV.1)}$$

 Average values of synthetic seawater temperature, salinity and δ^{11}B values were used

for the vesicle pH in different treatments.

IV.5 Acknowledgments

IV.7 References

Allison, N., I. Cohen, A. A. Finch, J. Erez, and A. W. Tudhope (2014), Corals concentrate dissolved inorganic carbon to facilitate calcification, *Nat Commun*, *5*.

Anthony, K. R. N., D. I. Kline, G. Diaz-Pulido, S. Dove, and O. Hoegh-Guldberg (2008), Ocean acidification causes bleaching and productivity loss in coral reef builders, *Proceedings of the National Academy of Sciences*, *105*(45), 17442-17446.

Ariovich, D., and R. N. Pienaar (1979), The role of light in the incorporation and utilization of Ca++ ions by Hymenomonas carterae (Braarud et Fagerl.) Braarud (Prymnesiophyceae), *British Phycological Journal*, *14*(1), 17-24.

Atkinson, M. Elemental composition of commercial seasalts, *Journal of Aquariculture and Aquatic Sciences*, *8*(2), 39.

Bach, L. T., L. C. M. Mackinder, K. G. Schulz, G. Wheeler, D. C. Schroeder, C. Brownlee, and U. Riebesell (2013), Dissecting the impact of CO_2 and pH on the mechanisms of photosynthesis and calcification in the coccolithophore *Emiliania huxleyi*, *New Phytol.*, *199*(1), 121-134.

Balestra, B., P. Ziveri, S. Monechi, and T. Simon (2004), Coccolithophorids from the Southeast Greenland Margin (Northern North Atlantic): Production, Ecology and the Surface Sediment Record, *Micropaleontology*, *50*, 23-34.

Bednarsek, N., et al. (2012), Extensive dissolution of live pteropods in the Southern Ocean, *Nature Geosci*, *5*(12), 881-885.

Brand, W. A., T. B. Coplen, J. Vogl, M. Rosner, and T. Prohaska (2014), Assessment of international reference materials for isotope-ratio analysis (IUPAC Technical Report), *Pure Appl. Chem.*, *86*(3), 425.

Buitenhuis, E. T., H. J. W. De Baar, and M. J. W. Veldhuis (1999), PHOTOSYNTHESIS AND CALCIFICATION BY EMILIANIA HUXLEYI (PRYMNESIOPHYCEAE) AS A FUNCTION OF INORGANIC CARBON SPECIES, *Journal of Phycology*, *35*(5), 949-959.

Casareto, B. E., M. P. Niraula, H. Fujimura, and Y. Suzuki (2009), Effects of carbon dioxide on the coccolithophorid Pleurochrysis carterae in incubation experiments, *Aquatic Biology*, *7*(1-2), 59-70.

Coplen, T. B., et al. (2002), Compilation of Minimum and Maximum Isotope Ratios of Selected Elements in Naturally Occurring Terrestrial Materials and Reagents, *Geological Survey Water-Resources Investigations Report*, *01-4222*.

Crenshaw, M. A. (1965), [Intracellular] Coccolith formation by two marine coccolithophorids, *Coccolithus huxleyi Hymenomonas* sp., *DISS ABSTR*, *25*(11), 6722.

Delille, B., et al. (2005), Response of primary production and calcification to changes of pCO_2 during experimental blooms of the coccolithophorid *Emiliania huxleyi*, *Global Biogeochem. Cycles*, *19*(2), GB2023.

Dong, L. F., N. A. Nimer, E. Okus, and M. J. Merrett (1993), Dissolved Inorganic Carbon Utilization in Relation to Calcite Production in *Emiliania huxleyi* (Lohmann) Kamptner, *New Phytol.*, *123*(4), 679-684.

Hemming, N. G., and G. N. Hanson (1992), Boron isotopic composition and concentration in modern marine carbonates, *Geochim. Cosmochim. Acta*, *56*(1), 537-543.

Herfort, L., B. Thake, and J. Roberts (2002), Acquisition and Use of Bicarbonate by *Emiliania huxleyi*, *New Phytol.*, *156*(3), 427-436.

Krief, S., E. J. Hendy, M. Fine, R. Yam, A. Meibom, G. L. Foster, and A. Shemesh (2010), Physiological and isotopic responses of scleractinian corals to ocean acidification, *Geochim. Cosmochim. Acta*, *74*(17), 4988-5001.

Liu, Y.-W., S. M. Aciego, A. D. Wanamaker, and B. K. Sell (2013), A high-throughput system for boron microsublimation and isotope analysis by total evaporation thermal ionization mass spectrometry, *Rapid Commun. Mass Spectrom.*, *27*(15), 1705-1714.

Liu, Y.-W., S. M. Aciego, and A. D. Wanamaker Jr (2015), Environmental controls on the boron and strontium isotopic composition of aragonite shell material of cultured *Arctica islandica*, *Biogeosciences*, *12*(11), 3351-3368.

Marulla, M., and T. O'Toole (2005a), Inland Reef Aquaria Salt Study, Part II, *Advanced Aquarist's Online Magazine*, *IV (XII)*.

Marulla, M., and T. O'Toole (2005b), Inland Reef Aquaria Salt Study, Part I, *Advanced Aquarist's Online Magazine*, *IV (XI)*.

Moheimani, N. R. (2005), The culture of coccolithophorid algae for carbon dioxide bioremediation, Murdoch University, Murdoch.

Moheimani, N. R., and M. A. Borowitzka (2006), The long-term culture of the coccolithophore *Pleurochrysis carterae* (Haptophyta) in outdoor raceway ponds, *Journal of Applied Phycology*, *18*(6), 703-712.

Moheimani, N. R., and M. A. Borowitzka (2011), Increased CO_2 and the effect of pH on growth and calcification of *Pleurochrysis carterae* and *Emiliania huxleyi* (Haptophyta) in semicontinuous cultures, *Appl. Microbiol. Biotechnol.*, *90*(4), 1399-1407.

Moheimani, N. R., J. P. Webb, and M. A. Borowitzka (2012), Bioremediation and other potential applications of coccolithophorid algae: A review, *Algal Research*, *1*(2), 120-133.

Nimer, N. A., G. K. Dixon, and M. J. Merrett (1992), Utilization of inorganic carbon by the coccolithophorid *Emiliania huxleyi* (Lohmann) Kamptner, *New Phytol.*, *120*(1), 153-158.

Nimer, N. A., and M. J. Merrett (1992), Calcification and utilization of inorganic carbon by the coccolithophorid *Emiliania huxleyi* Lohmann, *New Phytol.*, *121*(2), 173-177.

Paasche, E. (1964), A tracer study of the inorganic carbon uptake during coccolith formation and photosynthesis in the coccolithophorid *Coccolithus huxleyi*, *Physiologia Plantarum Suppl*, *3*, 1-82.

Rahbari, M. (2009), Physical characteristics of Pleurochrysis carterae in relation to harvesting potential for biodiesel production, The University of Adelaide, Adelaide.

Ries, J. B., A. L. Cohen, and D. C. McCorkle (2009), Marine calcifiers exhibit mixed responses to CO_2-induced ocean acidification, *Geology*, *37*(12), 1131-1134.

Ries, J. B. (2011), A physicochemical framework for interpreting the biological calcification response to CO_2-induced ocean acidification, *Geochim. Cosmochim. Acta*, *75*(14), 4053-4064.

Seki, M., T. Hirokawa, H. Hasegawa, and S. Furusaki (1995), Effect of CO_2 Concentration on Growth and Carbon Fixation Rate of *Pleurochrysis carterae*, *J. Chem. Eng. Jpn.*, *28*(4), 474-476.

Talmage, S. C., and C. J. Gobler (2010), Effects of past, present, and future ocean carbon dioxide concentrations on the growth and survival of larval shellfish, *Proc. Natl. Acad. Sci. U. S. A.*, *107*(40), 17246-17251.

Trotter, J., P. Montagna, M. McCulloch, S. Silenzi, S. Reynaud, G. Mortimer, S. Martin, C. Ferrier-Pagès, J.-P. Gattuso, and R. Rodolfo-Metalpa (2011), Quantifying the pH 'vital effect' in the temperate zooxanthellate coral *Cladocora caespitosa*: Validation of the boron seawater pH proxy, *Earth Planet. Sci. Lett.*, *303*(3-4), 163-173.

Westbroek, P., J. R. Young, and K. Linschooten (1989), Coccolith Production (Biomineralization) in the Marine Alga *Emiliania huxleyi*, *The Journal of Protozoology*, *36*(4), 368-373.

Winter, A., R. W. Jordan, and P. H. Roth (1994), Biogeography of living coccolithophores in ocean waters, edited, pp. 161-177, Cambridge University Press.

Zeebe, R. E., and D. A. Wolf-Gladrow (2001), *CO_2 in seawater: equilibrium, kinetics, isotopes*, Gulf Professional Publishing.
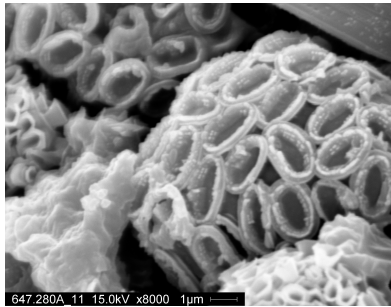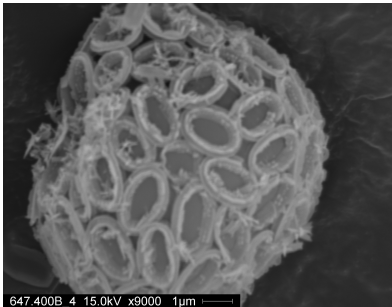
IV.8 Supplementary materials

IV.8.1 Results

Carbonate chemistry during the culture is shown in Figure S. 1. Temperature and salinity are nearly identical in different pCO_2 treatments for both strains, and with averages of 25.1 ± 0.5 °C and 35.9 ± 0.3 psu, respectively (Figure S. 1(a) and (b)). Measured synthetic seawater DIC and alkalinity range from 2370 to 3384 µmol/kg and 3000 to 3900 µmol/kg (Figure S. 1(c) and (d)). The DIC and alkalinity values show offsets between two culture sets, but both sets have increasing DIC as pH_{sw} decreases and the same alkalinity under different pH levels. Calculated seawater $HCO3^-$, CO_3^{2-}, $CO_{2(aq)}$ and pCO_2 concentrations are in ranges of 1800 to 3000 µmol/kg, 300 to 650 µmol/kg, 5 to 22 µmol/kg and 200 to 800 ppmv, respectively (Figure S. 1 (e) to (h)).

The SEM images suggest that there is no distinctive size change for coccolith scales, as well as the diameter of coccolithosphere. However, we do observe malformation of the coccoliths under low pH (Table S. 1).

Table S. 1   Typical SEM images from three different pCO_2 treatments in the culture experiment

pCO_2 = 280 ppmv	pCO_2 = 440 ppmv	pCO_2 = 520 ppmv
pH = 8.32	pH = 8.18	pH = 8.05

Trace elemental compositions of the synthetic seawater and cultured coccoliths under different treatments are showed in Figure S. 2. The calcium and trace elemental compositions ([Ca], B/Ca, Mg/Ca and Sr/Ca) in the synthetic seawater are identical or within a narrow range under different treatments and consistent with the natural seawater in general. The coccolith trace elemental results (B/Ca, Mg/Ca and Sr/Ca) are showed in Figure S. 3. The B/Ca, Mg/Ca and Sr/Ca ratios are range from 0.2 mmol/mol

to 24.3 mmol/mol, 43 mmol/mol to 134 mmol/mol and 1.8 mmol/mol to 6.6 mmol/mol, respectively. The Sr/Ca ratios are lied in the normal range for marine biogenic carbonates, however, the B/Ca ratios in strain CCMP 874 and Mg/Ca ratios in both strains are at least two to three orders higher than the ratios in conventional tested marine carbonates. None of the metal/Ca ratio has correlation to environmental variables such as temperature, salinity, pH or any of the carbonate species, except for the B/Ca in the strain CCMP 647. There is a slightly positive correlation of B/Ca to seawater pH in strain CCMP 647 (R^2 = 0.47); however, no correlation was found between B/Ca to pH_{sw} in strain CCMP 874. Instead, the B/Ca, Mg/Ca and Sr/Ca have slightly positive correlations between each other, with R^2 = 0.71 and 0.66 between B/Ca and Mg/Ca and Mg/Ca to Sr/Ca, respectively.

The average $\delta^{11}B$ value in synthetic seawater is 0.74 ± 1.43 ‰ (n = 23, 2 σ) (Figure S. 4 (a)). The $\delta^{11}B$ values in coccoliths are about 20 ‰ lower than that in the synthetic seawater. A prediction line of coccolith $\delta^{11}B$ is made across a pH range between 7.9 and 8.4, and based on the averages of synthetic seawater temperature and salinity, and a boron fractionation factor = 1.0272, following Eq. IV. 1.

Radiogenic and stable Sr isotopic results are showed in Figure S. 5. The coccolith $^{87}Sr/^{86}Sr$ ratios are consistent to that in the culture medium, and identical in different in different treatments, with an average value about 0.70802. The average $\delta^{88/86}Sr$ value in coccoliths is -0.026 ± 0.049 ‰ (n = 12, 2 σ), which is about 0.14 ‰ lower than that in the culture medium ($\delta^{88/86}Sr$ = 0.114). There is no resolvable variation for stable strontium isotopic compositions in the coccoliths.

IV.8.2   Method

SEM images for coccoliths from individual treatment were taken with Hitachi S3200N Scanning Electron Microscope in The University of Michigan Electron Microbeam Analysis Laboratory. Carbon tape was used to mount the dry coccolith pellet. At least 120 s of gold coating was applied onto the samples to prevent charging effect from accumulation of static electric charges on the non-conducted specimen surface. A 15 kV beam voltage was used to irradiate the sample with 8 mm working distance. A

107

software EDAX Genesis was used to capture the SEM images with image resolution better than 1024 × 800.

Trace element measurements including B/Ca, Mg/Ca, and Sr/Ca were conducted on a Thermo Finnigan Element II sector field inductively coupled plasma mass spectrometer (ICP-MS) at ICP-MS Trace Element Laboratory at Institution of Arctic and Alpine Research at the University of Colorado, Boulder. Twelve point five µl of seawater sample was diluted with 2 % HNO_3 to 500 µl for analysis. Dry carbonate samples were dissolved in 100 µl of 0.075 N HNO_3 and diluted with 400 µl of 2 % HNO_3. The long-term 1σ precisions are 0.54 % and 0.57 % for Mg/Ca and Sr/Ca ratios, respectively (Marchitto *et al.*, 2000). For the B/Ca measurements, an extra fall-in laboratory boron blank correction was conducted during the ICP-MS measurements and the recurrent 1σ precision is 4.2 % (Doss and Marchitto, 2013).

Radiogenic and stable Sr isotopic analysis followed the procedure described in Liu *et al.* (2015). Briefly, the residuals of coccolith samples after boron microsublimation were redissolved in 7 N nitric acid. A ^{87}Sr-^{84}Sr double spike was used to determine the stable strontium composition in the culture medium and coccoliths, with a spike to sample ratio about 1 to 1. To separate Sr from other matrices, both unspiked and spiked samples were passed through a 50 – 100 µm Sr-spec resin (Eichrom). About 100 – 200 ng and 200 – 250 of Sr in unspiked and spiked sample were loaded on outgassed Re single filament for measurements conducted on Thermo Fisher Triton PLUS multicollector thermal ionization mass spectrometer at the Glaciochemistry and Isotope Geochemistry Lab (GIGL) at the Department of Earth and Environmental Sciences, University of Michigan. A total of 400 cycles of data were collected for each measurement to determine the Sr isotopic ratios with within run precision better than 10 ppm (2 SE). The reproducibility of Sr isotopic standard SRM987 is 0.719246 ± 13 (2 σ, n = 42). The reported $^{87}Sr/^{86}Sr$ data in this study were all normalized to SRM987 = 0.710250 for inter-laboratory comparisons. The reproducibility of $\delta^{88/86}Sr$ values in seawater standard IAPSO = 0.365 ± 73 ‰ (2 σ, n = 4) and inter-laboratory carbonate standard JCp-1 = 0.195 ± 21 ‰ (2 σ, n = 4).
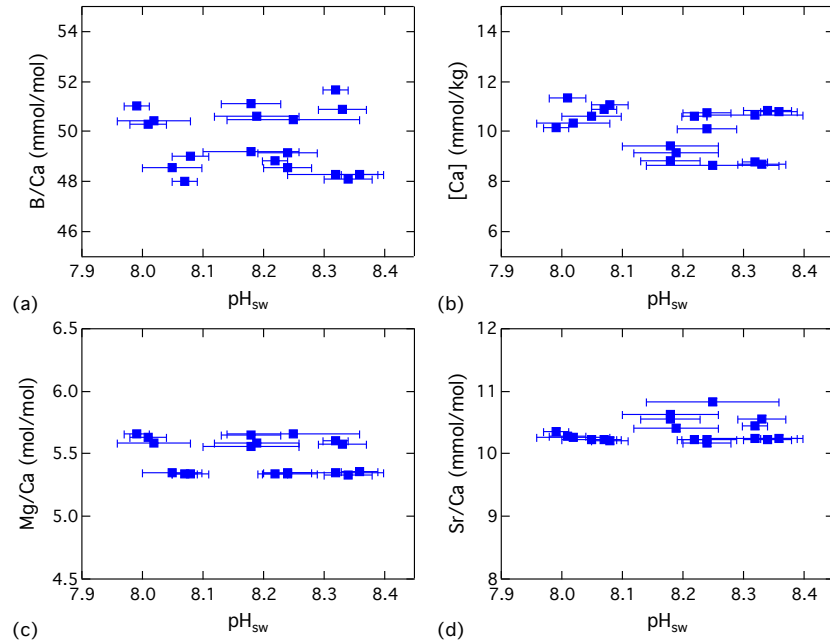
IV.8.3   Figures
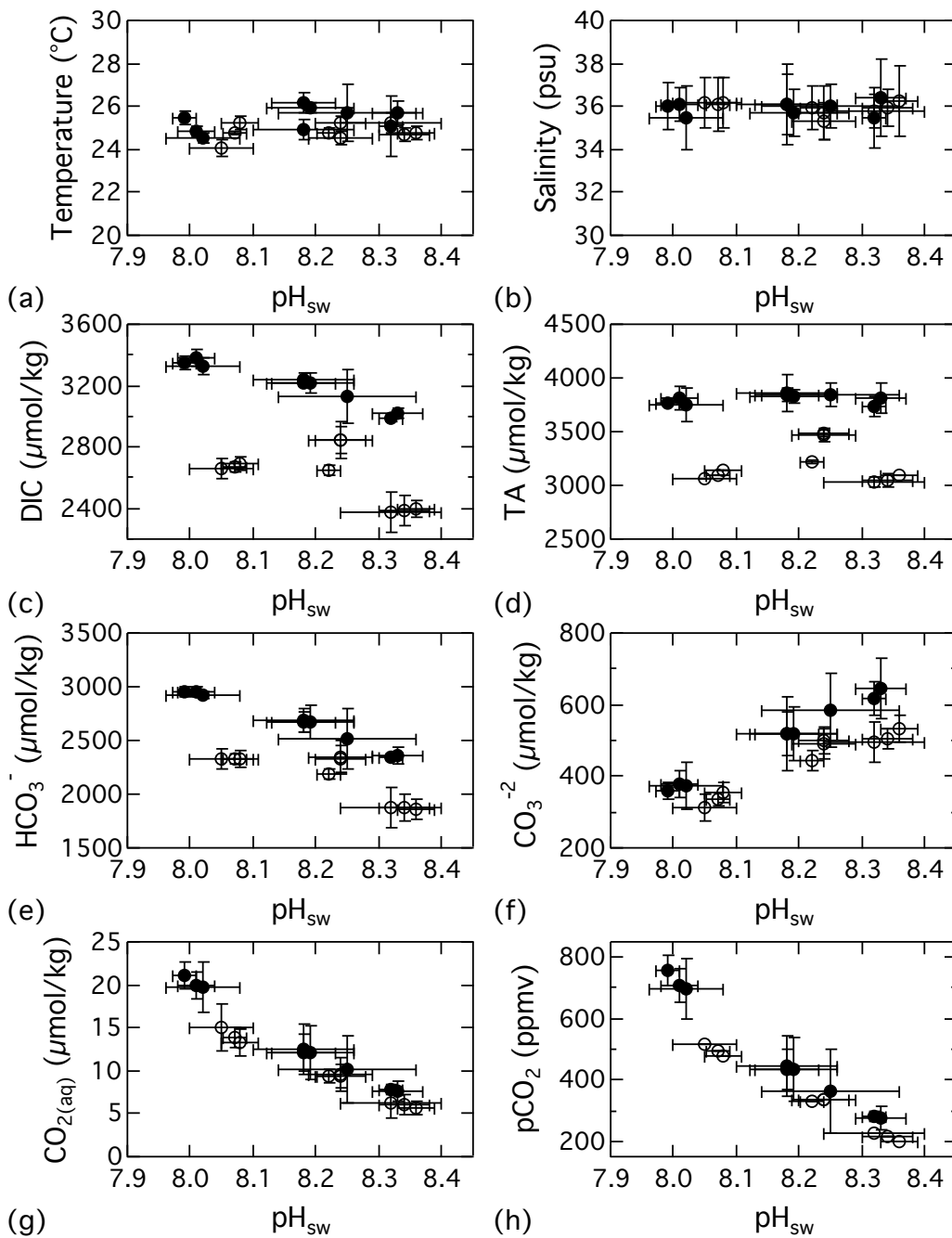
Figure S. 1   Culture carbonate system
Temperature, salinity, DIC and TA were monitored in different treatments. Water pH, HCO_3^-, CO_3^{2-}, $CO_{2(aq)}$ and pCO_2 contents were calculated based on the instrumental records. Solid circles represent data of strain CCMP647 and open circles represent data of strain CCMP 874.

Figure S. 2   **Trace element results of culture synthetic seawate**
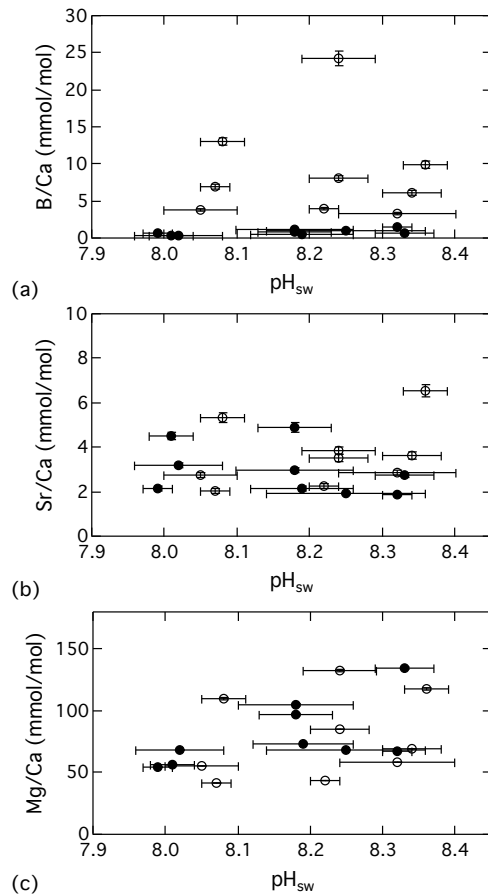
Figure S. 3   **Coccolith trace elements results**
Solid circles represent data of strain CCMP647 and open circles represent data of strain CCMP 874.

110
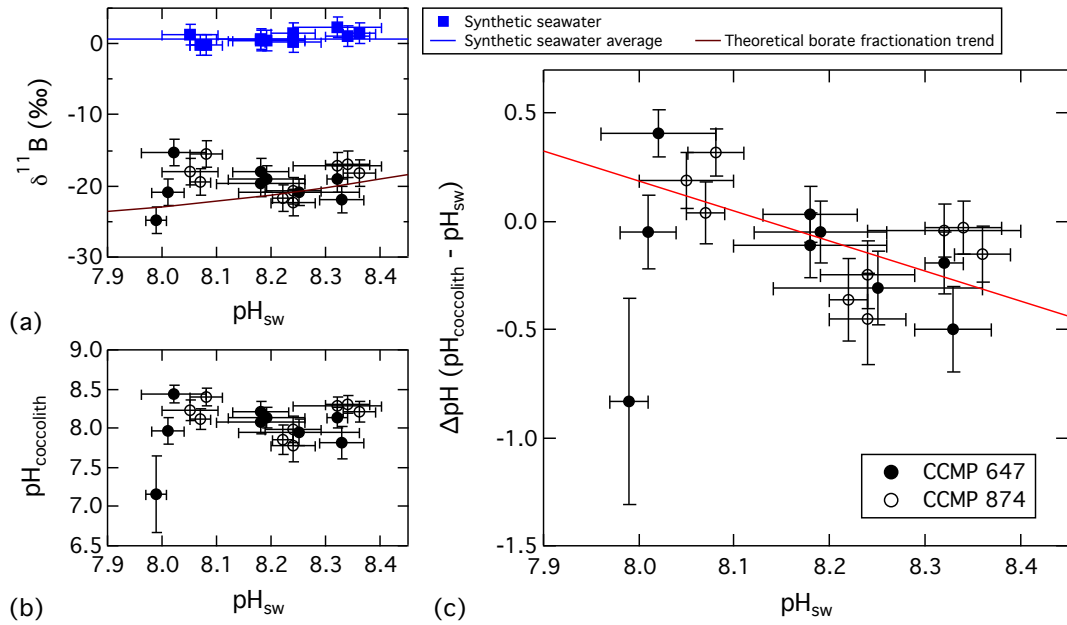
Figure S. 4 **(a) The coccolith and ambient seawater boron isotopic composition, (b) the boron-inferred coccolith calcification pH and (c) the pH offset between coccolith calcification site and ambient seawater were plotted with respect to the ambient seawater pH.**
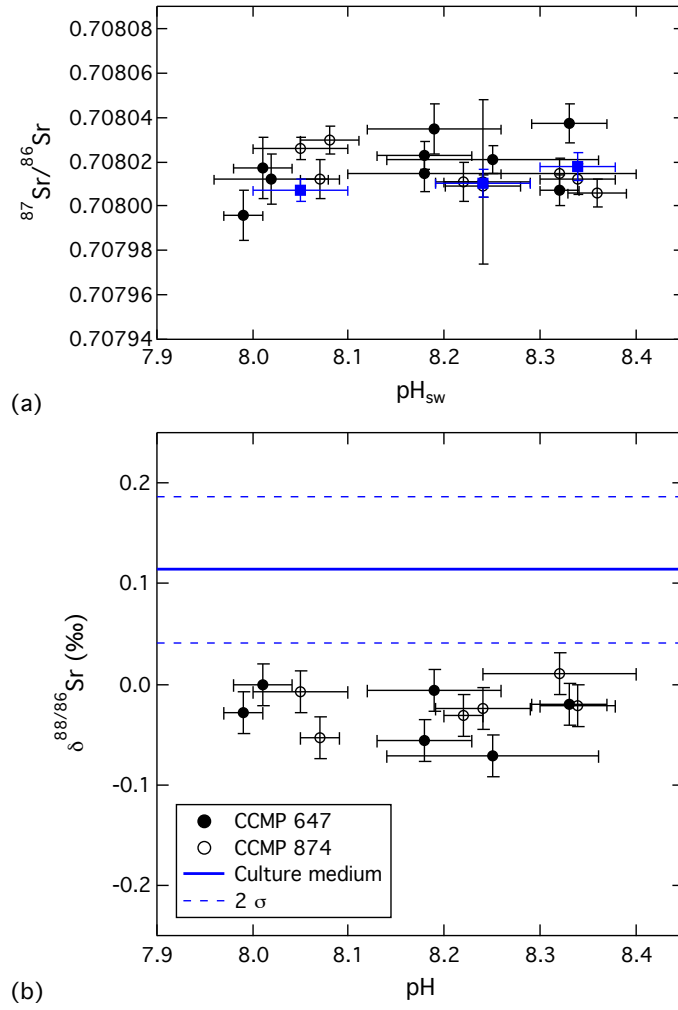
(a)

(b)

Figure S. 5 $^{87}Sr/^{86}Sr$ and $\delta^{88/86}Sr$ as a function of ambient seawater pH

IV.8.4 References

Doss, W., and T. M. Marchitto (2013), Glacial deep ocean sequestration of CO_2 driven by the eastern equatorial Pacific biologic pump, *Earth Planet. Sci. Lett.*, *377–378*, 43-54.

Liu, Y.-W., S. M. Aciego, and A. D. Wanamaker Jr (2015), Environmental controls on the boron and strontium isotopic composition of aragonite shell material of cultured *Arctica islandica*, *Biogeosciences*, *12*(11), 3351-3368.

Marchitto, T. M., G. A. Jones, G. A. Goodfriend, and C. R. Weidman (2000), Precise Temporal Correlation of Holocene Mollusk Shells Using Sclerochronology, *Quaternary Research*, *53*(2), 236-246.

Chapter V Summary and Outlook

V.1 Improved ability to investigate the vesicle pH in unconventional biogenic carbonates: what we have learned from them

In this Ph. D. dissertation project, we have developed a high-throughput boron purification technique. Coupled with negative mode thermal ionization mass spectrometry, less than 1 ng of boron is required for δ^{11}B analysis. This development allows us to investigate a wide range of biogenic carbonate samples, especially those unconventional marine archives that have a limited sample size and/or low boron concentrations. Extended studies from a wider range of biogenic archives should provide more opportunities to apply the δ^{11}B-pH proxy, and therefore expand seawater pH records both temporarily and geographically. Additionally, we can investigate the different biological responses to elevated pCO_2. The combination of these two study aspects can further help us to predict the potential buffering capacity of the ocean via bioremediation.

However, the developed technique still has limitations. The precision of δ^{11}B is ~ 1 – 2 ‰, which makes it hard to differentiate pH variations within 0.2 – 0.3 pH units. A better cleaning procedure for high organic carbonate samples is needed to reduce the potential interferences from $^{12}C^{14}N^{16}O$ compound. Treating samples with peroxide for a longer time or use of mixed reagents might improve the cleaning efficiency. Better maintenance of instrument conditions such as ion source and sample wheel chamber cleanness might also reduce the interferences from organics/contaminations during measurements (See Appendix A).

From the bivalve case study, we learned that *A. islandica* regulates internal pH so a species-specific transfer function is required for applying the δ^{11}B-pH proxy in *A. islandica.* Furthermore, there is likely a temperature threshold for boron uptake in this species. Thus better constraints culture experiments are required to determine the usage of this wide distributed geological archive, and potentially to develop the *A. islandica* δ^{11}B-pH transfer function.

From the coccolithophore case study, we found the adaptation ability of coccolithophore species *P. carterae* to ocean acidification. Our results suggest that with decreasing seawater pH (increasing DIC), *P. carterae* will not change its photosynthetic to calcification ratio, which might be due to increasing available DIC for photosynthesis and pH self-regulation for calcification. Further, we found that *P. carterae* might take more CO_2 instead of HCO_3^- at low pH condition.

The two different case studies both suggest the need to improve constraints on culture experiments and the information on species-specific responses to ocean acidification. Hence, some implications of this dissertation work are listed here.

V.2 Better constraints on culture experiments

V.2.1 *Arctica islandica* pH controlled incubation experiment

The cold-water species *A. islandica* shell has very wide distribution range in the northern Atlantic (Figure I. 3). Our result suggests when it grows in high seasonality environment, temperature might influence the boron incorporation into the aragonite shells. To differentiate the temperature effect from seawater pH to boron isotopic composition in the shell, a better constraint culture experiment is highly required to calibrate the δ^{11}B-pH proxy. The high latitude Atlantic region has lower seasonality, providing a nature constrain in temperature and salinity, therefore is ideal for calibrating the δ^{11}B-pH relation ship in *A. islandica*. In addition to low seasonality, it has been suggested *A. islandica* grows better under cooler environment. After calibrating the δ^{11}B-pH relationship, studies of boron isotopic composition in *A. islanidca* will extend

our seawater pH records to further north part of the Atlantic region and how the regional seawater pH vary with respect to increasing pCO_2.

V.2.2   Short-term and long-term pH controlled culture experiments on multiple coccolithophore speicies

V.2.2.1   *Short-term culture experiments on E. huxlyei*

Emiliania huxlyei is the most abundant coccolithophore species in the ocean (Bach *et al.*, 2013; Winter *et al.*, 1994). It has also a very wide distribution from tropical to sub-arctic ocean (Balestra *et al.*, 2004; Winter *et al.*, 1994). Different from *P. carterae, E. huxlyei* has several layers of calcite coccoliths cover one single cell, and it does not possess an organic base-plate scale associated with the mature coccoliths (Winter *et al.*, 1994). It has been intensively studied not only because its abundant distribution was thought to be an important biological pump for CO_2, but also because their coccolith scales are largely preserved in marine sediments, which provide important geochemical records for paleoceanographical or paleoclimatic studies. However, the organic and inorganic production reactions with respect to increasing pCO_2 and the corresponding inorganic carbon species uptake mode are still not fully understood.

Therefore, an extended study with additional boron isotopes, ratios of trace elements to calcium, stable carbon and oxygen isotopes in inorganic calcite and stable carbon isotopes in organic portion data from a pH-controlled culture experiment might provide more information to address those questions.

V.2.2.2   *Long-term culture experiments on P. carterae*

As we know that many of the marine biogenic carbonates are important geological archives, additional study with long-term culture is vital to evaluate the evolutionary effect on the adaptation in those organisms to ocean acidification. Compared to high organisms, the unicellular marine calcifying species has a shorter lifetime, typically 1 – 1.5 days/generation (Riebesell *et al.*, 2008), which is more applicable for evaluations of their long-term evolution, and can therefore provide more insights to the biological

evolvement. More specifically, this culture study can also expand our knowledge in interpreting those geological data, such as the increasing coccolithophore precipitation in the marine sedimentary core record since the Industrial Revolution, when we expect those marine calcifiers should suffer from more acidic and harsh environment.

V.3 Extended studies to wider range of marine calcifying organisms or invertebrates

In addition to those well-studied coral (e.g., *Porites species, Acropora species*), foraminifera (e.g., *Globigerinoides ruber, Globigerinoides sacculifer*), bivalve (e.g., *Mytilus edulis, A. islandica*) and coccolithophore species (e.g., *E. huxlyei, P. carterae*), it is also important and interesting to learn calcification processes in a wider range of marine organisms. Ries *et al.* (2009) presented calcification rate as a function of carbonate saturation state in 18 different species from a 60 days culture experiment and revealed their different calcification responses. Their result indicated various abilities to regulate pH for calcification in different species. Later, Ries (2011) further summarized previous work into six different biological calcification responses to CO_2-induced ocean acidification and proposed a proton-pumping model to explain the different responses. The proposed model was evaluated with *in situ* pH microelectrode probing in the temperate coral *Astrangia poculata* calcifying fluid under control and acidified conditions. However, it might not be applicable to conduct direct measurements in various species under different pCO_2 treatments. Hence, boron isotopic compositions might open a new window to uncover the vesicle pH and provide more information to assess the model.

V.4 Conclusion

The newly developed high-throughput boron purification method coupled with negative ion mode thermo ionization mass spectrometry in this study allow us to examine the boron isotopic composition in boron limited unconventional biogenic carbonate archives. We applied this technique to investigate how different environmental factors influence

boron isotope incorporation in aragonite bivalve shell, *A. islandica* in a culture experiment with instrumental sea. We found *A. islandica* will regulate the internal pH for calcification, and there might be a temperature threshold that will influence the boron incorporation. The lower seasonality, high latitude Atlantic region is ideal to avoid the environmental effect, however, a species-specific calibration is highly required for applying the δ^{11}B-pH proxy in the future. Our technique was also applied to investigate the impact from ocean acidification to coccolithophore *P. cartarae*. The boron isotopic composition data suggests this species will regulate the vesicle pH for calcification and is therefore insensitive to increasing pCO_2. This dissertation study indicates the wide implications of boron isotopic composition in unconventional biogenic archive, which helps to better understand the different biologic responses to ocean acidification, and further evaluate the potential use of δ^{11}B-pH proxy in a new species to extend our pH record in a wider region.

V.5 References

Bach, L. T., L. C. M. Mackinder, K. G. Schulz, G. Wheeler, D. C. Schroeder, C. Brownlee, and U. Riebesell (2013), Dissecting the impact of CO_2 and pH on the mechanisms of photosynthesis and calcification in the coccolithophore *Emiliania huxleyi*, *New Phytol.*, *199*(1), 121-134.

Balestra, B., P. Ziveri, S. Monechi, and T. Simon (2004), Coccolithophorids from the Southeast Greenland Margin (Northern North Atlantic): Production, Ecology and the Surface Sediment Record, *Micropaleontology*, *50*, 23-34.

Riebesell, U., R. G. J. Bellerby, A. Engel, V. J. Fabry, D. A. Hutchins, T. B. H. Reusch, K. G. Schulz, and F. M. M. Morel (2008), Comment on "Phytoplankton Calcification in a High-CO_2 World", *Science*, *322*(5907), 1466.

Ries, J. B., A. L. Cohen, and D. C. McCorkle (2009), Marine calcifiers exhibit mixed responses to CO_2-induced ocean acidification, *Geology*, *37*(12), 1131-1134.

Ries, J. B. (2011), A physicochemical framework for interpreting the biological calcification response to CO_2-induced ocean acidification, *Geochim. Cosmochim. Acta*, *75*(14), 4053-4064.

Winter, A., R. W. Jordan, and P. H. Roth (1994), Biogeography of living coccolithophores in ocean waters, edited, pp. 161-177, Cambridge University Press.

Appendices

Appendix A   Maintenance of standards, filaments and TIMS for precise δ^{11}B measurements with N-TIMS technique

Small boron sample is highly sensitive to surrounding environment. We monitored long-term variations of multiple boron isotopic standards to improve δ^{11}B reproducibility. According to our boric acid boron isotope standard record, sample and filaments stored in N_2 desiccator box can reduce the influence humidity and improve the analytical precision. However, filaments after outgassed should be oxidized with high purity oxygen gas for 3 days in the desiccator box, or the ionization efficiency would be largely reduced. Gain calibration before each measurements can potentially improve the measurements, however, more importantly, the cleanness of ion source and working standard solution are more critical to improve the precision (Figure A. 1). Long source bake out (10 hours) between barrels and change ion source when switch from other isotope measurements to boron analysis can keep low contamination level. Regular replacement with working standard solution is highly required to sustain high quality control. Using liquid nitrogen cold trap during analysis can improve the vacuum pressure and can potentially reduced the influences from water drop in the sample wheel chamber, which might be vaporized and bring organic dirt attached on the chamber wall to the system.

Results of inter-laboratory boron isotope seawater standard IAEA B-1, coral *Porites* standard JCp-1 and in-lab bivalve *A. islandica* working standard are showed in Figure A. 2. The results suggest that additional treatment with 2 µl H_2O_2 after microsublimation purification procedure can further improve the reproducibility for different natural samples due to the reduction of organic matters. Additional cleaning for nature samples before dissolution might also help to improve analytical precision in the future.
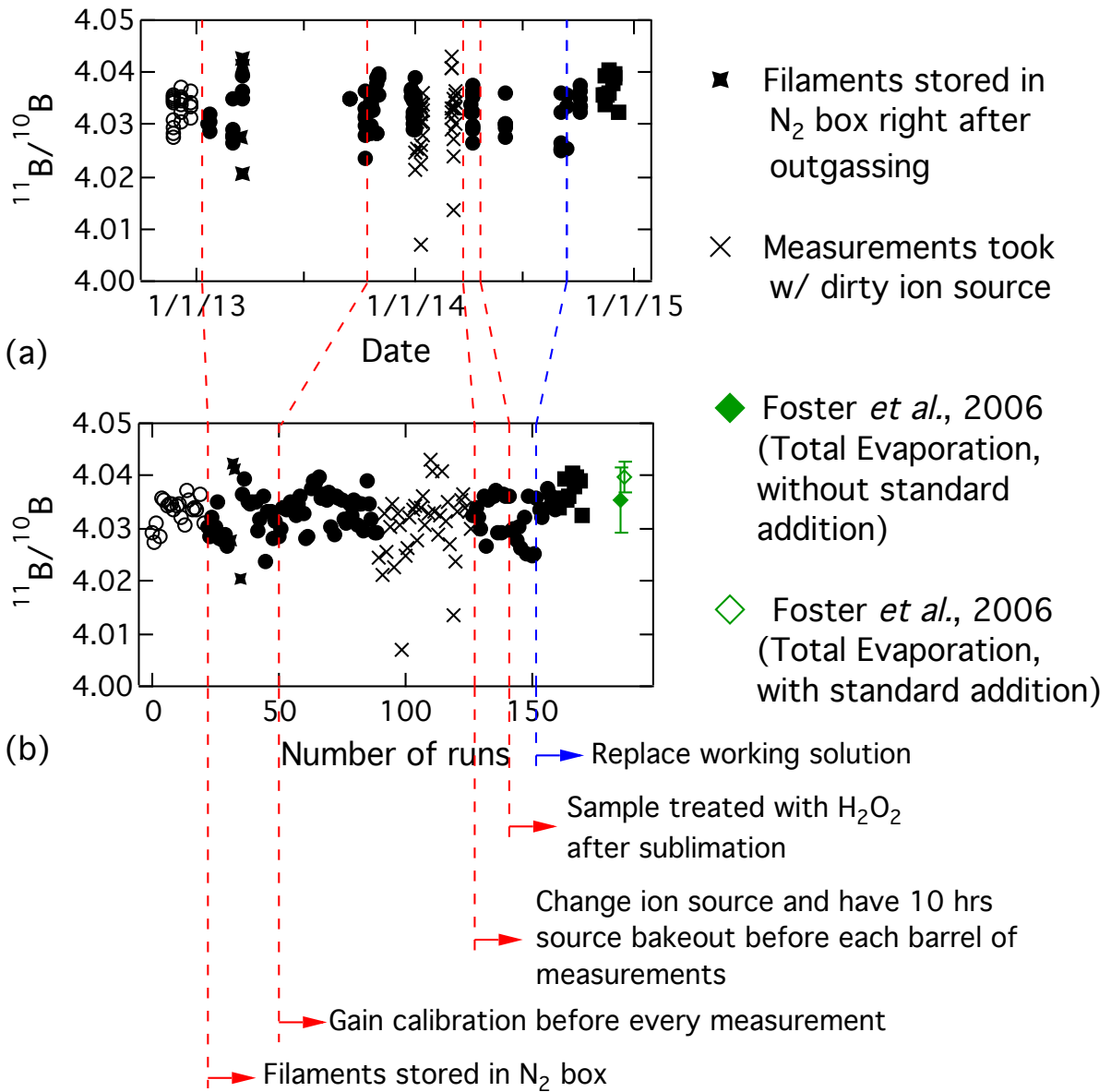
Figure A. 1   Long-term reproducibility of SRM 951a
Different trials of treatments were listed to show the potential improving method for boron isotope measurements with NTIMS method.
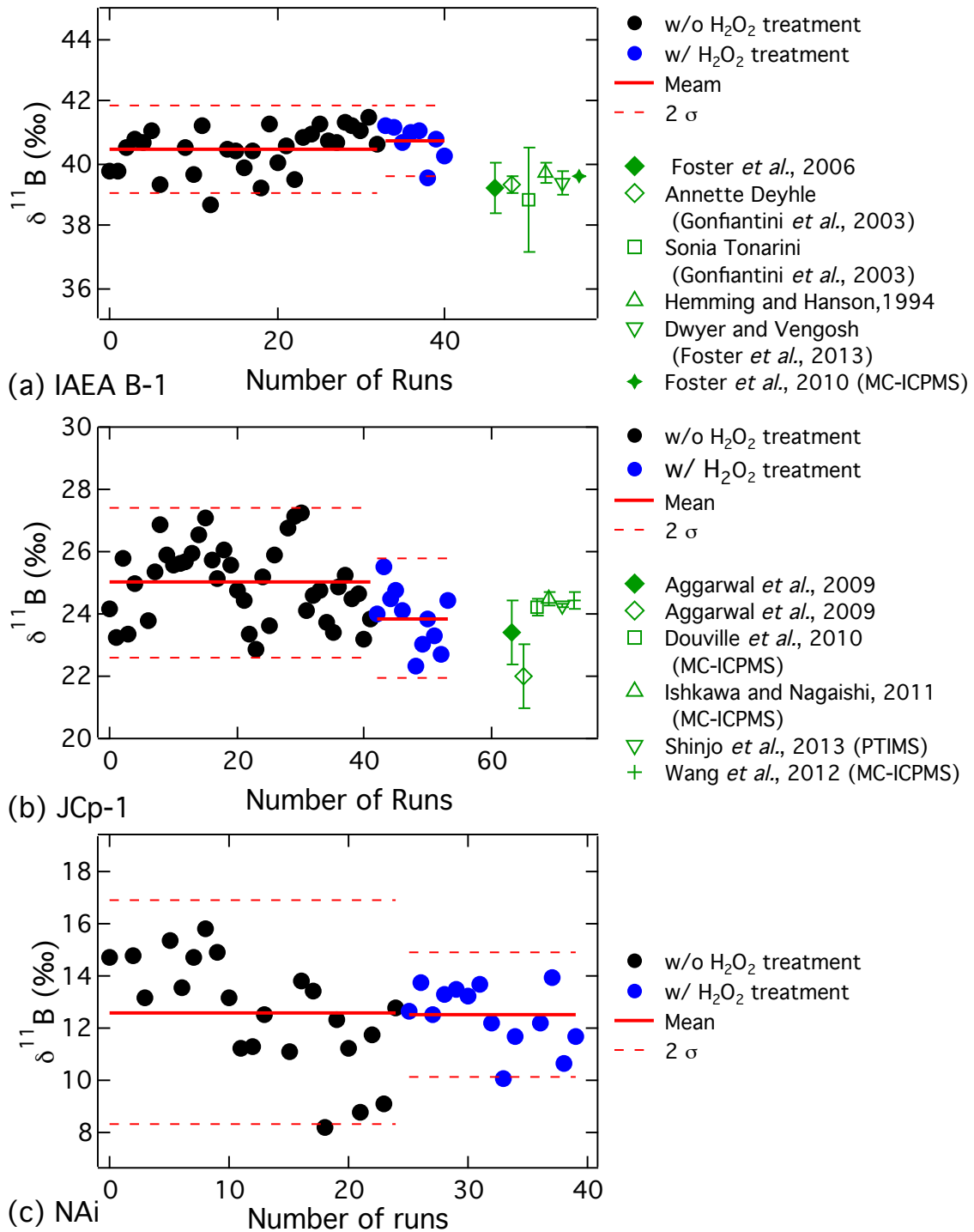
Figure A. 2　　　Long-term reproducibility of inter-laboratory boron isotope standards (a) IAEA B-1 (b) JCp-1 and *Arctica islandica* shell working standard (c) NAi

Blank dots represent data without H_2O_2 treatment after sublimation. The isotopic ratios were normalized to the average [11]B/[10]B ratio of SRM951a before H_2O_2 treatment. Blue dots represent data with H_2O_2 treatment after sublimation and the isotopic ratios were normalized to average [11]B/[10]B ratio of SRM951a after the blue dash line shown in Figure A. 1. Some reported values were listed in green for reference. The reference values were obtain by TIMS method if not specified in the legend.

Appendix B   *Arctica islandica* pH controlled incubation experiment at Fram Center for Climate and Environment, Tromsø

An ongoing extended study for the bivalve shell *A. islandica* with relative constant seawater temperature and salinity but a larger pH variation were set up to differentiate the influence from seawater pH to the shell boron isotopes uptake. The primary objective of this experiment is therefore to confirm the relationship between boron isotopic compositions in the bivalve mollusk *A. islandica* and the ambient seawater pH, so that we might use the δ^{11}B-pH proxy to reconstruct the seawater pH records in higher latitude of coastal Atlantic region.

B.1   Experimental settings

Living adult and juvenile animals were collected from January 31st to February 6th 2014 from Ingøy, Norway. The experiment was built in Troms Marin Yngel, a research facility owned by Akvaplan-niva, Tromsø, Norway. We conducted five-months of calibration work from February to July 2014. Our experiment consists of organisms cultured at four different pH treatments: 7.5, 7.7, 7.9 and 8.1 (normal seawater pH, control treatment) at near constant seawater temperature (7 °C ± 1 °C) and salinity (34.5 ± 1 PSU). Overall 108 clams were divided into nine tanks at four pH levels (12 clams/tray, two trays/pH level, one extra tray under control pH treatment). *Arctica islandica* clams were stained at the start of the experiment (after a one-week acclimation period) and were stained in May to constrain individual growth rates: distance between stain marks will indicate the new growth and the dates of staining will provide a time reference. The initial size distribution of shells is not significantly different among the tanks (ANOVA, p = 0.99). A schematic of the experimental setup is shown in Figure B. 1.

Water samples were collected and filtered with a 0.45 μm PES filter at the start of the experiment and every month thereafter for determining dissolved inorganic carbon, alkalinity, major nutrients (ammonium, nitrite, nitrate and phosphate), water isotopes (δD, δ^{18}O, δ^{11}B) and major and trace elements (limiting micronutrients Si, Fe, Co, Mn and tracers Ca, B, Mg) at the Universiy of Tromsø, the University of Michigan (UM) and

Iowa State University (ISU). The ongoing work includes shell section observations under microscope and multiple geochemical proxies analysis for water and shell carbonate samples. In order to investigate potential vital effects during the culture experiment, shell growth and major and micronutrients will be monitored. The micronutrients (Fe, Co, and Mn) will be extracted and concentrated by processing through a Nobias-chelate PA1 resin for analysis on ICP-MS with medium resolution following the procedures described in Sohrin et al. (2008) and Biller and Bruland (2012). Ca, B, Mg and Sr will be measured directly after diluting the water sample to proper Ca and Mg concentrations by ICP-MS under low-resolution mode. Monitoring of stable isotopes and trace elements ratios will aid in evaluating the equilibrium state between the shell and the seawater from which it is precipitating. Major and micronutrient measurements will be made at UM, while water isotopes will be measured at ISU.
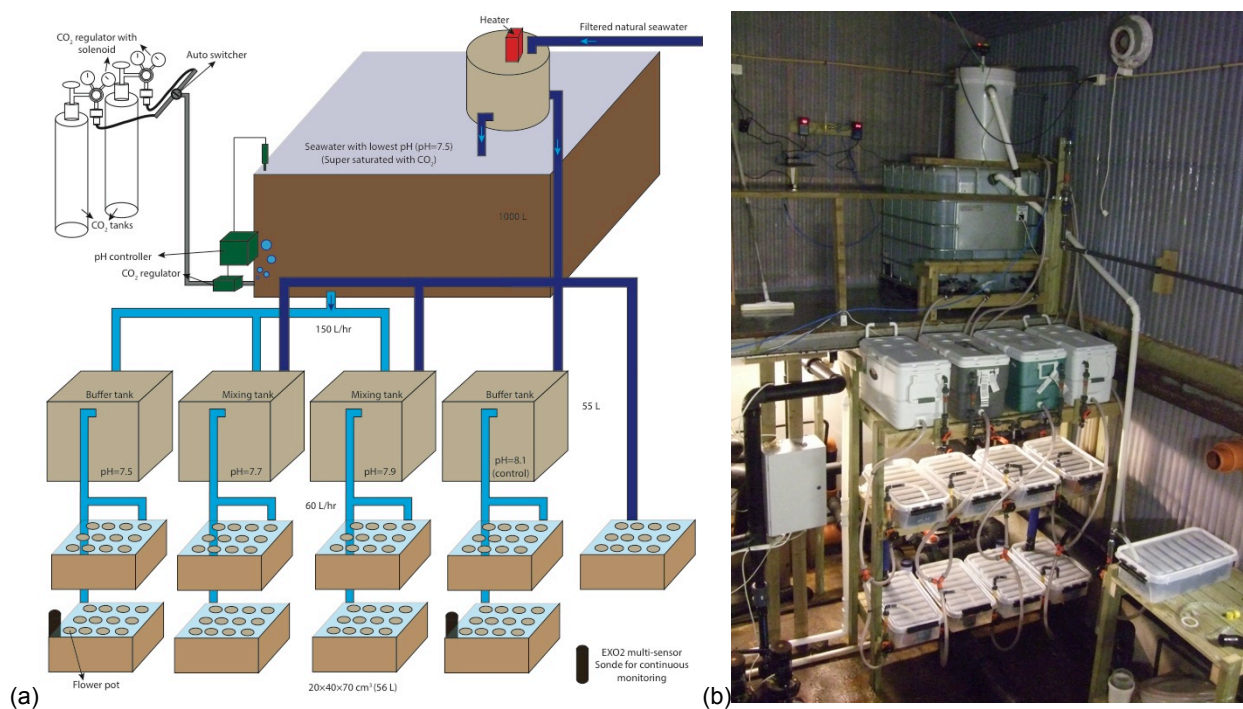

Figure B. 1   The experimental setup of pH controlled culture experiment in Tromsø, Norway.
To maintain the pH levels, we injected high pressure CO_2 into seawater to achieve a pH level about 7.5 in a 1000 L tank in this experiment. Seawater was piped through a 60 µm filter into the tank with a water intake located at a depth of 60 m. The CO_2-enriched seawater was heated to 7 °C and mixed with different amounts of seawater to achieve different pH levels. The pH of each tank was regulated and maintained by adjusting the flow rates of seawater and CO_2-enriched seawater in a buffer tank. To prevent pH buffering from the dissolution of calcium carbonates, artificial calcium carbonate-free sediment was used as substrate in the trays. For *in situ* water monitoring, two multiparameter instruments were mounted in the pH end-member tanks for continuous data recording. Four pH meters were mounted in the buffer tanks to monitor the pH levels in different treatments.

B.2　Instrumental records and expected outcomes

We grew the shells under a nearly constant temperature (7.5 ± 0.5 °C) and salinity (34.5 ± 0.5 PSU) for five months. Because we limited water temperature and salinity variability to near constant values during the experiment (Figure B. 2), the shell $\delta^{11}B$ values are expected to be controlled only by the pH. The 0.6 pH unit offset in this experiment should correspond to a variation in the $\delta^{11}B$ value by as much as 3.1‰, which can be estimated through the equation Eq. I.4. Our instrumental temperature and salinity data will be used to determine the corresponding pK_b value and the $\delta^{11}B_{sw}$ used for pH calculation will based on the average value measured from the tank water. In general, we predict a shift in $\delta^{11}B$ for the calibration experiment outside of our measurement error. Deviations from this prediction will be used to determine the overall transfer function, in a way with a species-specific correction factor to the original transfer function (Eq. I.4) and/or an additional ΔpH (pH_{EPF} - pH_{sw}) to pH_{sw} correction.
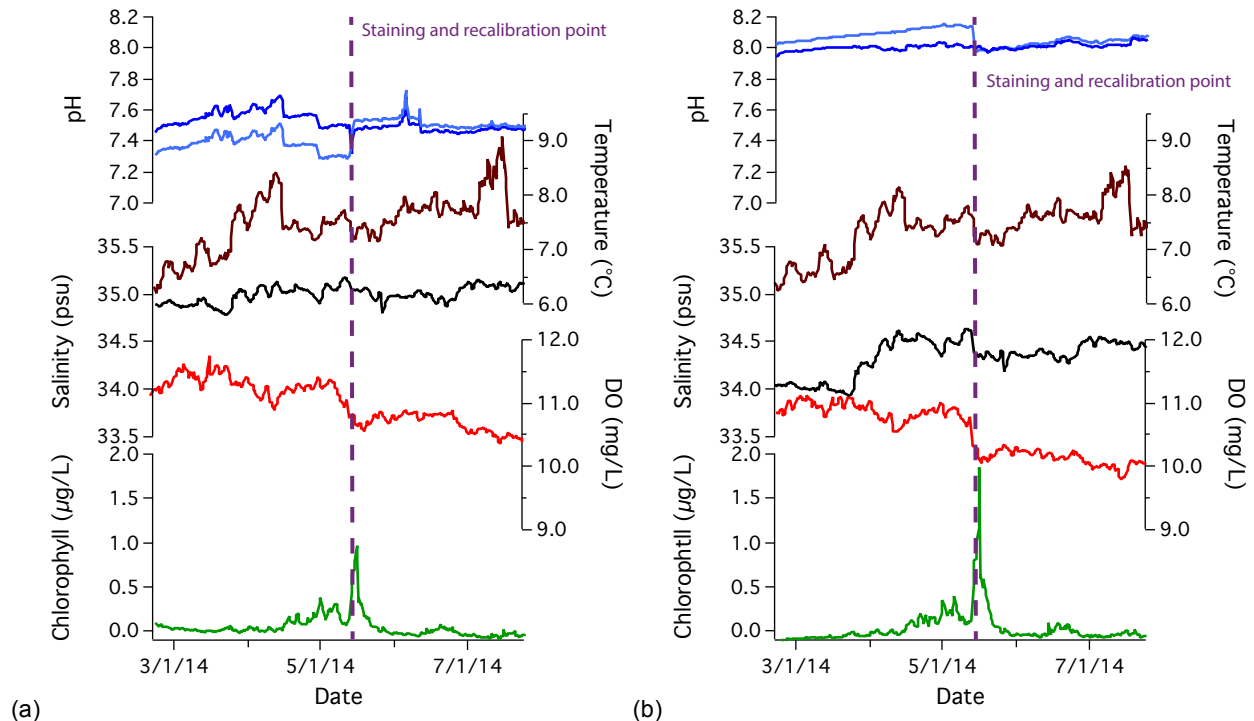
Figure B. 2　　　Continuous instrumental monitoring of the pH controlled experiment.
These two figures show continuous tank water pH, temperature, salinity, dissolved oxygen and chlorophyll for treatment (a) pH = 7.5 and (b) pH = 8.1 (ambient condition)

B.3 *In situ* pH measurements in *A. islandica*

In Stemmer (2013) thesis study, she examined the inner extrapallial fluid (EPF) pH in *A. islandica* (Figure B. 3 (a)) with a liquid membrane microsensor. In her short-term observation (< 1 hour) she found that in general, the inner EPF pH decreases from shell side to tissue side, but occasionally the pH close to the tissue side raised up from 6.7 – 9.1 pH unit. In her long-term observation (7 yours) the overall pH is about 0.2 – 0.6 lower than the ambient seawater pH, but the pH discrimination between inner EPF and ambient seawater baseline decrease overtime. Her work showed the pH regulation of *A. islandica*, however, only two specimens were observed in less than 7 hours in this experiment. How the shells will respond to different environmental pH is still unclear. Therefore, an improved method to obtain in situ EPF pH measurements during pH control culture experiment is also desired to constrain the bivalve $\delta^{11}B$ and calcification pH relationship. Figure B. 3 (b) to (g) show some ideas about the experimental design that was adapted from Stemmer (2013). Note that during a culture, living shell will move in the substrates (e.g., carbonate-free sands), so the entrance hole for in situ EPF pH measurements should be firmly mounted and sealed. Instead of parafilm, other toxic-free material might be used here.

(a)
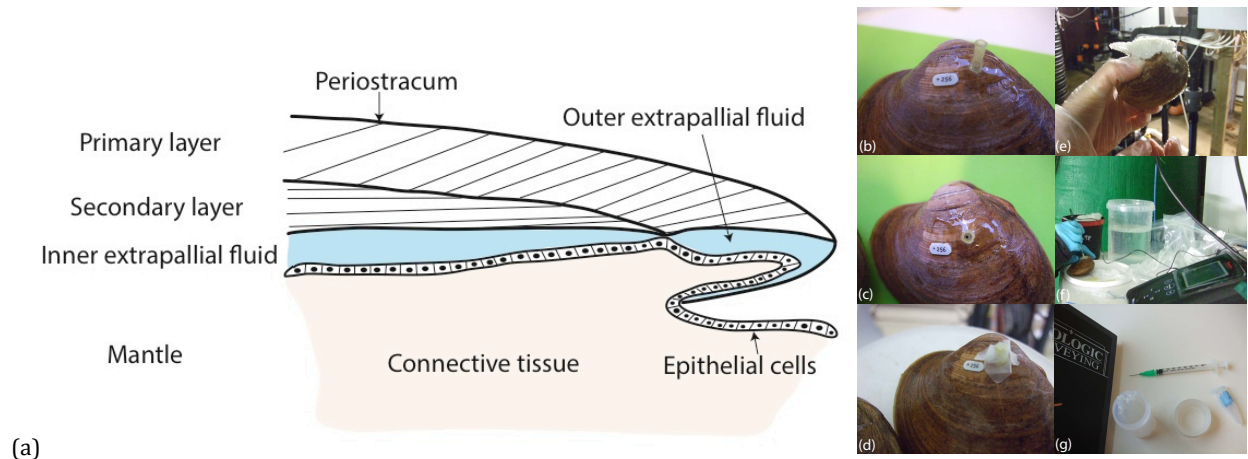
Figure B. 3   (a) Sketch of bivalve shell and the inner and outer EPF sites. (b) to (g) show some ideas to measure in situ EPF pH during a pH control culture experiment.
A cut pipette tip can be mounted on the hole drilled on one of the valve. The hole might be sealed with parafilm or toxic-free material. In (g), a syringe with acid cleaned PE tube was used to extract inner EPF for boron isotopic measurement.

B.4   References

Biller, D. V., and K. W. Bruland (2012), Analysis of Mn, Fe, Co, Ni, Cu, Zn, Cd, and Pb in seawater using the Nobias-chelate PA1 resin and magnetic sector inductively coupled plasma mass spectrometry (ICP-MS), *Mar. Chem.*, *130-131*, 12-20.

Sohrin, Y., S. Urushihara, S. Nakatsuka, T. Kono, E. Higo, T. Minami, K. Norisuye, and S. Umetani (2008), Multielemental Determination of GEOTRACES Key Trace Metals in Seawater by ICPMS after Preconcentration Using an Ethylenediaminetriacetic Acid Chelating Resin, *Anal. Chem.*, *80*(16), 6267-6273.

Stemmer, K. (2013), Shell formation and microstucture of the ocean quahog Arctica islandica: Does ocean acidification matter?, 143 pp, Staats- und Universitaetsbibliothek Bremen, Bremen.